Supporting Information for

Customizing Circularly Polarized Afterglow by Stepwise Chiral Amplification in BINAPs/BINAPOs

*Bo Yang[§], Suqiong Yan[§], Shirong Ban[§], Hui Ma[§], Yuan Zhang[§], Fanda Feng[§], and Wei Huang[§‡]**

§State Key Laboratory of Coordination Chemistry, School of Chemistry and Chemical Engineering, Nanjing University, Nanjing 210023, P. R. China
‡Shenzhen Research Institute of Nanjing University, Shenzhen 518057, P. R. China
Email: whuang@nju.edu.cn

CONTENTS

A: Experimental section

Unless other noted, all reagents and solvents used in the experiments were purchased from commercial sources without further purification. The compounds were purified by column chromatography and then characterized by NMR. The highly purified chiral compounds were received after being resolved by high-performance chiral preparative chromatography (used for optical studies). Nuclear magnetic resonance (NMR) spectra were measured with a Bruker-advance ^{1}H (400 MHz), ^{31}P (160 MHz), and ^{13}C (100 MHz) spectrometer. Trace tetramethylsilane (TMS, δ = 0.0 ppm) was used as an internal standard for the ^{1}H NMR spectra, and $CDCl_3$ (δ = 77.0 ppm) was used as an internal standard for the ^{13}C NMR spectra. SCXRD data were collected at 173 K using a Bruker diffractometer with an X-ray tube with Ga/Kα (λ = 1.34139 Å) radiation. Program APEX4 was used for the data collection and reduction. The structures were solved with an intrinsic phasing of SHELXT and refined by full-matrix least-squares on F^2 using OLEX2 software,[1] which utilizes the SHELX-2013-2 module.[2] The detailed crystallographic data and experimental details of all complexes were shown in this ESI. Crystallographic data were deposited with the Cambridge Crystallographic Data Centre (CCDC number 2344550). Ultraviolet-visible absorption spectra were measured on a Shimadzu UV-2600 spectrophotometer by using a 10 mm optical-path quartz cell at room temperature. The photoluminescence (PL) spectra were measured on the HITACHI F-4600 and HORIBA-FL3. Absolute quantum yields were measured using the calibrated integrating sphere system (λ_{ex}=365 nm, Labsphere Inc). The time-resolved PL measurements were taken on the HORIBA-FL3 instrument to measure the excited state lifetime. A NanoLED-370 (372 nm) or SpectraLED-370 (374 nm) was used as the excitation source, and the time-correlated single-photon counting (TCSPC) method and bi-exponential fitting ($\boldsymbol{R(t) = S_1 e^{\left(-\frac{t}{\tau 1}\right)} + S_2 e^{\left(-\frac{t}{\tau 2}\right)}}$) were used to quantify the emission lifetime (Lifetime data were analyzed with Data Station v6.6 (Horiba Scientific)). Photographs were taken by the Panasonic GX-95 camera. Circular dichroism (CD) spectra were measured on a JASCO J-810 spectrometer. Circularly polarized luminescence (CPL) spectra were recorded on a JASCO CPL-300 spectrophotometer, the excitation wavelength was 365 nm for all samples. The gabs value was determined by $\boldsymbol{g_{abs} = \frac{\Delta\varepsilon}{\varepsilon} = 2\frac{\varepsilon_L - \varepsilon_R}{\varepsilon_L + \varepsilon_R}}$ $= \frac{\boldsymbol{CD(mdeg)}}{\boldsymbol{32980 \times Abs}}$, where ε_L and ε_R are the ellipticities of the left- and right-handed circularly polarized absorptions. The g_{lum} value of CPL was determined by $\boldsymbol{g_{lum} = \frac{\Delta I}{I} = 2\frac{I_L - I_R}{I_L + I_R}}$, where I_L and I_R are the intensities of the left- and right-handed circularly polarized emissions.

B: Synthesis of procedures for substrates and products

The synthesis method is identical to our previous work.[3]

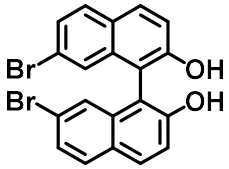

Synthesis of 7,7'-dibromo-[1,1'-binaphthalene]-2,2'-diol: In a 250 mL round-bottomed flask was placed 7-bromonaphthalen-2-ol (10 g, 44.8 mmol), $FeCl_3$ (3.0 eq), tetramethylethylenediamine (TMEDA, 1.0 eq) and 100 mL of mixed solvent (EtOH/H2O = 1:1). The mixture was refluxed at 90 °C in O_2 for 48 h. The mixture was extracted successively with water and DCM solution. The organic phase is dried with anhydrous $MgSO_4$ and filtered. The organic solvent was removed by decompressing vaporization. The resulting residue was purified by column chromatography with PE : DCM (1:3), and then the grey solid powder was obtained with 93% yield. ^{1}H NMR (400 MHz, $CDCl_3$) δ 7.96 (d, J = 8.9 Hz, 2H), 7.77 (d, J = 8.7 Hz, 2H), 7.48 (dd, J = 8.7, 1.9 Hz, 2H), 7.39 (d, J = 8.9 Hz, 2H), 7.23 (d, J = 1.8 Hz, 2H), 5.08 (s, 2H).

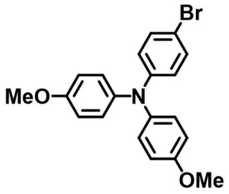

Synthesis of 4-bromo-N,N-bis(4-methoxyphenyl)aniline: In a 250 mL round-bottomed flask was placed bis(4-methoxyphenyl)amine (5.0 g, 21.8 mmol), 1-bromo-4-iodobenzene (3.16 g, 1.0 eq), $Pd(dppf)Cl_2$ (0.16 g 1 mol%,), Sodium tert-butoxide (NaO-*t*Bu, 4.2 g, 2.0 eq), and 100 mL of dry toluene (50 mL). The mixture was refluxed at 90 °C in Ar for 24 h. The cooling mixture was extracted successively with water and DCM solution. The organic phase is dried with anhydrous $MgSO_4$ and filtered. The organic solvent was removed by decompressing vaporization. The resulting residue was purified by column chromatography with PE : DCM (5:1), and then the white solid was obtained with 94% yield. ^{1}H NMR (400 MHz, $CDCl_3$) δ 7.23 (dd, *J* = 9.9, 3.0 Hz, 2H), 7.13 – 6.93 (m, 4H), 6.91 – 6.70 (m, 6H), 3.78 (s, 6H).

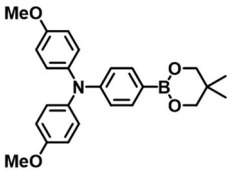

Synthesis of 4-(5,5-dimethyl-1,3,2-dioxaborinan-2-yl)-N,N-bis(4-methoxyphenyl)aniline: In a 250 mL round-bottomed flask was placed 4-bromo-N,N-bis(4-methoxyphenyl)aniline (5.0 g, 13.0 mmol), 5,5,5',5'-tetramethyl-2,2'-bi(1,3,2-dioxaborinane) (3.24 g, 1.1 eq), $Pd(dppf)Cl_2$ (0.19 g 2 mol%,), dry KOAc (2.56 g, 2.0 eq), and 100 mL of dry dioxane (50 mL). The mixture was refluxed at 100 °C in Ar for 24 h. The cooling mixture was extracted successively with water and DCM solution. The organic phase is dried with anhydrous $MgSO_4$ and filtered. The organic solvent was removed by decompressing vaporization. The resulting residue was purified by column chromatography with PE : DCM (10 : 1 to 6 : 1), and then the white solid was obtained with 97% yield. ^{1}H NMR (400 MHz, $CDCl_3$) δ 7.64 – 7.50 (m, 2H), 7.06 (d, J = 8.9 Hz, 4H), 6.93 – 6.83 (m, 2H), 6.86 – 6.69 (m, 6H), 3.78 (s, 6H), 3.71 (d, J = 11.8 Hz, 6H), 1.00 (s, 6H).

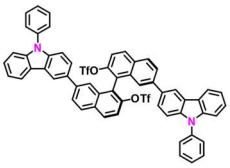

Synthesis of P1-OTf: (1) In a 100 mL Schlenk flask was placed 7,7'-dibromo-[1,1'-binaphthalene]-2,2'-diol (3.0 g, 6.77 mmol), (9-phenyl-9H-carbazol-3-yl)boronic acid (4.86 g, 2.5 eq), $Pd(PPh_3)_4$ (1 mol%,), K_2CO_3 (NaO-tBu, 4.2 g, 2.0 eq), and 100 mL of mixed toluene/EtOH/H_2O (4 : 2 : 4). The mixture was refluxed at 90 °C in Ar for 24 h. The cooling mixture was extracted successively with water and DCM solution. The organic phase is dried with anhydrous $MgSO_4$ and filtered. The organic solvent was removed by decompressing vaporization. The resulting residue was purified by column chromatography with PE : DCM (1:3), and then the grey crud solid was obtained with 85% yield. This grey crud product was directly used for esterification.

(2) In a 100 mL Schlenk flask was placed **P1-OH** (1.0 g, 0.97 mmol) and 20 mL of dry DCM. NEt_3 in DCM (2.5 eq) was added dropwise at 0 °C for 10 min. The $(Tf)_2O$ in DCM was added dropwise at 0 °C for about 15 min. The reaction was reacted at room temperature for 3 hours. The mixture was extracted successively with brine and DCM solution. The organic layer was dried with $MgSO_4$ and filtered. The organic solvent was removed by decompressing vaporization. The resulting residue was purified by column chromatography with PE : DCM (8 : 1), and then the white solid was obtained with 94%. ^{1}H NMR (400 MHz, $CDCl_3$) δ 8.15 (d, *J* = 9.0 Hz, 2H), 8.05 (d, *J* = 8.6 Hz, 2H), 7.83 (dd, *J* = 8.6, 1.6 Hz, 2H), 7.60 (d, *J* = 9.0 Hz, 2H), 7.43 (s, 2H), 7.24 (d, *J* = 8.7 Hz, 4H), 7.07 (d, *J* = 8.3 Hz, 8H), 6.96 (dd, *J* = 16.1, 8.5 Hz, 12H), 2.32 (s, 12H).

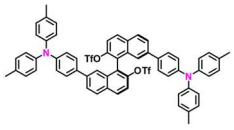

Synthesis of P2-OTf: Prepared by the aforementioned method from (4-(di-p-tolylamino)phenyl)boronic acid with 87% yield. ^{1}H NMR (400 MHz, $CDCl_3$) δ 8.15 (d, *J* = 9.0 Hz, 2H), 8.05 (d, *J* = 8.6 Hz, 2H), 7.83 (dd, *J* = 8.6, 1.6 Hz, 2H), 7.60 (d, *J* = 9.0 Hz, 2H), 7.43 (s, 2H), 7.24 (d, *J* = 8.7 Hz, 4H), 7.07 (d, *J* = 8.3 Hz, 8H), 6.96 (dd, *J* = 16.1, 8.5 Hz, 12H), 2.32 (s, 12H).

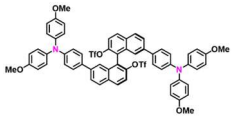

Synthesis of P3-OTf: Prepared by the aforementioned method from (4-(bis(4-methoxyphenyl)amino)phenyl)boronic acid with 91% yield. ^{1}H NMR (400 MHz, $CDCl_3$) δ 8.10 (d, *J* = 9.0 Hz, 2H), 8.00 (d, *J* = 8.6 Hz, 2H), 7.78 (dd, *J* = 8.6, 1.7 Hz, 2H), 7.55 (d, *J* = 9.0 Hz, 2H), 7.37 (d, *J* = 0.7 Hz, 2H), 7.18 (d, *J* = 8.8 Hz, 4H), 7.03 – 6.97 (m, 8H), 6.84 – 6.77 (m, 12H), 3.77 (s, 12H).

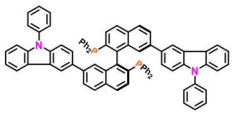

Synthesis of P1: In a 50 mL Schlenk flask was placed **P1-OTf** (1.0 g, 0.9 mmol), $Ni(dppe)Cl_2$ (10 mol%,), Zn powder (3.0 eq), and 100 mL of dry DMF (50 mL, 4 : 2 : 4). The mixture was degassed and injected with Ar (3 times). The fresh PPh_2Cl was injected into the tube. The mixture was reacted at 110 °C in Ar for 2−3 days. The cooling mixture was extracted successively with water and DCM solution. The organic layer was washed with brine about 3–4 times to remove DMF, dried with $MgSO_4$, and filtered. The organic solvent was removed by decompressing vaporization. The resulting residue was purified by column chromatography with PE : DCM (5 : 1 to 2 : 1), and then the white solid was obtained with 40% yield. ^{1}H NMR (400 MHz, $CDCl_3$) δ 8.00 – 7.92 (m, 6H), 7.89 (d, *J* = 1.4 Hz, 2H), 7.78 (dd, *J* = 8.5, 1.7 Hz, 2H), 7.57 (dd, *J* = 10.8, 4.5 Hz, 6H), 7.52 – 7.47 (m, 4H), 7.46 – 7.41 (m, 2H), 7.38 – 7.34 (m, 4H), 7.25 – 7.10 (m, 20H), 7.07 (dd, *J* = 8.6, 1.8 Hz, 2H), 7.03 – 6.96 (m, 6H). ^{31}P NMR (162 MHz, $CDCl_3$) δ -15.29 (s). ^{13}C NMR (101 MHz, $CDCl_3$) δ 141.25 (s), 140.17 (s), 139.41 (s), 137.61 (s), 136.16 (d, *J* = 5.4 Hz), 134.81 – 133.81 (m), 133.12 (s), 132.93 – 132.44 (m), 132.27 (s), 130.28 (s), 129.87 (s), 128.53 (d, *J* = 19.5 Hz), 128.30 – 127.89 (m), 127.42 (d, *J* = 9.0 Hz), 127.01 (s), 126.82 (s), 125.93 (d, *J* = 12.0 Hz), 125.49 (s), 123.44 (d, *J* = 9.5 Hz), 120.40 (s), 119.92 (s), 119.11 (s), 96.00 (s). HRMS found $[P1+H]^+$: 1105.3802 (cal. 1105.3835).

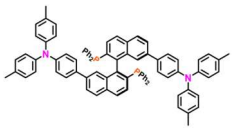

Synthesis of P2: Prepared by the aforementioned method from **P2-H-Me-OTf** with 38% yield. ^{1}H NMR (400 MHz, $CDCl_3$) δ 7.93 (dd, *J* = 8.5, 5.5 Hz, 4H), 7.67 (dd, *J* = 8.5, 1.6 Hz, 2H), 7.54 – 7.48 (m, 2H), 7.19 – 6.95 (m, 42H), 6.89 (d, *J* = 8.6 Hz, 4H), 2.33 (s, 12H). ^{31}P NMR (162 MHz, $CDCl_3$) δ -15.64 (s). ^{13}C NMR (101 MHz, $CDCl_3$) δ 147.39 (s), 145.94 (s), 145.51 (s), 145.21 (s), 138.44 (d, *J* = 12.1 Hz), 137.87 (d, *J* = 47.0 Hz), 137.50 (s), 135.98 (d, *J* = 7.3 Hz), 134.22 (d, *J* = 11.0 Hz), 134.07 – 132.39 (m), 132.36 – 129.63 (m), 129.86 (s), 129.86 (s), 128.47 (d, *J* = 16.8 Hz), 128.26 – 127.93 (m), 127.97 – 127.93 (m), 127.61 (d, *J* = 43.5 Hz), 127.97 – 124.37 (m), 122.52 (s), 77.35 (s), 77.04 (s), 76.72 (s), 20.82 (s). HRMS found $[P2+H]^+$: 1229.4514 (cal. 1229.4570).

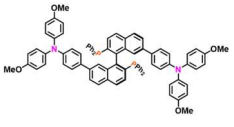

Synthesis of P3: Prepared by the aforementioned method from **P2-H-OMe-OTf** with 42% yield. ^{1}H NMR (400 MHz, $CDCl_3$) δ 7.92 – 7.85 (m, 4H), 7.63 (dd, *J* = 8.5, 1.4 Hz, 2H), 7.48 (d, *J* = 8.3 Hz, 2H), 7.04 (tt, *J* = 11.2, 8.1 Hz, 34H), 6.91 (d, *J* = 8.6 Hz, 4H), 6.84 – 6.74 (m, 14H), 3.79 (s, 12H). ^{31}P NMR (162 MHz, $CDCl_3$) δ -15.59 (s). ^{13}C NMR (101 MHz, $CDCl_3$) δ 155.80 (s), 147.89 (s), 145.50 (s), 140.90 (s), 138.20 (s), 137.61 (d, *J* = 13.6 Hz), 135.90 (d, *J* = 7.0 Hz), 134.16 (d, *J* = 21.6 Hz), 132.67 (t, *J* = 9.8 Hz), 132.19 (s), 130.36 (s), 128.81 – 127.95 (m), 127.76 (s), 127.38 (s), 127.08 – 126.30 (m), 125.98 (s), 124.56 (s), 120.62 (s), 114.67 (s), 77.35 (s), 77.03 (s), 76.72 (s), 55.50 (s). HRMS found $[P3+H]^+$: 1165.4713 (cal. 1165.4774).

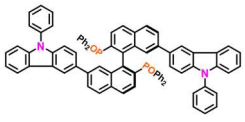

Synthesis of (*S*)-PO1: In a 25 mL round-bottomed flask was placed **(*S*)-P1** (0.1 g, 0.9 mmol) and 10 mL of DCM/EtOH (1 : 1). The mixtures were slowly injected with H_2O_2 (excess, ~10.0 eq). The mixture was reacted at 25 °C in air for 20 min. The reaction mixtures were extracted successively with water and DCM solution. The organic layer was washed with brine about 3-4 times to remove H_2O_2, dried with $MgSO_4$, and filtered. The organic solvent was removed by decompressing vaporization. The resulting residue was purified by column chromatography with DCM: EA (5 : 1 to 3 : 1), and then the white gray was obtained with an equivalent yield. ^{1}H NMR (400 MHz, $CDCl_3$)

δ 7.86 (dd, *J* = 13.9, 5.2 Hz, 6H), 7.75 (dd, *J* = 8.5, 1.4 Hz, 2H), 7.73 – 7.63 (m, 6H), 7.53 – 7.34 (m, 16H), 7.29 (dd, *J* = 9.7, 3.6 Hz, 6H), 7.19 – 6.98 (m, 16H), 6.88 (dd, *J* = 8.6, 1.5 Hz, 2H). ^{31}P NMR (162 MHz, $CDCl_3$) δ 28.83 (s). ^{13}C NMR (101 MHz, $CDCl_3$) δ 143.42, 141.25, 140.19, 139.49, 137.56, 134.27, 134.15, 132.98, 132.82, 132.70, 132.59, 131.87, 131.78, 131.21, 129.88, 128.55, 128.15, 128.02, 127.91, 127.72, 127.49, 126.99, 126.03, 125.79, 125.03, 123.44, 123.32, 120.36, 119.92, 119.03, 109.84, 109.60, 77.34, 77.02, 76.71. HRMS found $[PO1+H]^+$: 1137.3682 (cal. 1137.3733). The **(*R*)-PO1** was prepared by the aforementioned method from **(*R*)-P1** with an equivalent yield. The NMR was the same as that of **(*S*)-**isomer.

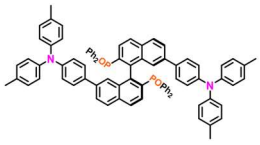

Synthesis of (*S*)-PO2: Prepared by the aforementioned method from **(*S*)-P2** with an equivalent yield. ^{1}H NMR (400 MHz, $CDCl_3$) δ 7.86 (t, *J* = 6.1 Hz, 4H), 7.74 – 7.62 (m, 6H), 7.44 (dd, *J* = 10.7, 8.0 Hz, 6H), 7.36 – 7.32 (m, 2H), 7.23 – 7.02 (m, 20H), 6.94 (d, *J* = 8.3 Hz, 8H), 6.86 – 6.77 (m, 8H), 2.30 (s, 12H). ^{31}P NMR (162 MHz, $CDCl_3$) δ 28.58 (s). ^{13}C NMR (101 MHz, $CDCl_3$) δ 147.43, 145.15, 138.14, 134.15, 133.36, 132.95, 132.60, 132.56, 132.50, 131.84, 131.75, 131.15, 131.12, 131.08, 131.06, 129.84, 128.45, 128.11, 127.98, 127.86, 127.75, 127.30, 127.27, 127.17, 126.60, 124.56, 124.15, 122.39, 119.12, 77.34, 77.02, 76.70, 29.71, 20.80. HRMS found $[PO2+H]^+$: 1261.4400 (cal. 1261.4468). The **(*R*)-PO2** was prepared by the aforementioned method from **(*R*)-P2** with an equivalent yield. The NMR was the same as that of **(*S*)-**isomer.

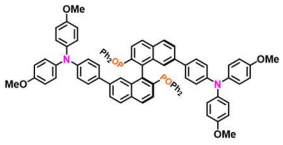

Synthesis of (*Rac*)-PO3: Prepared by the afore-mentioned method from **(*Rac*)-P3** with an equivalent yield. ^{1}H NMR (400 MHz, $CDCl_3$) δ 7.77 (t, *J* = 6.0 Hz, 4H), 7.71 – 7.52 (m, 6H), 7.36 (dt, *J* = 11.5, 8.3 Hz, 6H), 7.25 (d, *J* = 7.0 Hz, 2H), 7.17 – 7.08 (m, 6H), 7.02 (t, *J* = 6.2 Hz, 4H), 6.98 – 6.85 (m, 10H), 6.78 – 6.61 (m, 16H), 3.70 (s, 12H). *denote trace grease from PE or H_2O from $CDCl_3$. ^{31}P NMR (162 MHz, $CDCl_3$) δ 28.50. ^{13}C NMR (101 MHz, $CDCl_3$) δ 155.84, 147.95, 140.85, 138.26, 135.18, 134.07, 132.89, 132.60, 132.49, 132.36, 131.86, 131.77, 131.06, 129.57, 128.38, 128.08, 127.98, 127.86, 127.71, 127.11, 126.63, 126.45, 124.04, 120.49, 114.67, 77.36, 77.24, 77.04, 76.72, 55.51. HRMS found $[PO3+H]^+$: 1197.4599 (cal. 1197.4672)

C: Preparation procedures for emissive polymer and LC films

1) Firstly, the emitters (0.5 wt%) and PMMA/PVP/PMMA@PVP were placed in a clear glass bottle. DCM was added to the glass bottle to dissolve mixtures. After that, the DCM of mixtures was naturally volatilized to offer viscous solutions. The mixtures were drop-casted on glass plates (or pattern masking operation) to get polymer films after volatilization. The optical and chiroptical activities of transparent films were tested via PL, TRPL, ECD/CPL spectra, and digital camera.
2) Firstly, the emitters (0.2 wt%) and 5CB (50 mg) were placed in a clear glass bottle. DCM (0.2 mL) was added to the glass bottle to dissolve mixtures. After that, the DCM of mixtures was naturally volatilized to offer mixed LCs melt. The flowing LCs were drop-casted on the glass plate and then covered with another glass plate. The optical activities of glass films were tested via ECD/CPL spectra, POM, and digital camera.
3) First, the mixtures of RM257 (host, 98.5 wt%), chiral phosphor **PO1** (1.0 wt%), and photo-initiator Irg651 (0.5 wt%) were dissolved in DCM and then stirred and sonicated for 2 min. Second, 3 drops of the solution were dropped onto a glass plate (2.0 × 2.0 cm), and DCM was allowed to evaporate naturally at room temperature. The doped RM257 film was placed on a hot stage at 145 ºC for 5 minutes, after which the temperature was gradually lowered to 100 ºC and maintained for 10 minutes. Subsequently, a UV lamp (λ_{em} =365 nm) with a power of 15 W was employed to uniformly irradiate the film of LC films (100 ºC) for 5 minutes. The mobility of chiral LC films was lost because of cross-linking. Finally, the films (**PLC@PO1**) were cooled to room temperature.

D: DFT calculation methods

(1) Computational methods for molecular orbitals and excited states transition: For all structures presented in this article, calculations of grid data, and hole-electron analysis were acquired by Multiwfn version 3.8 (dev) software.[4] Isosurface maps were rendered by VMD 1.9.3 software.[5]

(2) The initial structures of the molecule were extracted from single crystals by the Mercury 2021.3.0 software. For the structurally optimized task, DFT/TD-DFT optimized structures were simulated at Gaussian 16 A.03 software in the gas phase at 298.15 K.[6] B3LYP exchange-correlation function and 6-31G(d) basis were set for all elements.[4-9] Vibrational frequencies were computed to ensure that the optimized geometries correspond to the true minima of the potential energy surfaces. The MOs isosurface value was set at 0.02. The single-point energy and TD-DFT tasks were performed at a B3LYP/6-31G(d) level, respectively. SOC coefficient (ξ_{soc}) for all conditions was calculated from ORCA 5.0 software via the spin-orbit mean-field (SOMF(1X)) method at the B3LYP/6-31G(d) level.[10]

(3) In order to facilitate the measurement and discussion of electronic excitation characteristics through some quantitative values, we illustrates the S_r, D_{index}, and t_{index} indices according to Lu's work.[4] The S_r is a function of overlap between hole distributions (more theoretical details could be found in handbook of Multiwfn[11]; http://sobereva.com/multiwfn/):

$$1).S_r\ index = \int S_r(r)d(r) = \int \sqrt{\rho^{hole}(r)\rho^{ele}(r)}\ d_{(r)}$$

The larger S_r suggests the higher the degree of overlap between hole and electron, vice versa. This value have limit ranges of [0 to1], where 1 means the holes and electrons are perfectly aligned (indicating a short-range local transition of charge), and 0 means there is no overlap at all (indicating a long-range ICT transition of electrons).

$$2).\ D_x = |X_{ele}| - |X_{hol}\ |;\ D_y = |Y_{ele}| - |Y_{hol}\ |;\ D_z = |Z_{ele}| - |Z_{hole}|$$

$$3).\ D_{index} = \sqrt{D_x^2 + D_y^2 + D_z^2}$$

$X/Y/Z$ is the $x/y/z$ coordinates of the center of mass of the hole/electron. The larger D_{index} suggests higher electron-hole separation distance.

$$4).\ t_{index} = D_{index} - H_{CT} = D_{index} - |\boldsymbol{H} \cdot \boldsymbol{u}_{CT}|$$

$$5).\ H_\alpha = \frac{\sigma_{ele,a} + \sigma_{hol\ ,a}}{2};\alpha = \{x, y, z\}$$

$\boldsymbol{H}$ is vector of H_x, H_y and H_z. $\boldsymbol{u}_{\mathrm{CT}}$ is the vector in the CT direction.

E: Additional Figures and Charts

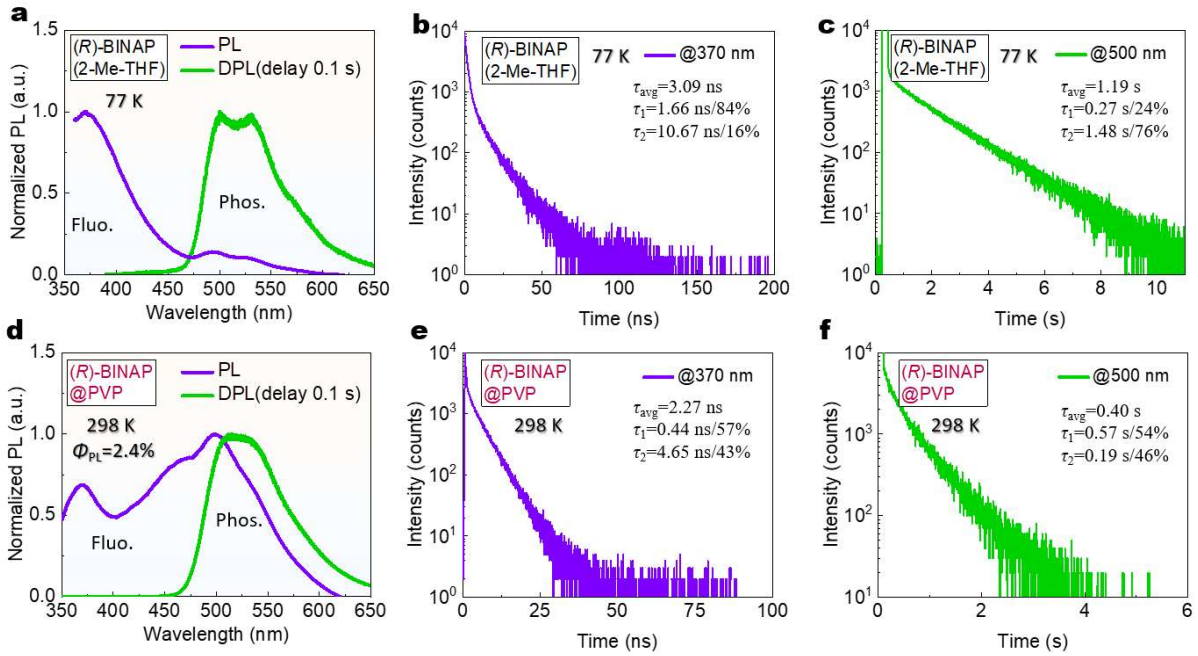

Figure S1. (a) PL and DPL spectra of (*R*)-BINAP in 2-Me-THF at 77 K (Ex at 320 nm). (b) Fluorescent lifetime of (*R*)-BINAP in 2-Me-THF at 77 K. (c) Phosphorescent lifetime of (*R*)-BINAP in 2-Me-THF at 77 K. (d) PL and DPL spectra of (*R*)-BINAP@PVP (0.5 wt%) at 298 K (Ex at 320 nm). (e) Fluorescent lifetime of (*R*)-BINAP@PVP at 298 K. (f) Phosphorescent lifetime of (*R*)-BINAP@PVP at 298 K.

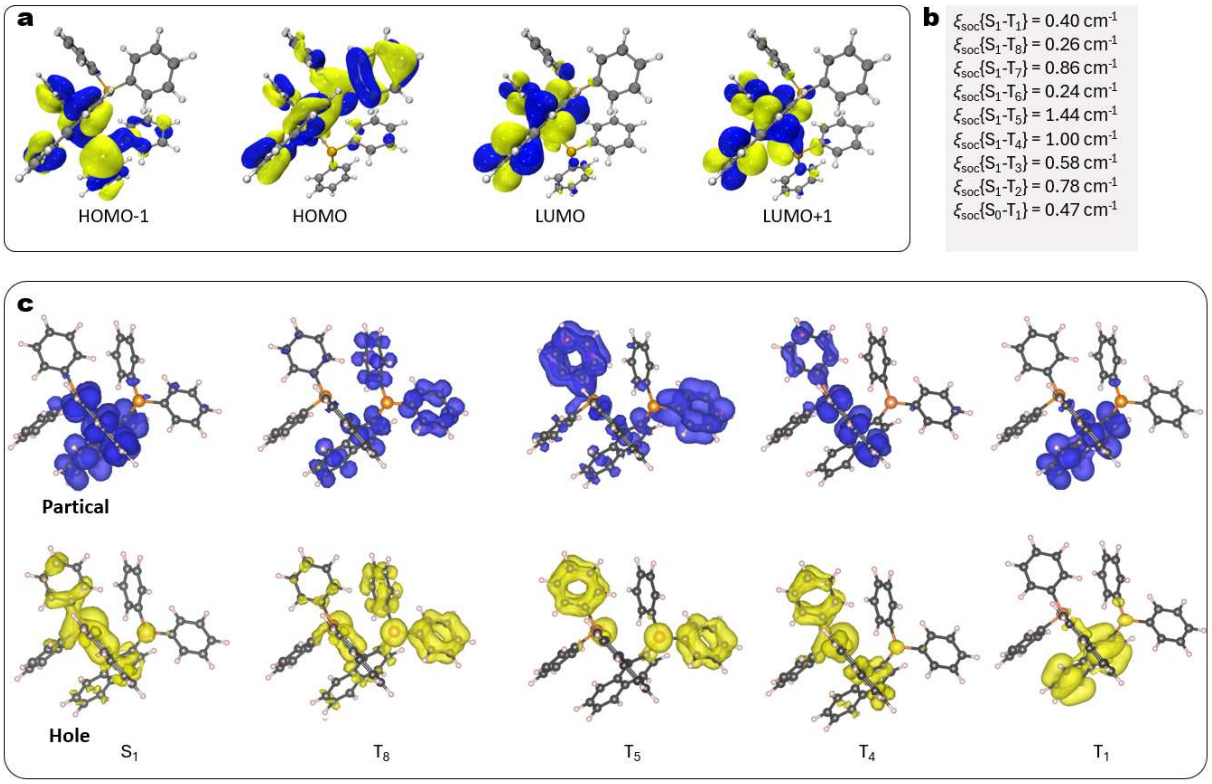

Figure S2. (a) HOMOs and LUMOs of BINAP at the ground state. (b) SOC coefficients (ξ_{soc}) of BINAP. (c) Electron (yellow)-hole (blue) distribution analysis of $S_0 \rightarrow S_1$ and $S_0 \rightarrow T_n$ transitions for BINAP at the S_1 geometry.

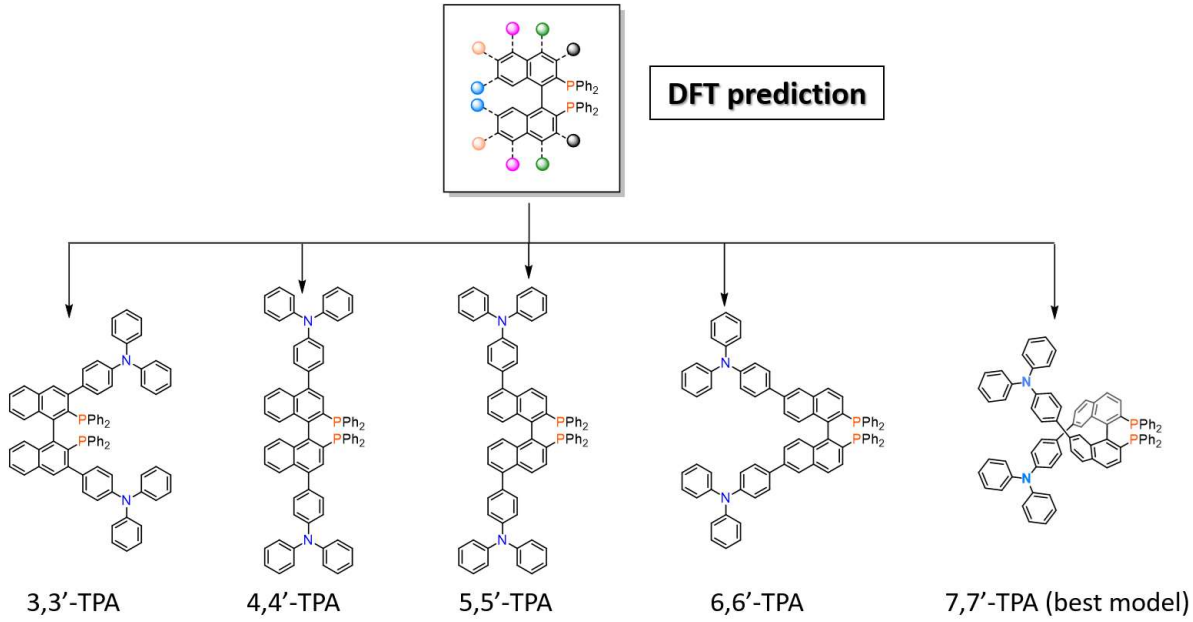

Name	θ (°)	μ_e (esu cm)	μ_m (erg/Gauss)	g_{abs}
3,3'-TPA	~90.0	7.5×10^{-19}	3.1×10^{-5}	0
4,4'-TPA	93.2	6.9×10^{-18}	7.2×10^{-21}	2.3×10^{-4}
5,5'-TPA	68.8	6.2×10^{-18}	4.9×10^{-21}	1.2×10^{-3}
6,6'-TPA	27.5	4.8×10^{-18}	6.8×10^{-21}	5.0×10^{-3}
7,7'-TPA	162.1	4.8×10^{-18}	1.5×10^{-20}	1.1×10^{-2}
$S_0 \rightarrow S_1$; $g = 4\|\mu_e\| \times \|\mu_m\| \times \cos\theta / \|\mu_e\|^2 + \|\mu_m\|^2$; Calculated at B3LYP/6-31G(d) level by TD-DFT				

Figure S3. TD-DFT predicted electric (μ_e), magnetic (μ_m) transition dipole moments, angles, and g_{abs} values at the B3LYP/6-31G(d) level for $S_0 \rightarrow S_1$.

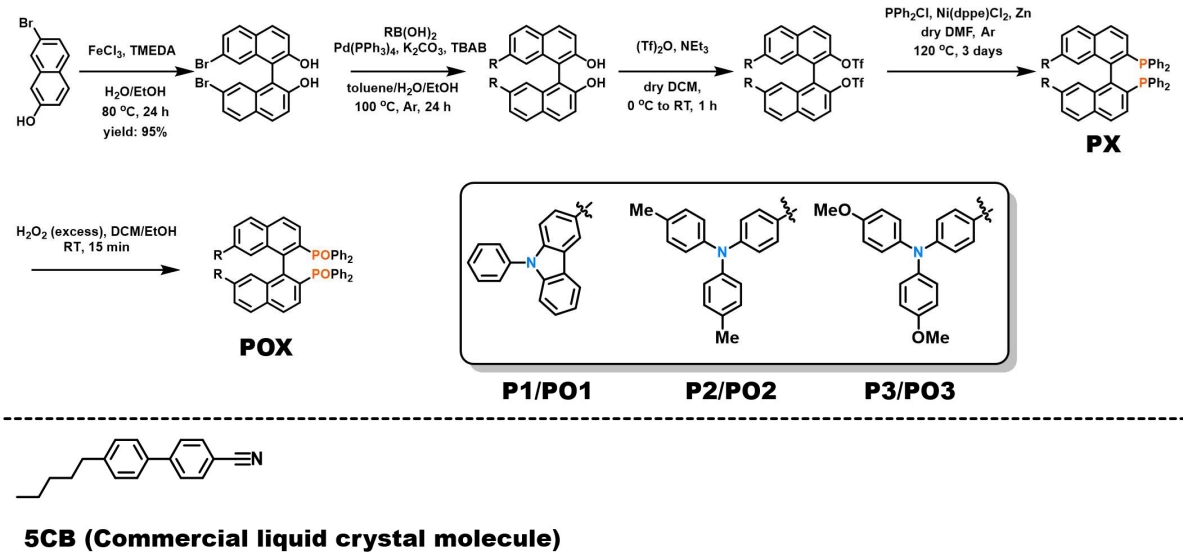

Figure S4. Synthetic route of target emitters and their corresponding precursors.

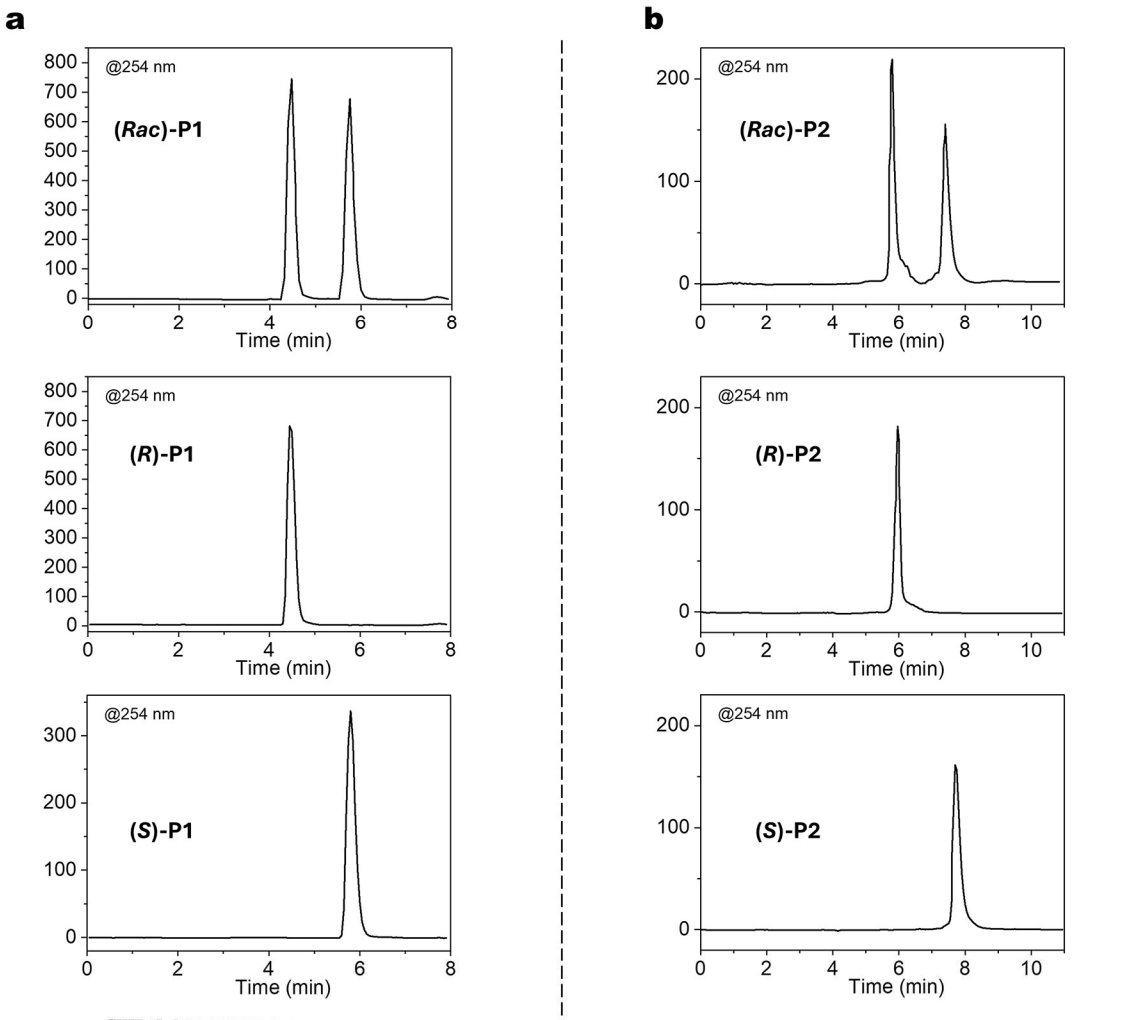

CHIRAL CHROMATOGRAPHY REPORT

Column	: CHIRALPAK IE(IE00CE-SB022)	
Column size	: 0.46 cm I.D. × 25 cm L	
Injection	: 10 ul	
Mobile phase	: Hexane/DCM=60/40(V/V)	
Flow rate	: 1 ml/min	
Wave length	: UV 254 nm	
Temperature	: 35 ℃	
HPLC equipment	: Shimadzu LC-20AD	CP-HPLC-05
Sample name	: Raw Material	

CHIRAL CHROMATOGRAPHY REPORT

Column	: CHIRALPAK IB N-5(IBN50CE-XA057)	
Column size	: 0.46 cm I.D. × 25 cm L	
Injection	: 10 ul	
Mobile phase	: Hexane/DCM=90/10(V/V)	
Flow rate	: 1.0 ml/min	
Wave length	: UV 254 nm	
Temperature	: 35 ℃	
HPLC equipment	: Shimadzu LC-20AT	CP-HPLC-06
Sample name	: Raw Material	

Figure S5. (a) Chiral HPLC data and experimental conditions of racemic **P1** and its enantiomers. (b) Chiral HPLC data and experimental conditions of racemic **P2** and its enantiomers. Based on the TD-DFT calculated ECD and experimental ECD signals, the first elution is (*R*)-isomer, and second elution is (*S*)-isomer.

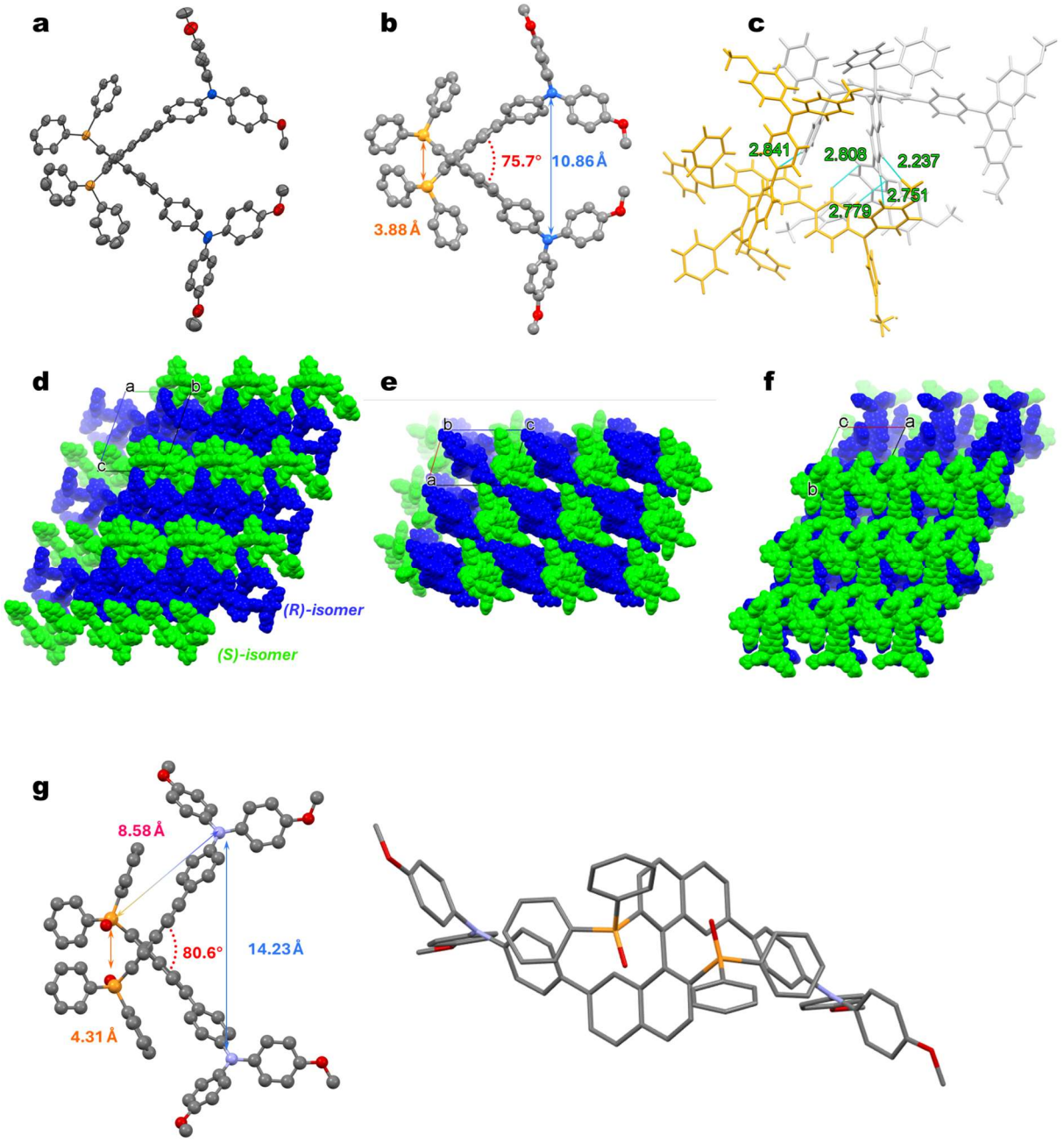

Figure S6. (a) ORTEP drawing of (*R*)-isomer in **(*Rac*)-P3** crystals (at 30% ellipsoid probability; CCDC number 2344550). (b−c) Structure and hydrogen bonding analysis for **(*Rac*)-P3**. (d−f) Crystal packing of **(*Rac*)-P3**. (g) DFT optimized structure of **(*R*)-PO3** at the ground state.

Table S1. Crystallographic data and structure refinement parameters	
Name	**(*Rac*)-P3**
CCDC	2344550
Empirical formula	$C_{84}H_{66}N_2O_4P_2$
Temperature/K	193(2)
Formula weight	1129.32
Crystal system	Triclinic
Space group	$P\bar{1}$
a/Å	17.3151(8)
b/Å	19.7760(9)
c/Å	24.0152(10)
α/°	104.281(2)
β/°	99.666(2)
γ/°	110.711(2)
Volume/Å^3	7152.9(6)
Z	2
ρ_{calc}(g/cm^3)	1.142
μ/mm^{-1}	0.612
F(000)	2584.0
Radiation (Å)	GaKα (λ = 1.34139)
Index ranges	$-20 \le h \le 20$, $-23 \le k \le 23$, $-26 \le l \le 28$
Reflections collected	93757 ($3.442° \le 2\theta \le 108.312°$)
Independent reflections	26167 [R_{int}= 0.0618, R_{sigma}= 0.0744]
Goodness-of-fit on F^2	1.020
Final R indexes [all data]	R_1 = 0.1840, wR_2 = 0.2830
Final R indexes [I>=2σ (I)]	R_1 = 0.1083, wR_2 = 0.2529
Largest diff. peak/hole / e Å^{-3}	0.94 / -0.75

Table S2. Bond lengths for two isomer units in **(*Rac*)-P3**					
Atoms	Atoms	Length (Å)	Atoms	Atoms	Length (Å)
C1	C2	1.385(5)	C85	C86	1.390(6)
C1	C10	1.415(6)	C85	C94	1.427(7)
C1	P1	1.825(5)	C85	P3	1.832(5)
C2	C3	1.422(6)	C86	C87	1.426(6)
C2	C11	1.509(6)	C86	C95	1.524(6)
C3	C4	1.417(5)	C87	C88	1.411(6)
C3	C8	1.426(6)	C87	C92	1.434(7)
C4	C5	1.373(6)	C88	C89	1.391(7)
C5	C6	1.410(6)	C89	C90	1.410(7)
C5	C21	1.497(6)	C89	C105	1.487(8)
C6	C7	1.354(6)	C90	C91	1.348(7)
C7	C8	1.401(6)	C91	C92	1.412(7)
C8	C9	1.405(6)	C92	C93	1.401(7)
C9	C10	1.346(6)	C93	C94	1.355(7)
C11	C12	1.353(6)	C95	C96	1.375(7)
C11	C20	1.435(6)	C95	C104	1.425(7)
C12	C13	1.433(6)	C96	C97	1.433(7)
C12	P2	1.846(5)	C96	P4	1.812(6)
C13	C14	1.362(7)	C97	C98	1.330(8)
C14	C15	1.394(7)	C98	C99	1.398(8)
C15	C16	1.408(6)	C99	C100	1.405(8)
C15	C20	1.424(6)	C99	C104	1.446(7)
C16	C17	1.340(7)	C100	C101	1.350(8)
C17	C18	1.440(6)	C101	C102	1.429(7)
C18	C19	1.381(6)	C102	C103	1.377(7)
C18	C41	1.455(6)	C102	C125	1.463(7)
C19	C20	1.398(6)	C103	C104	1.391(7)
C21	C22	1.385(7)	C105	C106	1.380(8)
C21	C26	1.385(7)	C105	C110	1.386(9)
C22	C23	1.377(6)	C106	C107	1.392(9)
C23	C24	1.393(8)	C107	C108	1.373(10)
C24	C25	1.386(8)	C108	C109	1.374(9)
C24	N1	1.420(6)	C108	N3	1.435(8)
C25	C26	1.383(6)	C109	C110	1.404(8)
C27	C28	1.363(10)	C111	C116	1.353(11)
C27	C32	1.428(9)	C111	N3	1.373(10)
C27	N1	1.442(9)	C111	C112	1.461(7)
C28	C29	1.380(10)	C112	C113	1.323(10)
C29	C30	1.374(10)	C113	C114	1.366(8)
C30	O1	1.346(12)	C114	C115	1.378(11)
C30	C31	1.390(14)	C114	O5	1.425(10)
C31	C32	1.341(14)	C115	C116	1.422(11)
C33	O1	1.282(14)	C117	O5	1.502(12)

C34	C39	1.369(13)	C118	C119	1.365(9)
C34	C35	1.370(11)	C118	C123	1.384(9)
C34	N1	1.381(10)	C118	N3	1.453(9)
C35	C36	1.507(13)	C119	C120	1.370(10)
C36	C37	1.420(14)	C120	C121	1.381(10)
C37	C38	1.180(12)	C121	C122	1.348(9)
C37	O2	1.522(8)	C121	O6	1.378(9)
C37	O2'	1.556(9)	C122	C123	1.383(10)
C38	C39	1.404(12)	C124	O6	1.431(9)
C40	O2	1.56(2)	C125	C126	1.401(7)
C41	C46	1.398(6)	C125	C130	1.404(7)
C41	C42	1.398(6)	C126	C127	1.357(8)
C42	C43	1.366(7)	C127	C128	1.381(8)
C43	C44	1.391(7)	C128	C129	1.380(7)
C44	N2	1.376(7)	C128	N4	1.409(8)
C44	C45	1.421(7)	C129	C130	1.360(7)
C45	C46	1.361(7)	C131	C136	1.361(9)
C47	C52	1.361(8)	C131	C132	1.363(8)
C47	C48	1.378(8)	C131	N4	1.423(8)
C47	N2	1.435(7)	C132	C133	1.372(8)
C48	C49	1.384(9)	C133	C134	1.342(8)
C49	C50	1.349(10)	C134	O7	1.368(8)
C50	C51	1.378(9)	C134	C135	1.382(10)
C50	O3	1.391(8)	C135	C136	1.372(11)
C51	C52	1.372(9)	C137	O7	1.411(8)
C53	O3	1.461(10)	C138	C143	1.374(8)
C54	C55	1.371(9)	C138	C139	1.377(9)
C54	C59	1.371(9)	C138	N4	1.435(8)
C54	N2	1.421(7)	C139	C140	1.396(10)
C55	C56	1.444(10)	C140	C141	1.350(10)
C56	C57	1.391(11)	C141	C142	1.352(9)
C57	C58	1.341(12)	C141	O8	1.422(8)
C57	O4	1.450(10)	C142	C143	1.362(8)
C58	C59	1.359(9)	C144	O8	1.494(10)
C60	O4	1.210(15)	C145	C146	1.391(7)
C61	C62	1.373(7)	C145	C150	1.392(7)
C61	C66	1.411(8)	C145	P3	1.824(6)
C61	P1	1.805(6)	C146	C147	1.376(8)
C62	C63	1.410(8)	C147	C148	1.389(7)
C63	C64	1.390(9)	C148	C149	1.360(7)
C64	C65	1.387(10)	C149	C150	1.355(8)
C65	C66	1.351(9)	C151	C152	1.356(8)
C67	C72	1.371(8)	C151	C156	1.384(8)
C67	C68	1.391(8)	C151	P3	1.839(5)
C67	P1	1.855(5)	C152	C153	1.415(8)

C68	C69	1.410(9)	C153	C154	1.363(9)
C69	C70	1.371(11)	C154	C155	1.361(10)
C70	C71	1.332(11)	C155	C156	1.387(9)
C71	C72	1.384(9)	C157	C162	1.370(10)
C73	C78	1.363(9)	C157	C158	1.395(9)
C73	C74	1.367(9)	C157	P4	1.816(8)
C73	P2	1.829(7)	C158	C159	1.362(10)
C74	C75	1.362(12)	C159	C160	1.370(12)
C75	C76	1.326(12)	C160	C161	1.394(12)
C76	C77	1.375(12)	C161	C162	1.366(11)
C77	C78	1.404(10)	C163	C168	1.380(10)
C79	C84	1.383(8)	C163	C164	1.387(10)
C79	C80	1.389(9)	C163	P4	1.827(8)
C79	P2	1.805(7)	C164	C165	1.379(12)
C80	C81	1.404(11)	C165	C166	1.313(16)
C81	C82	1.371(12)	C166	C167	1.383(16)
C82	C83	1.348(10)	C167	C168	1.421(12)
C83	C84	1.377(9)	C40'	O2'	1.43(2)

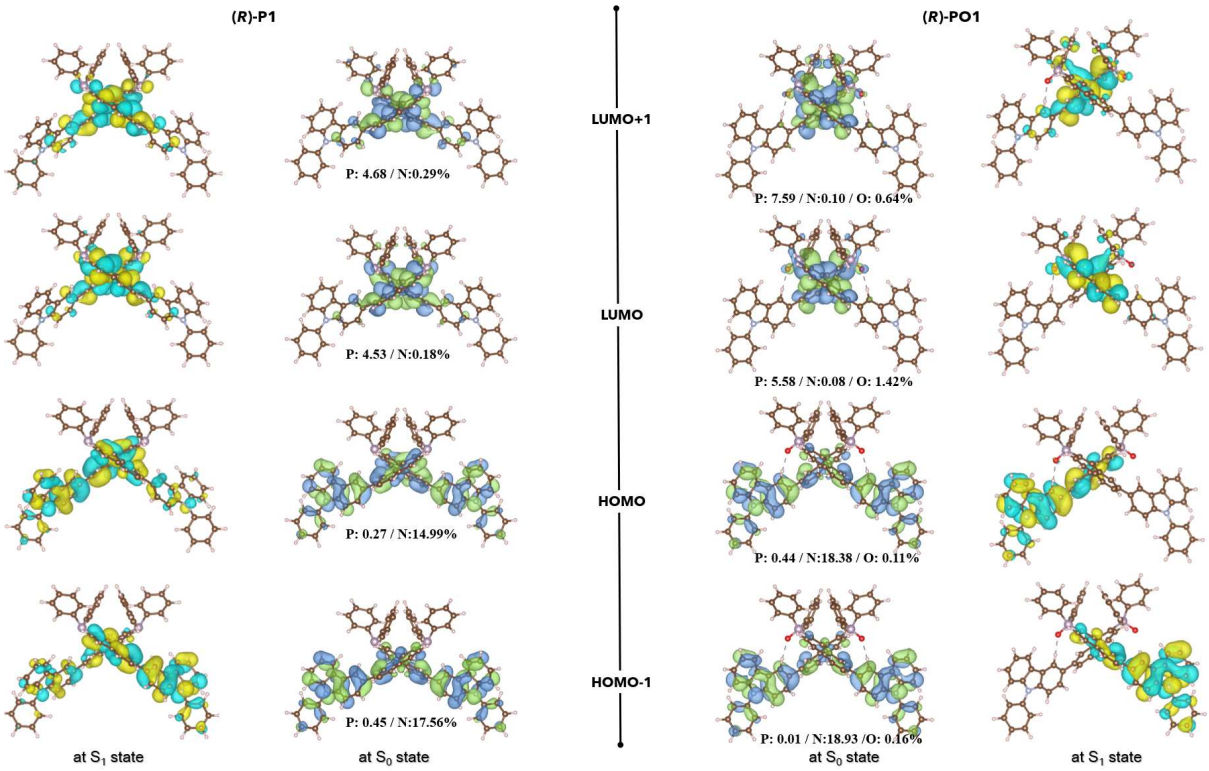

Figure S7. Calculated spatial distributions of the HOMOs and LUMOs of **(*R*)-P1** and **(*R*)-PO1** (iso = 0.02).

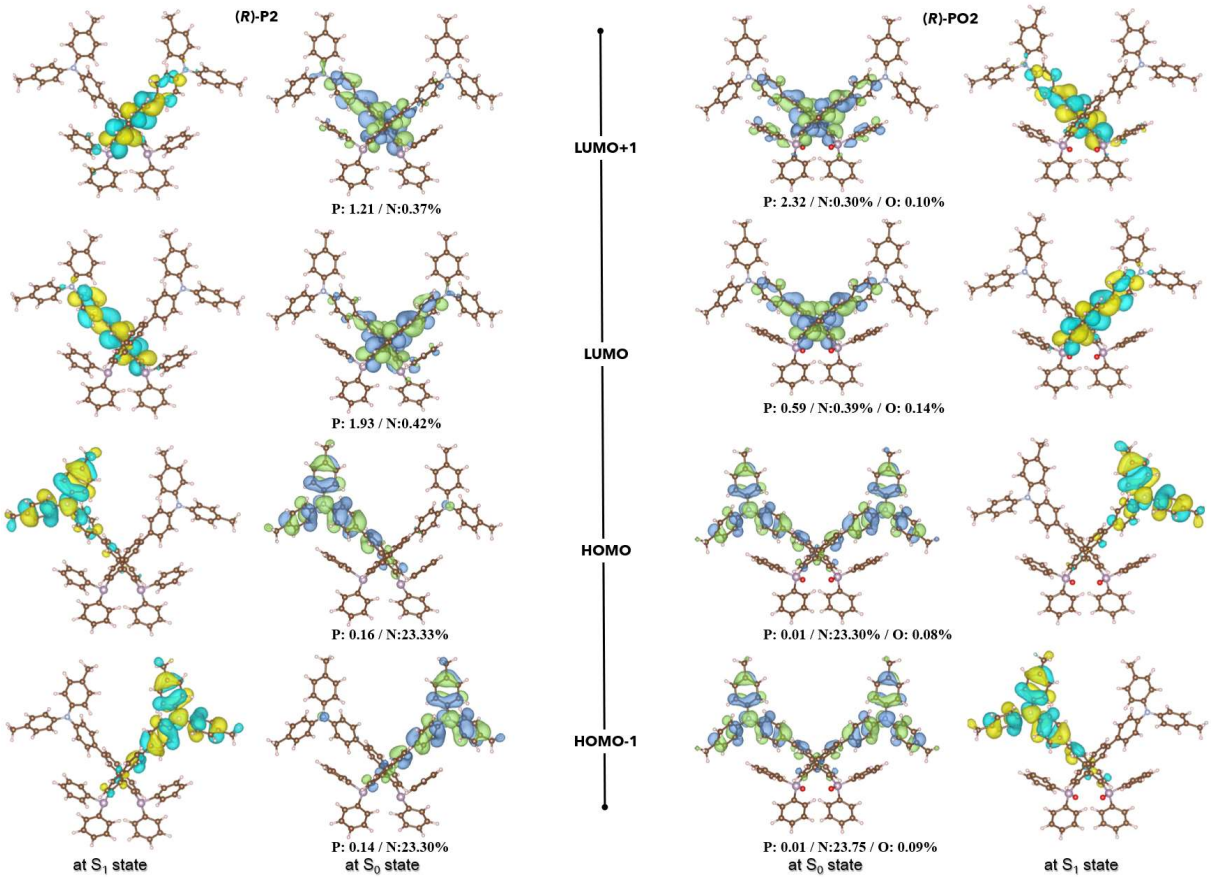

Figure S8. Calculated spatial distributions of the HOMOs and LUMOs of **(*R*)-P2** and **(*R*)-PO2** (iso = 0.02).

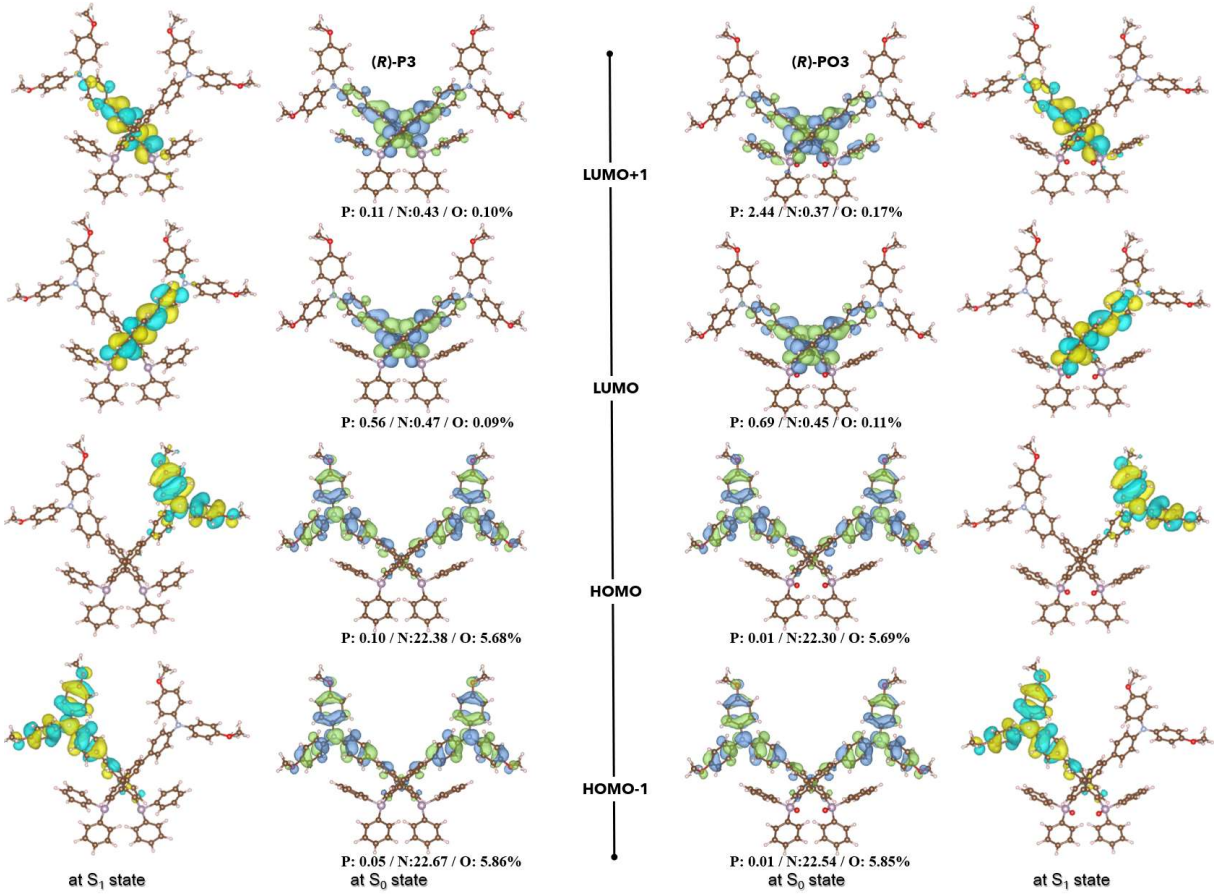

Figure S9. Calculated spatial distributions of the HOMOs and LUMOs of **(*R*)-P3** and **(*R*)-PO3** (iso = 0.02).

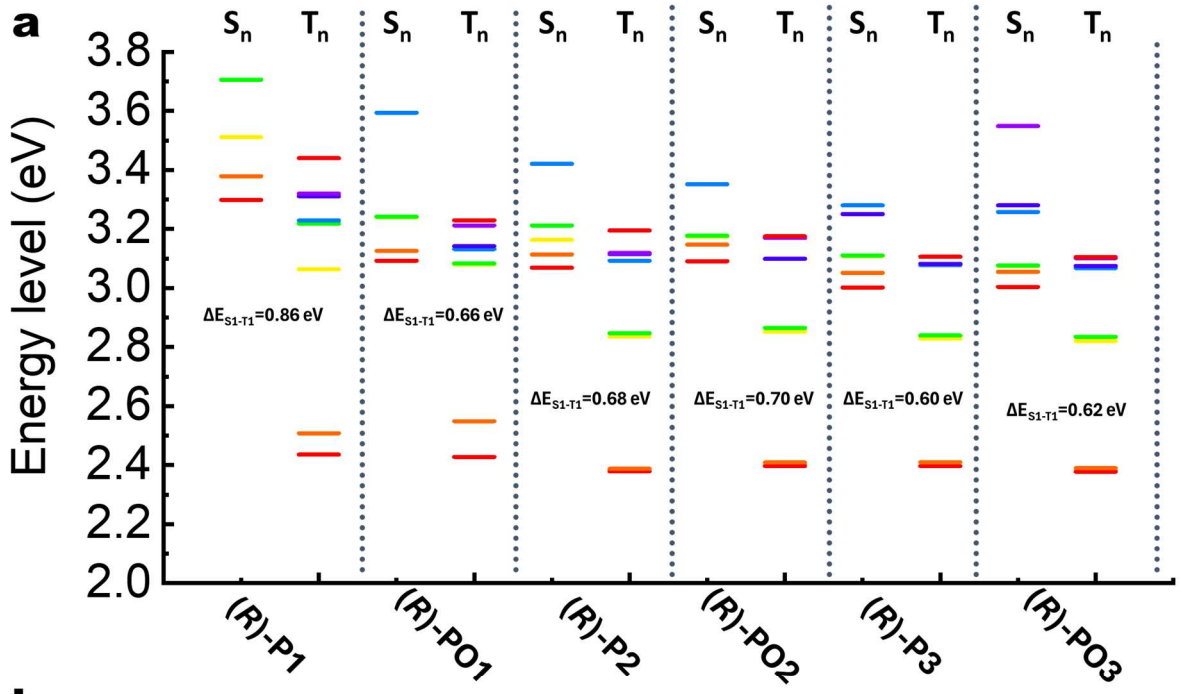

b

(*R*)-P1	(*R*)-PO1	(*R*)-P2
$\xi_{soc}\{S_1\text{-}T_1\}$ = 0.02 cm^{-1}	$\xi_{soc}\{S_1\text{-}T_1\}$ = 0.08 cm^{-1}	$\xi_{soc}\{S_1\text{-}T_1\}$ = 0.16 cm^{-1}
$\xi_{soc}\{S_1\text{-}T_2\}$ = 0.78 cm^{-1}	$\xi_{soc}\{S_1\text{-}T_2\}$ = 0.26 cm^{-1}	$\xi_{soc}\{S_1\text{-}T_2\}$ = 0.17 cm^{-1}
$\xi_{soc}\{S_1\text{-}T_3\}$ = 0.26 cm^{-1}	$\xi_{soc}\{S_1\text{-}T_3\}$ = 0.14 cm^{-1}	$\xi_{soc}\{S_1\text{-}T_3\}$ = 0.18 cm^{-1}
$\xi_{soc}\{S_1\text{-}T_4\}$ = 0.14 cm^{-1}	$\xi_{soc}\{S_1\text{-}T_4\}$ = 0.21 cm^{-1}	$\xi_{soc}\{S_1\text{-}T_4\}$ = 0.14 cm^{-1}
$\xi_{soc}\{S_1\text{-}T_5\}$ = 0.07 cm^{-1}	$\xi_{soc}\{S_1\text{-}T_5\}$ = 0.12 cm^{-1}	$\xi_{soc}\{S_1\text{-}T_5\}$ = 0.30 cm^{-1}
$\xi_{soc}\{S_1\text{-}T_6\}$ = 0.12 cm^{-1}	$\xi_{soc}\{S_1\text{-}T_6\}$ = 0.05 cm^{-1}	$\xi_{soc}\{S_1\text{-}T_6\}$ = 0.32 cm^{-1}
$\xi_{soc}\{S_0\text{-}T_1\}$ = 4.82 cm^{-1}	$\xi_{soc}\{S_0\text{-}T_1\}$ = 0.71 cm^{-1}	$\xi_{soc}\{S_0\text{-}T_1\}$ = 1.59 cm^{-1}

(*R*)-PO2	(*R*)-P3	(*R*)-PO3
$\xi_{soc}\{S_1\text{-}T_1\}$ = 0.12 cm^{-1}	$\xi_{soc}\{S_1\text{-}T_1\}$ = 0.15 cm^{-1}	$\xi_{soc}\{S_1\text{-}T_1\}$ = 0.12 cm^{-1}
$\xi_{soc}\{S_1\text{-}T_2\}$ = 0.15 cm^{-1}	$\xi_{soc}\{S_1\text{-}T_2\}$ = 0.21 cm^{-1}	$\xi_{soc}\{S_1\text{-}T_2\}$ = 0.13 cm^{-1}
$\xi_{soc}\{S_1\text{-}T_3\}$ = 0.06 cm^{-1}	$\xi_{soc}\{S_1\text{-}T_3\}$ = 0.07 cm^{-1}	$\xi_{soc}\{S_1\text{-}T_3\}$ = 0.03 cm^{-1}
$\xi_{soc}\{S_1\text{-}T_4\}$ = 0.24 cm^{-1}	$\xi_{soc}\{S_1\text{-}T_4\}$ = 0.19 cm^{-1}	$\xi_{soc}\{S_1\text{-}T_4\}$ = 0.23 cm^{-1}
$\xi_{soc}\{S_1\text{-}T_5\}$ = 0.53 cm^{-1}	$\xi_{soc}\{S_1\text{-}T_5\}$ = 0.46 cm^{-1}	$\xi_{soc}\{S_1\text{-}T_5\}$ = 0.84 cm^{-1}
$\xi_{soc}\{S_1\text{-}T_6\}$ = 0.32 cm^{-1}	$\xi_{soc}\{S_1\text{-}T_6\}$ = 0.03 cm^{-1}	$\xi_{soc}\{S_1\text{-}T_6\}$ = 0.05 cm^{-1}
$\xi_{soc}\{S_0\text{-}T_1\}$ = 0.47 cm^{-1}	$\xi_{soc}\{S_0\text{-}T_1\}$ = 0.89 cm^{-1}	$\xi_{soc}\{S_0\text{-}T_1\}$ = 0.42 cm^{-1}

Figure S10. (a) TD-DFT calculated excitation energy diagrams and (b) SOC coefficients (ξ_{soc}) for six emitters at the S_0 geometry.

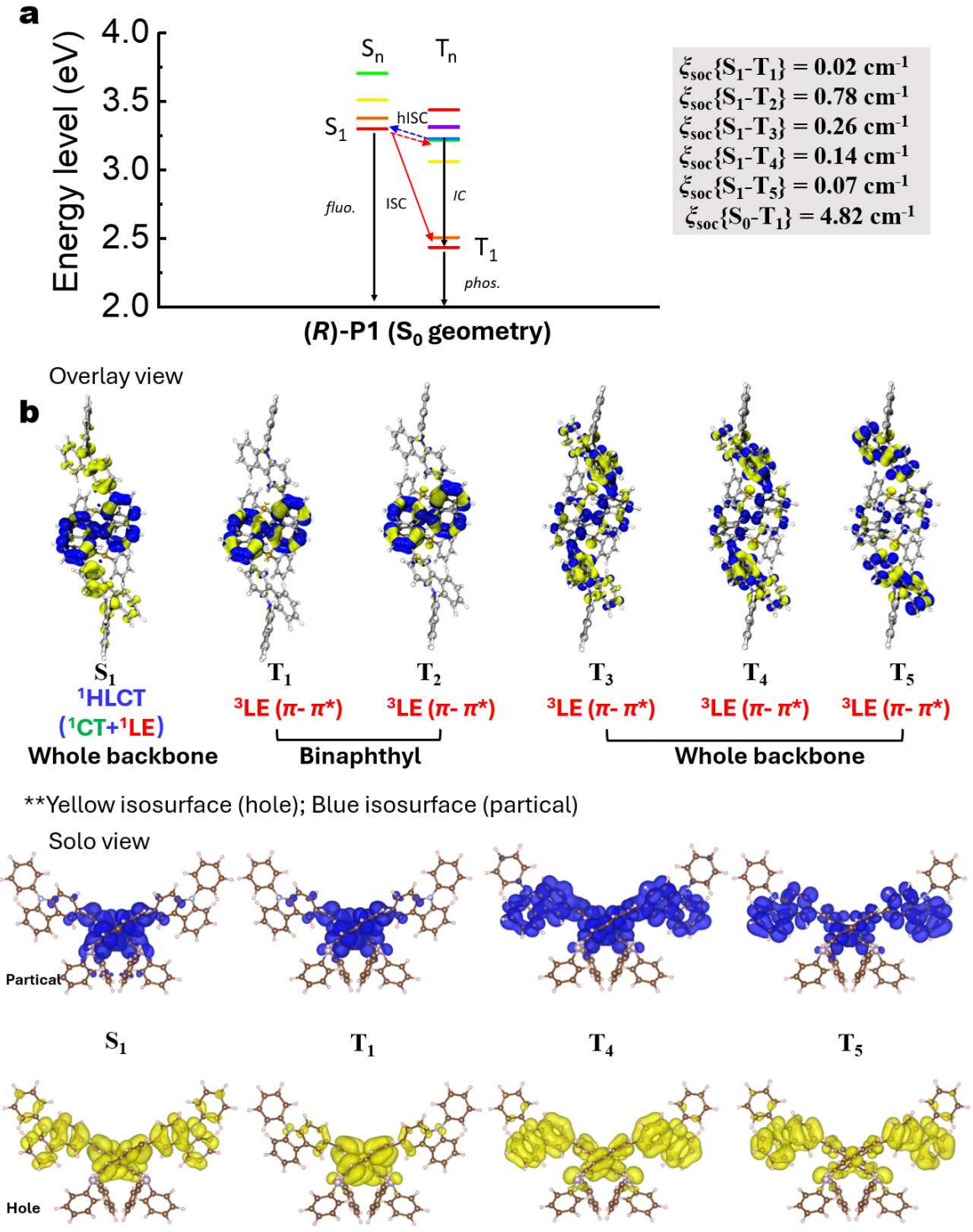

Figure S11. (a) TD-DFT calculated energy diagrams and SOC coefficients (ξ_{soc}) for **(*R*)-P1**. (b) Electron (yellow)-hole (blue) distribution analysis of $S_0 \rightarrow S_1$ and $S_0 \rightarrow T_n$ transitions for **(*R*)-P1** at the S_0 geometry (isovalue: 0.0003 a.u.).

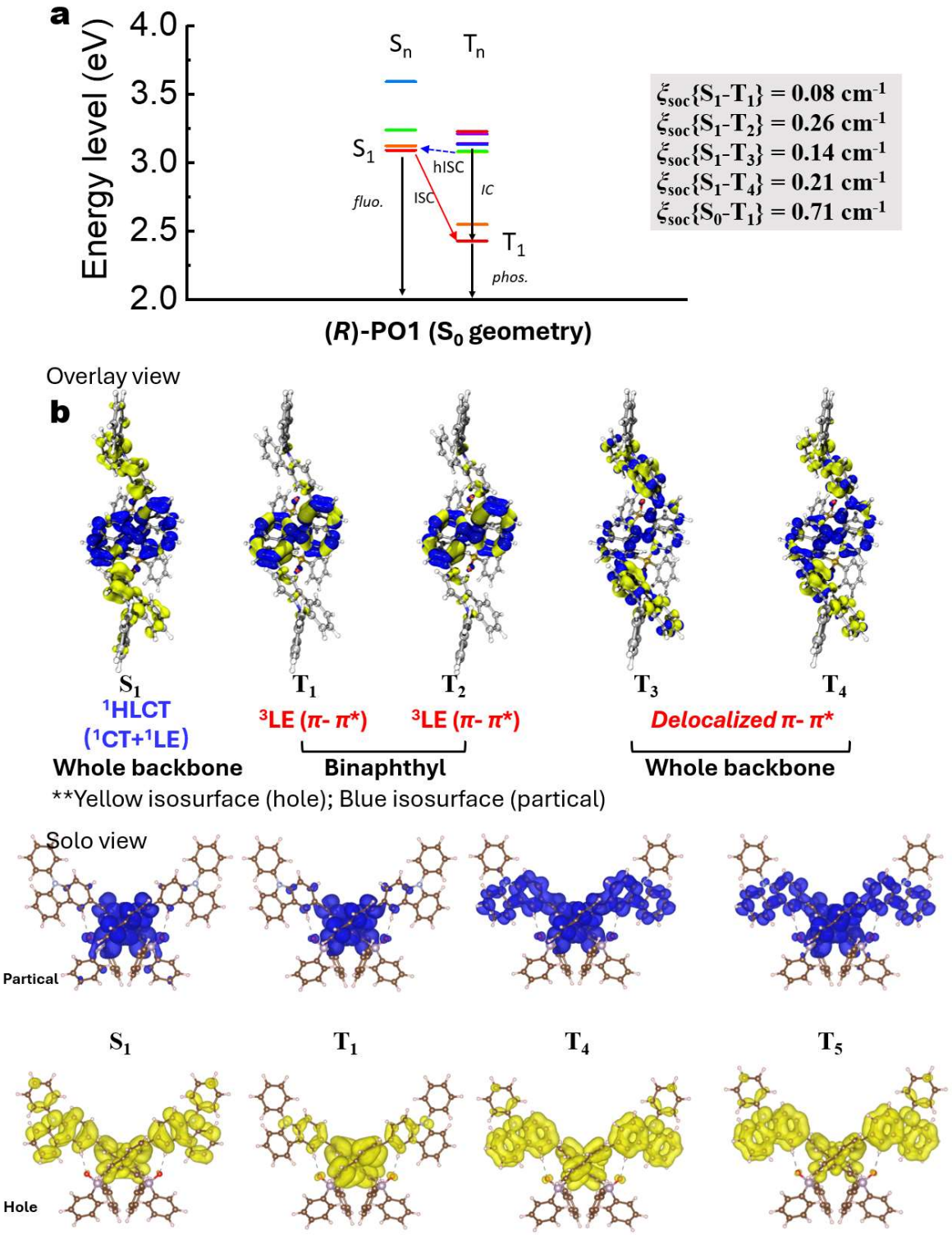

Figure S12. (a) TD-DFT calculated energy diagrams and SOC coefficients (ξ_{soc}) for **(*R*)-PO1**. (b) Electron (yellow)-hole (blue) distribution analysis of $S_0 \rightarrow S_1$ and $S_0 \rightarrow T_n$ transitions for **(*R*)-PO1** at the S_0 geometry (isovalue: 0.0003 a.u.).

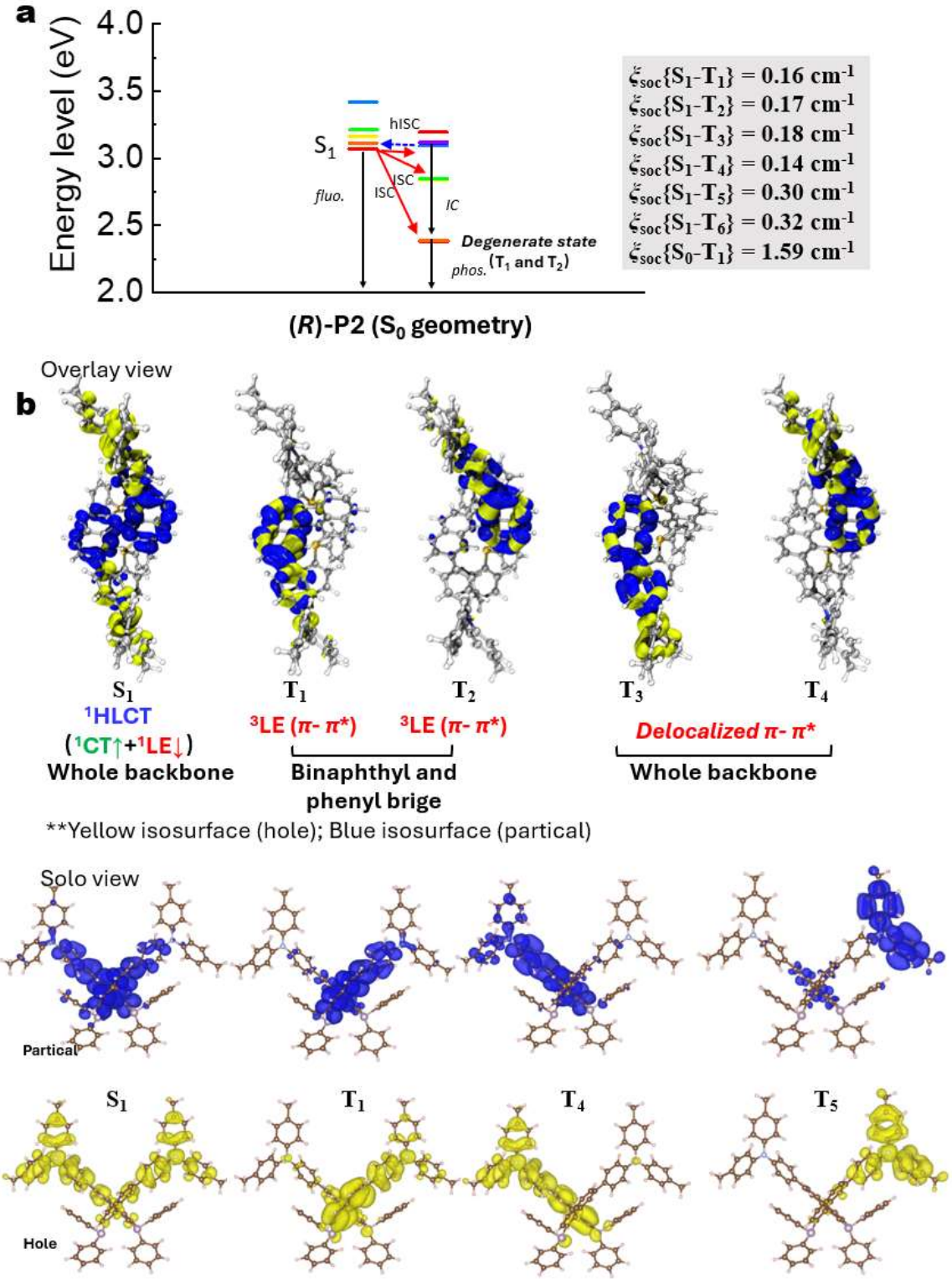

Figure S13. (a) TD-DFT calculated energy diagrams and SOC coefficients (ξ_{soc}) for **(*R*)-P2**. (b) Electron (yellow)-hole (blue) distribution analysis of $S_0 \rightarrow S_1$ and $S_0 \rightarrow T_n$ transitions for **(*R*)-P2** at the S_0 geometry (isovalue: 0.0003 a.u.).

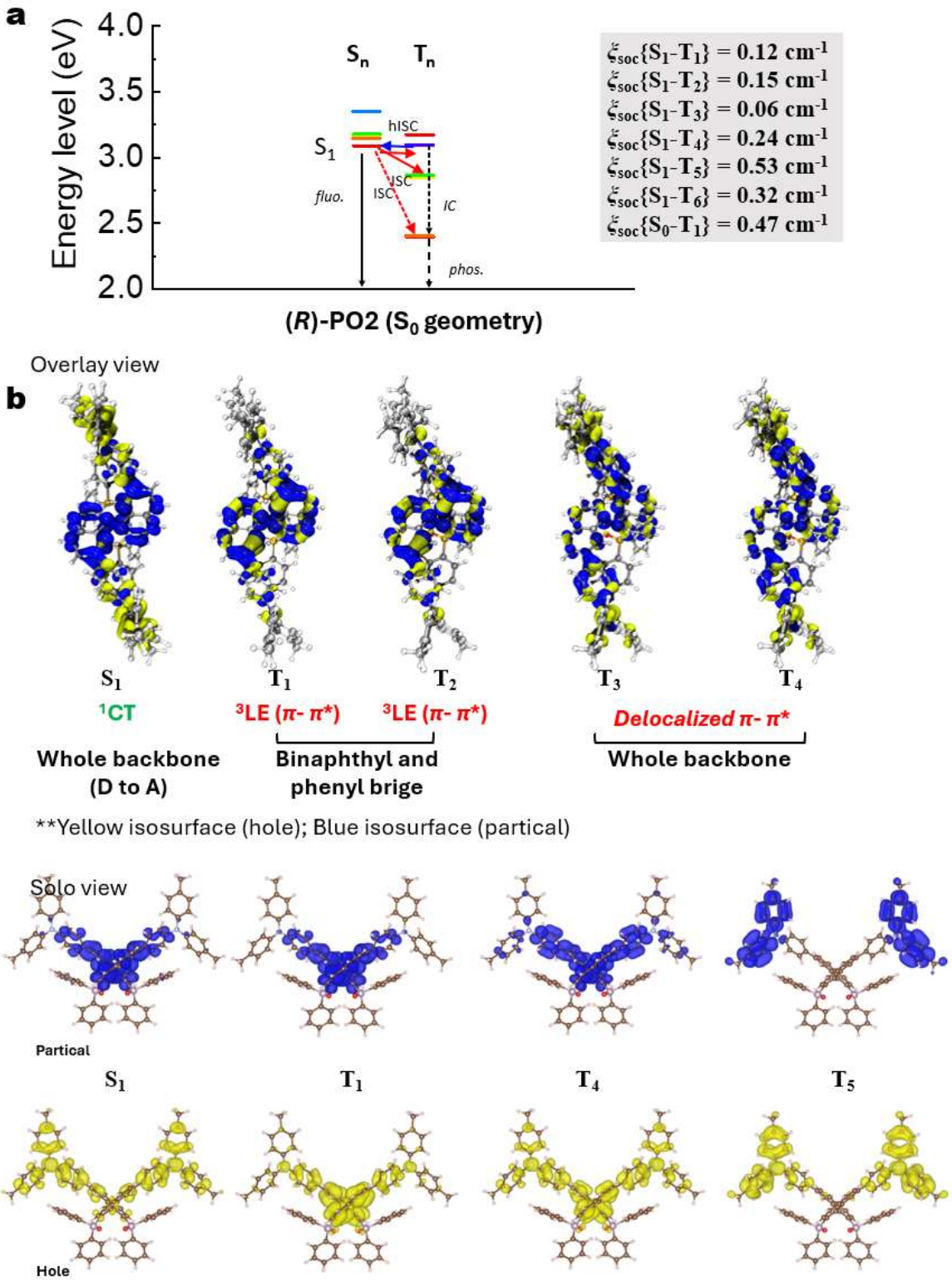

Figure S14. (a) TD-DFT calculated energy diagrams and SOC coefficients (ξ_{soc}) for **(*R*)-PO2**. (b) Electron (yellow)-hole (blue) distribution analysis of $S_0 \rightarrow S_1$ and $S_0 \rightarrow T_n$ transitions for **(*R*)-PO2** at the S_0 geometry (isovalue: 0.0003 a.u.).

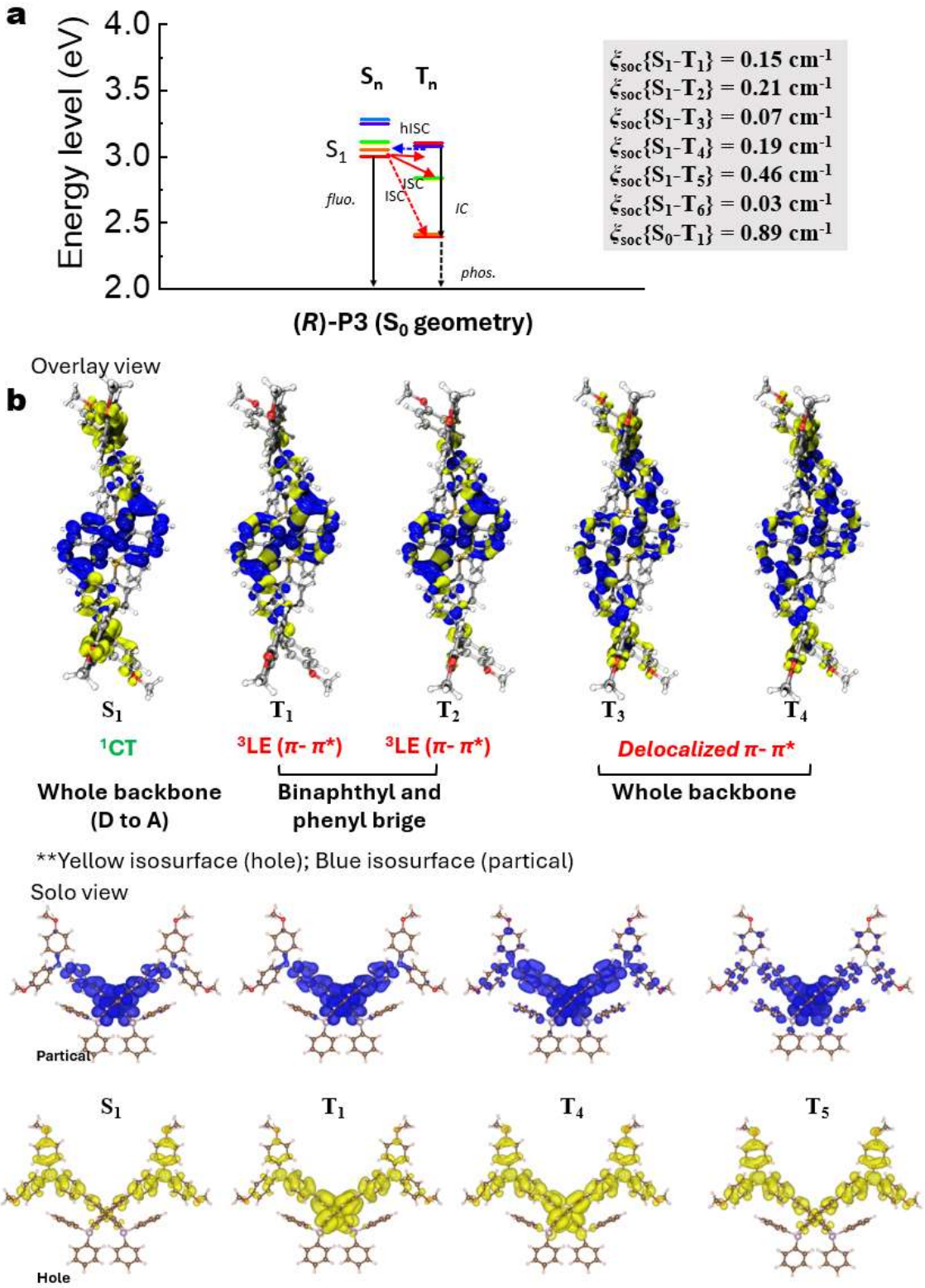

Figure S15. (a) TD-DFT calculated energy diagrams and SOC coefficients (ξ_{soc}) for **(*R*)-P3**. (b) Electron (yellow)-hole (blue) distribution analysis of $S_0 \rightarrow S_1$ and $S_0 \rightarrow T_n$ transitions for **(*R*)-P3** at the S_0 geometry (isovalue: 0.0003 a.u.).

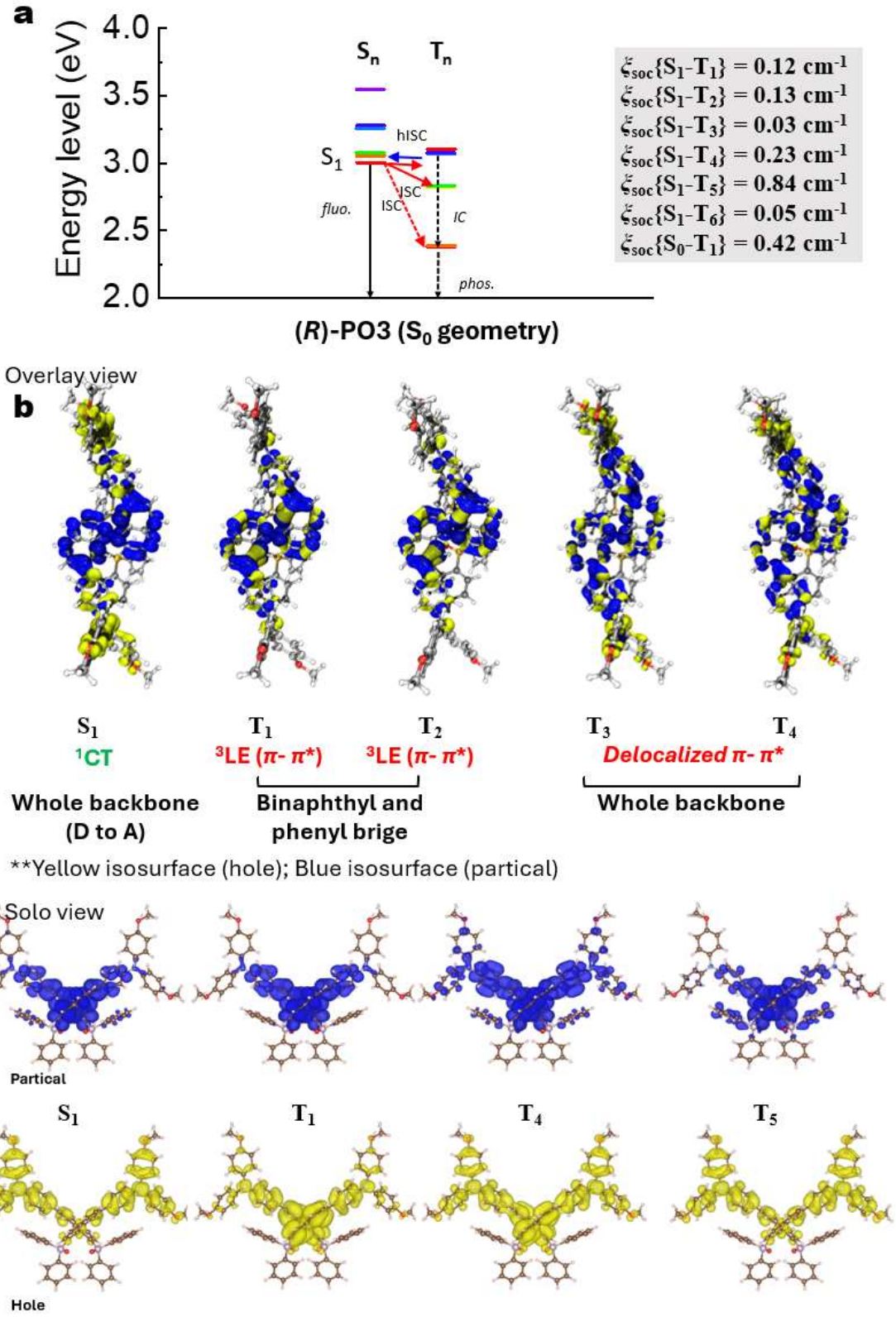

Figure S16. (a) TD-DFT calculated energy diagrams and SOC coefficients (ξ_{soc}) for **(*R*)-PO3**. (b) Electron (yellow)-hole (blue) distribution analysis of $S_0 \rightarrow S_1$ and $S_0 \rightarrow T_n$ transitions for **(*R*)-P3** at the S_0 geometry (isovalue: 0.0003 a.u.).

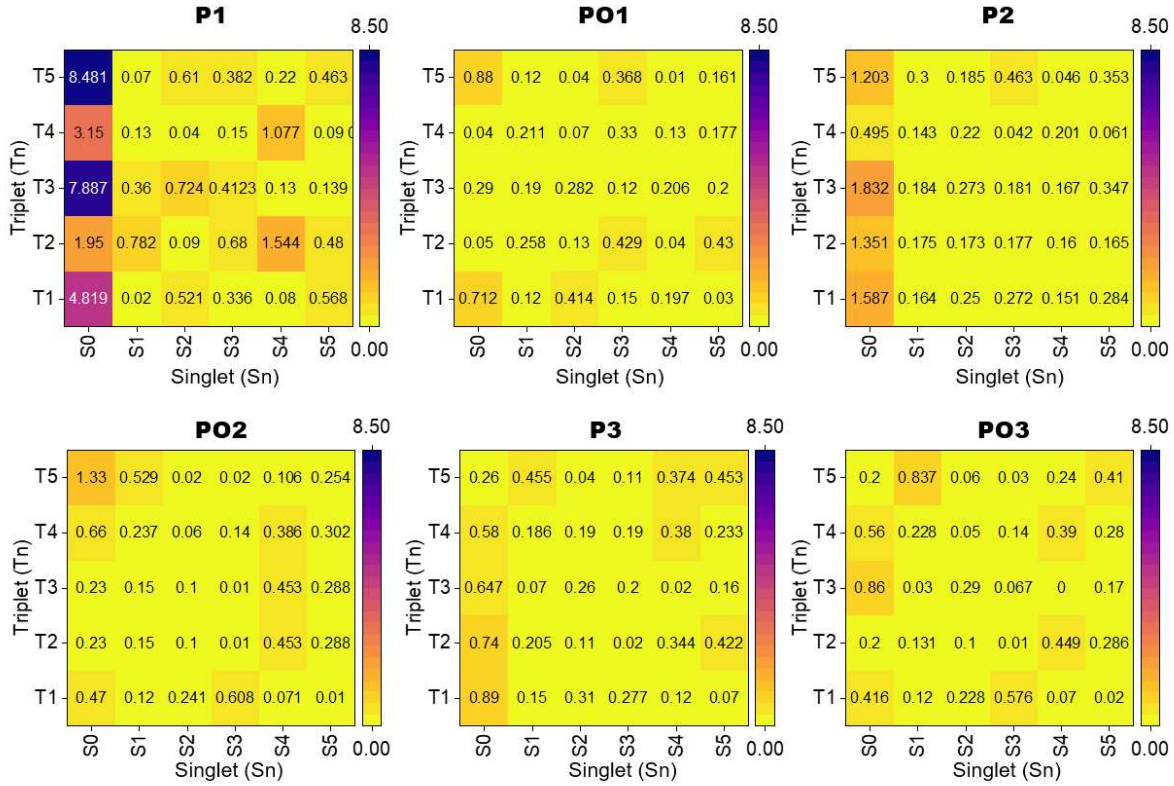

Figure S17. TD-DFT calculated heatmaps with ξsoc values between Sn and Tn (n = 0/1 to 5, at the S_0 geometry).

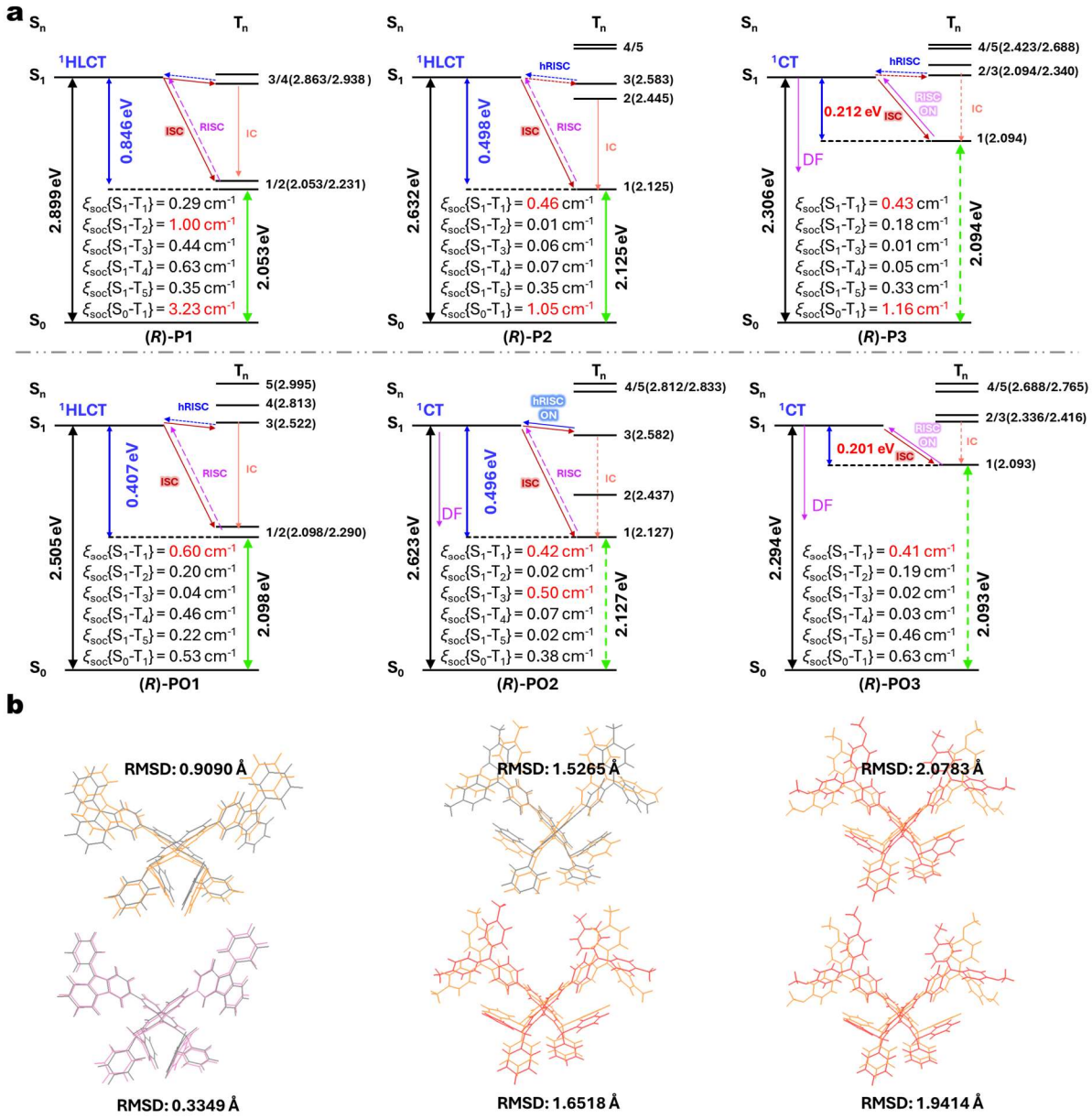

Figure S18. (a) TD-DFT calculated excitation energy diagrams and (b) SOC coefficients (ξ_{soc}) for six emitters at the S_1 geometry. (b) Root-mean-square error (RMSD) values of superimposed S_0–S_1 geometry (optimized at B3LYP/6-31G* level).

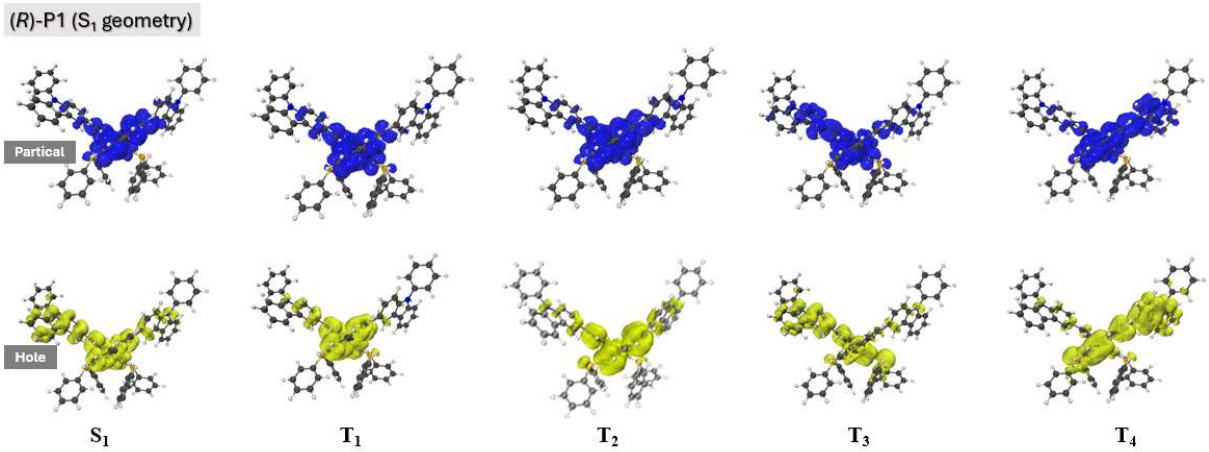

Figure S19. Electron (yellow)-hole (blue) distribution analysis of $S_0 \rightarrow S_1$ and $S_0 \rightarrow T_n$ transitions for **(*R*)-P1** at the S_1 geometry.

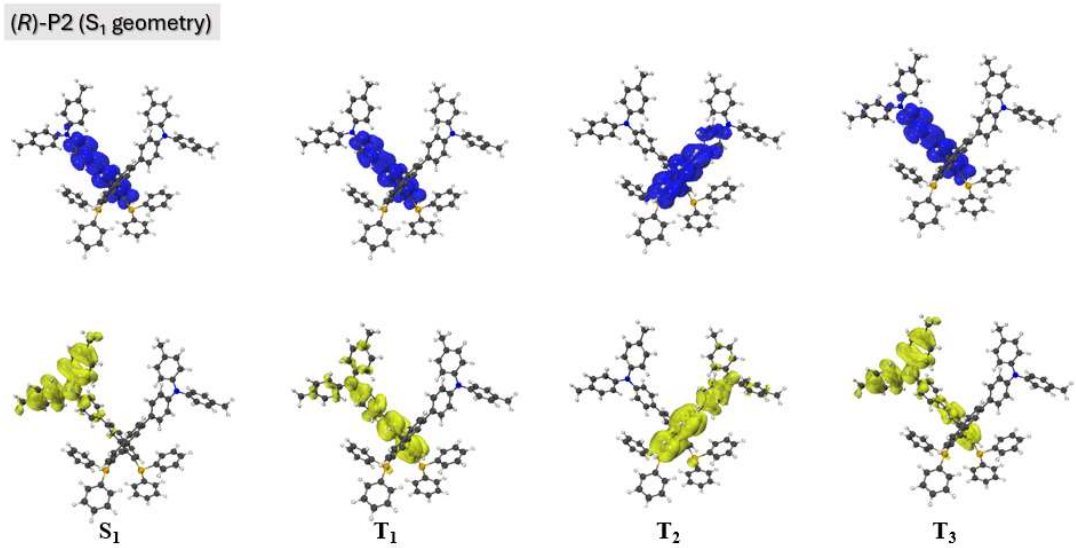

Figure S20. Electron (yellow)-hole (blue) distribution analysis of $S_0 \rightarrow S_1$ and $S_0 \rightarrow T_n$ transitions for **(*R*)-P2** at the S_1 geometry.

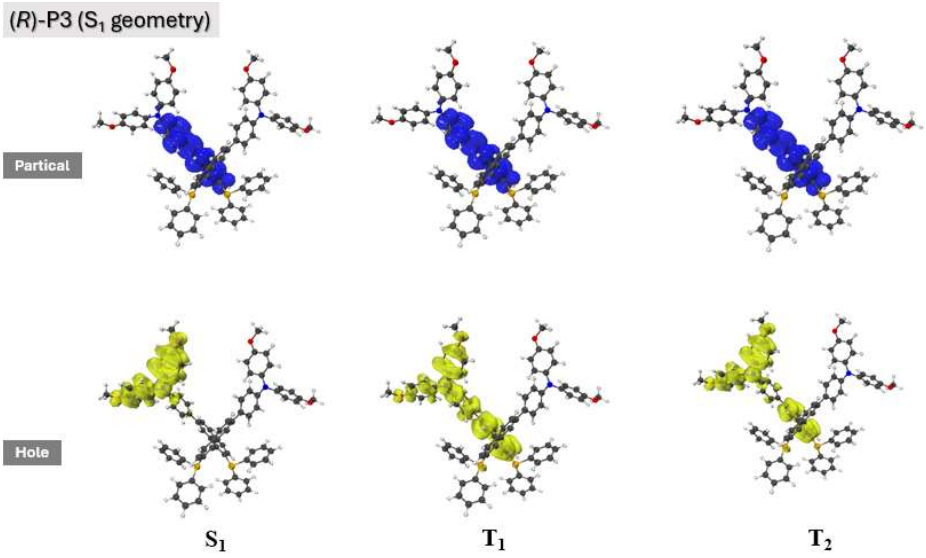

Figure S21. Electron (yellow)-hole (blue) distribution analysis of $S_0 \rightarrow S_1$ and $S_0 \rightarrow T_n$ transitions for **(*R*)-P3** at the S_1 geometry.

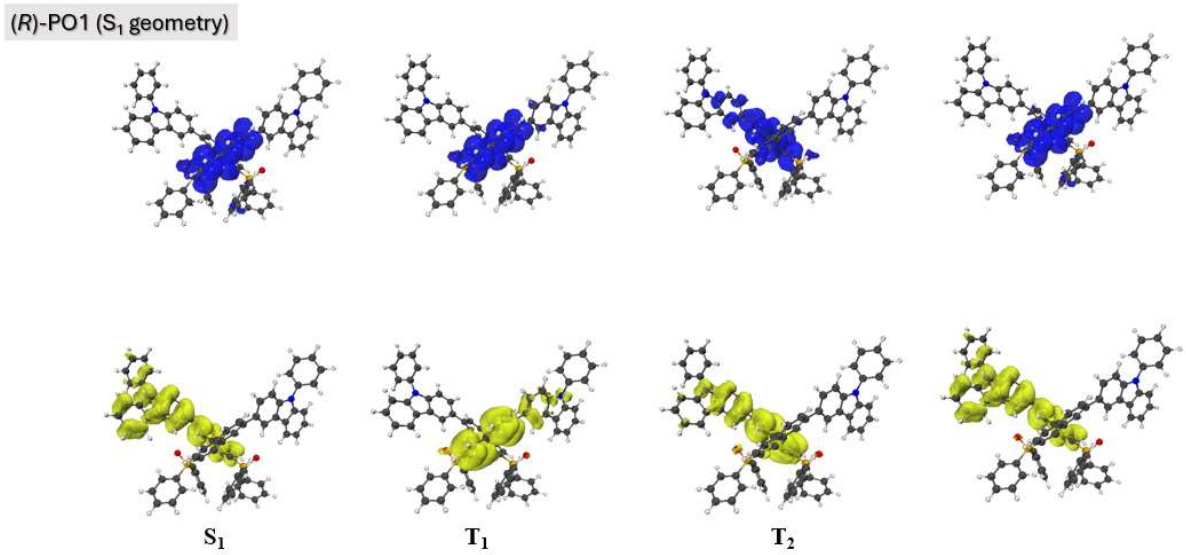

Figure S22. Electron (yellow)-hole (blue) distribution analysis of $S_0 \rightarrow S_1$ and $S_0 \rightarrow T_n$ transitions for **(*R*)-PO1** at the S_1 geometry.

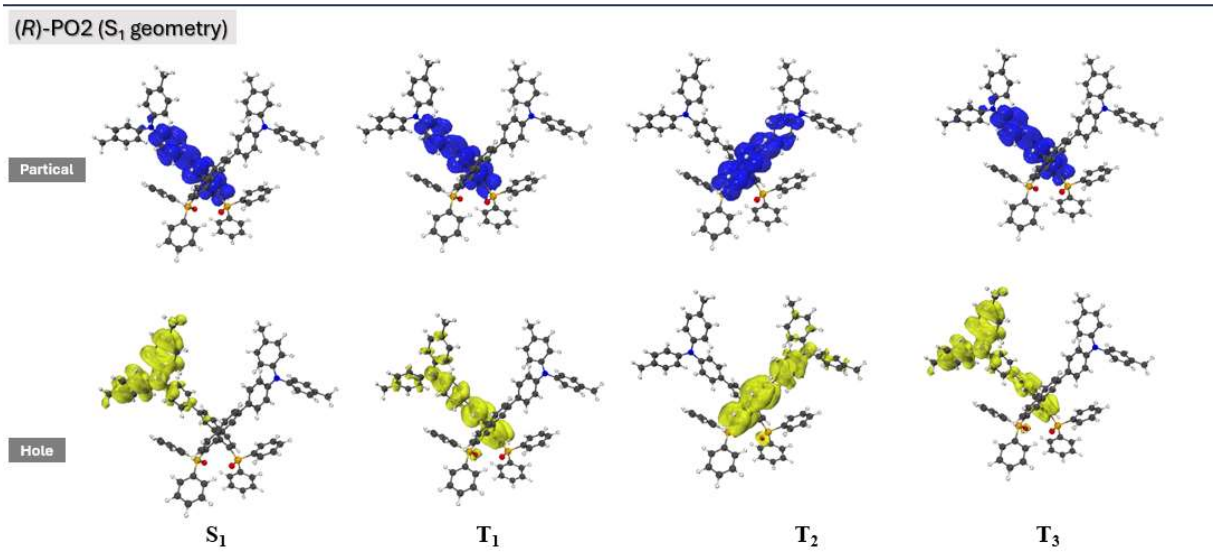

Figure S23. Electron (yellow)-hole (blue) distribution analysis of $S_0 \rightarrow S_1$ and $S_0 \rightarrow T_n$ transitions for **(*R*)-PO2** at the S_1 geometry.

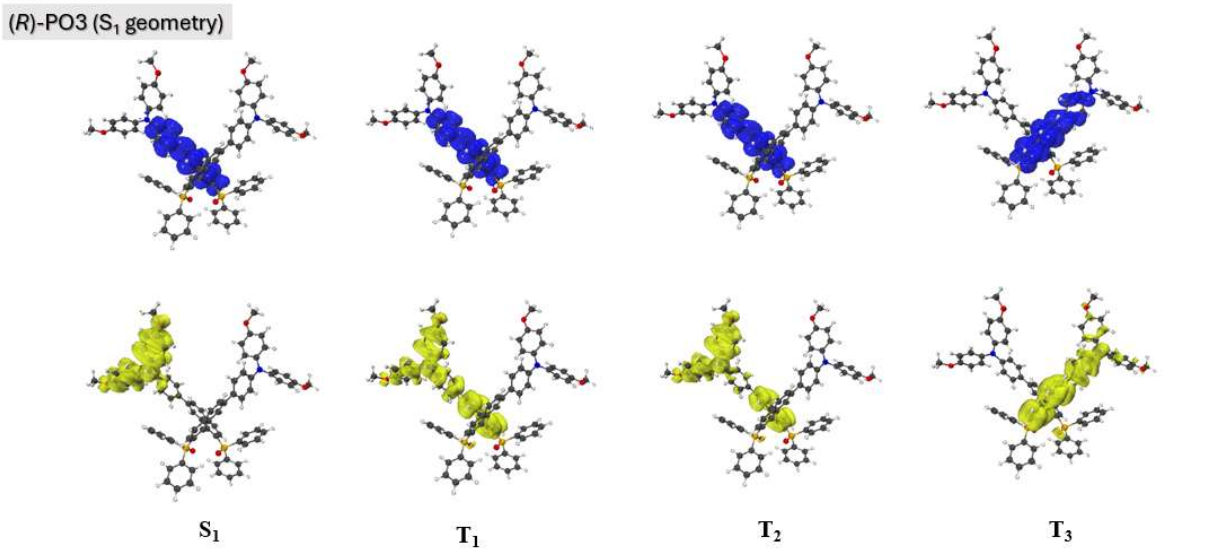

Figure S24. Electron (yellow)-hole (blue) distribution analysis of $S_0 \rightarrow S_1$ and $S_0 \rightarrow T_n$ transitions for **(*R*)-PO3** at the S_1 geometry.

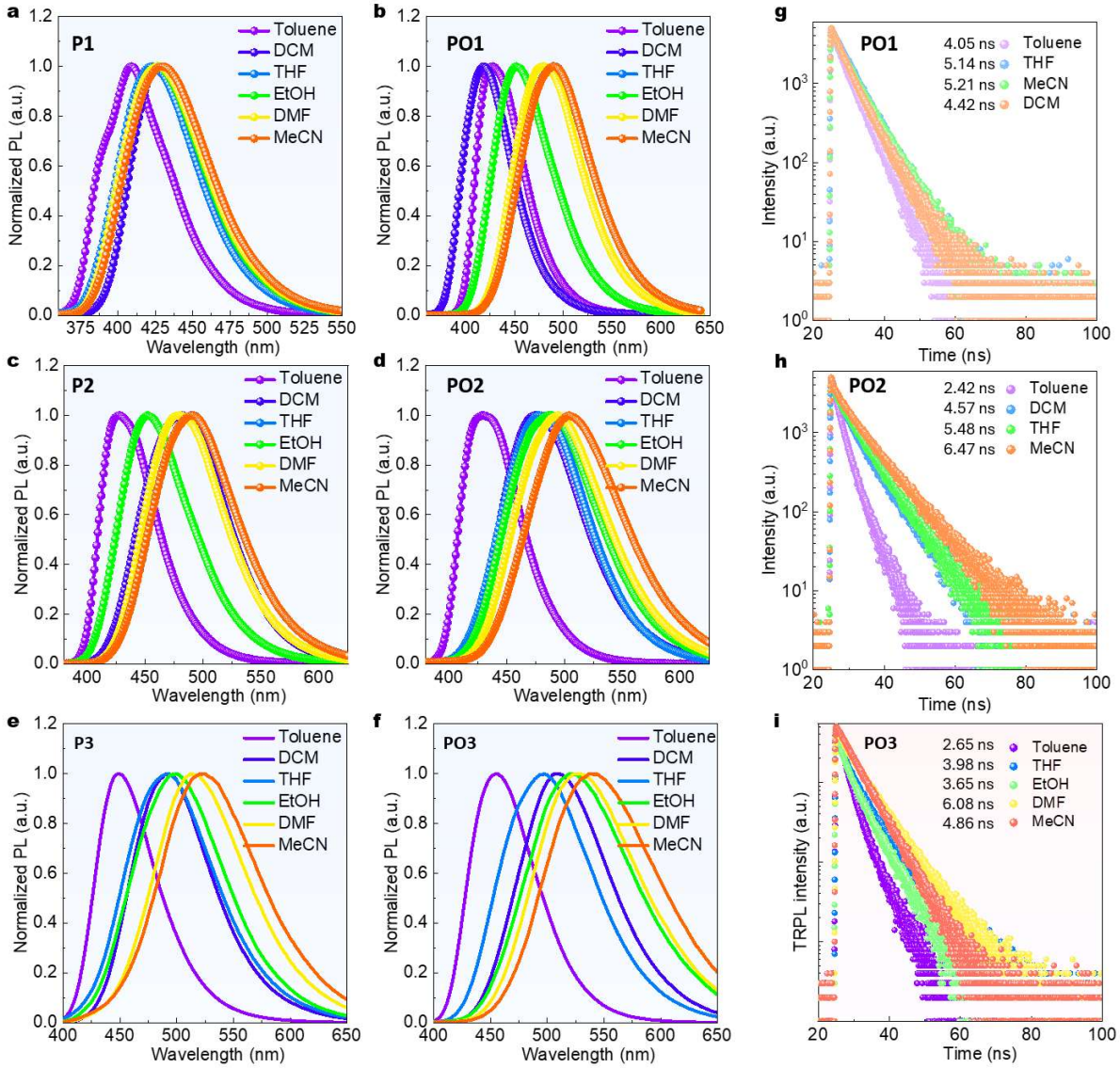

Figure S25. (a–f) PL spectra of **P1–PO3** emitters in different solvents, respectively. (g–i) Emission lifetimes of **PO1**, **PO2,** and **PO3** emitters in different solvents, respectively (lifetimes are revealed by bi-exponential fitting).

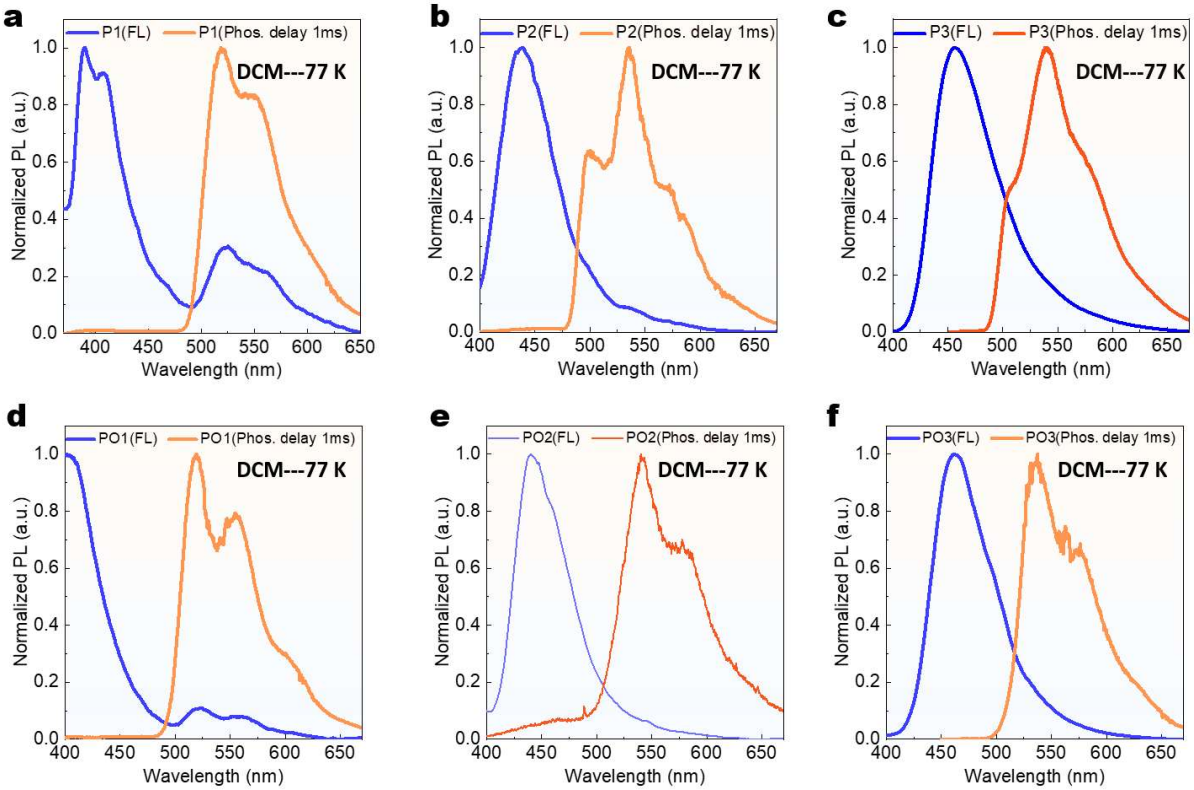

Figure S26. (a-f) PL and delayed PL spectra of six emitters in DCM at 77 K.

Table S3. Photophysical and chiroptical data of all compounds in DCM

name	states	[a]λ_{em} (nm)	[b]Φ_{em} (%)	[c]$\tau_{fluo.}$ (ns)	[d]$\tau_{phos.}$ (ms)	k_r (s^{-1})	[e]$\Delta E_{S1\text{-}T1}$ (eV)	Stokes shift (nm)	[f]$\lvert g_{abs}\rvert$ ($\times 10^{-3}$)	[g]$\lvert g_{lum}\rvert$ ($\times 10^{-3}$)
P1	DCM-RT	427	0.12/[h]6.7	4.1	–	2.9×10^5	–	108	6.5	~[h]3.4
	DCM-77 K	390,518	–	2.6	857(539*51%;1183*49%)	–	0.83	–	–	–
PO1	DCM-RT	418	63.1/[h]79.5	4.4	–	1.4×10^8	–	99	9.6	~[h]3.0
	DCM-77 K	401,519	–	2.9	898(556*53%;1285*47%)	–	0.85	–	–	–
P2	DCM-RT	482	33.7/[h]41.6	3.7	–	9.2×10^7	–	130	3.4	~[h]1.3
	DCM-77 K	438,532	–	2.1	783(213*29%;1019*71%)	–	0.56	–	–	–
PO2	DCM-RT	474	72.8/[h]83.1	4.6	–	1.6×10^8	–	124	4.1	~[h]1.1
	DCM-77 K	440,541	–	2.1	802(166*21%;976*79%)	–	0.55	–	–	–
P3	DCM-RT	491	59.1/[h]68.4	2.7	–	2.2×10^8	–	138	–	–
	DCM-77 K	455,543	–	4.4	801(153*17%;931*83%)	–	0.45	–	–	–
PO3	DCM-RT	508	81.5/[h]95.3	3.4	–	2.4×10^8	–	156	–	–
	DCM-77 K	462,535	–	2.6	881(292*18%;1007*82%)	–	0.50	–	–	–

[a]The main emission peaks. [b]Φ_{em} was determined by integrating the sphere system. [c]Fluorescent lifetimes can be revealed by bi-exponential fitting the decay curve of the time-resolved PL spectrum. [d]Phosphorescent lifetimes can be revealed by biexponential fitting the decay curve of the time-resolved phos. spectrum. [e]$\Delta E_{S1\text{-}T1}$ was determined by fitting the onset of the PL spectrum. [f]$\lvert g_{abs}\rvert$ was determined from the maximum from the CD spectrum. [g]$\lvert g_{lum}\rvert$ was determined from the maximum from the CPL spectrum. [h]Φ_{em} was determined from degassed solutions. [h]Collected in DCM solutions and PMMA films.

Table S4. Photophysical data of all compounds in doped polymers (298 K)

name	states	$\lambda_{fluo.}$ (nm)	$\lambda_{phos.}$ (nm)	$\Phi_{fluo.}$ (%)	$\tau_{fluo.}$ (ns)	$\tau_{phos.}$ (ms)	Exp, $\lvert g_{lum}\rvert$ ($\times 10^{-3}$)	Cal, $\lvert g_{lum}\rvert$ ($\times 10^{-3}$)
P1	PMMA	410	523, 550(sh)	11.2	8.6	269(478*48%;78*52%)	6.2	7.9
	PVP	412	524, 552(sh)	14.5	8.1	1020(345*27%;1267*73%)	6.4	
PO1	PMMA	413	524, 547(sh)	45.6	5.3	218(412*57%;39*43%)	7.0	4.8
	PVP	413	528, 550(sh)	56.2	4.9	880(342*39%;1226*61%)	~6.8	
P2	PMMA	448	542, 574(sh)	51.1	2.3	233(52*59%;339*41%)	1.5	2.2
	PVP	470	545, 577(sh)	60.7	2.6	780(329*47%;1169*53%)	1.2	
PO2	PMMA	440	536, 450(sh)	76.9	3.5	1.37(0.45*21%;1.61*79%)	1.3	0.66
	PVP	479	553	83.2	3.3	20(1.5*48%;37*52%)	1.1	
P3	PMMA	453	~459 (df.)	78.6	3.8	1.64(1.41*14%*;1.67*86%)	–	–
	PVP	462	453, 513(sh)	86.3	3.1	220(341*55%;72*45%)	–	
PO3	PMMA	459	~451 (df.)	94.2	4.9	1.03(0.74*35%;1.18*65%)	–	–
	PVP	485	490	97.4	4.3	18(1.1*57%;40*43%)	–	

Two fluorescent lifetimes ($\tau_{fluo.}$ and $\tau_{phos.}$) can be revealed by fitting the decay curve of the time-resolved PL spectra data. "sh" stands for shoulder peak. PLQY was determined by integrating the sphere system. Cal, $\lvert g_{lum}\rvert$ values were obtained by TD-DFT simulation at $S_1 \rightarrow S_0$ emission.

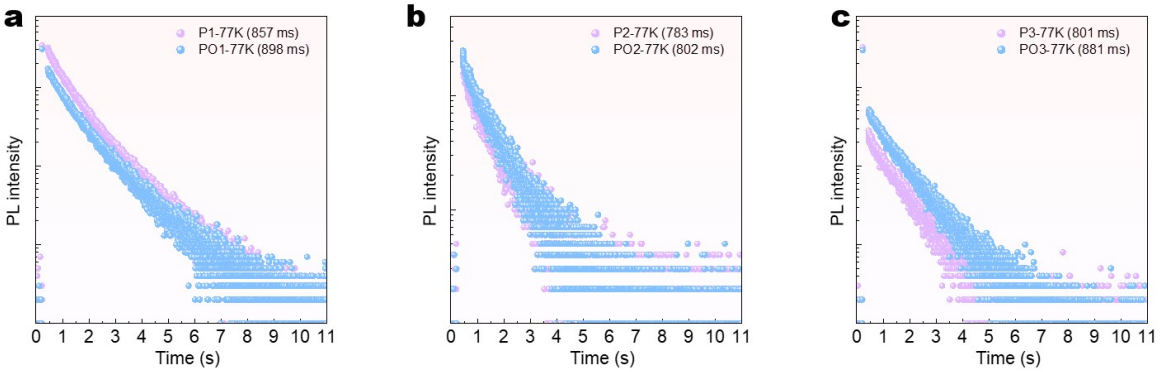

Figure S27. (a−c) Emission lifetimes of **P1**−**P3** and **PO1**−**PO3** emitters in DCM at 77 K (at phos. peak).

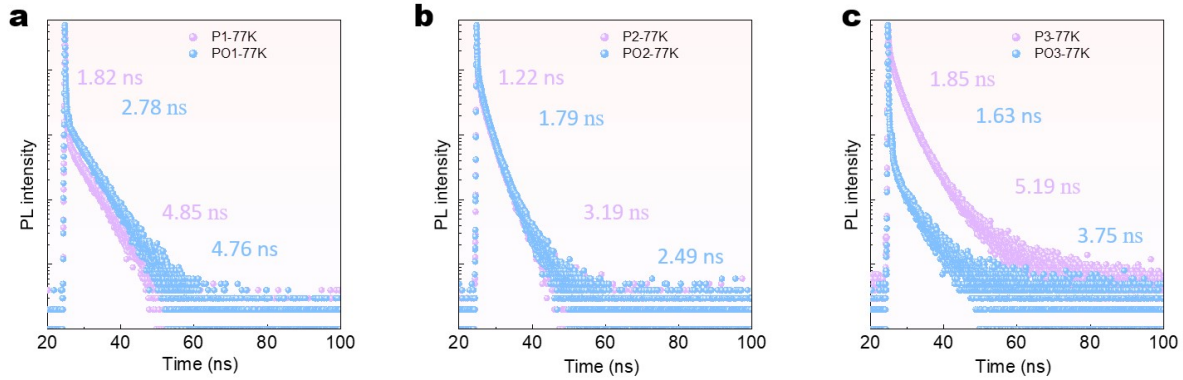

Figure S28. (a−c) Emission lifetimes of **P1**−**P3** and **PO1**−**PO3** emitters in DCM at 77 K (at fluo. peak).

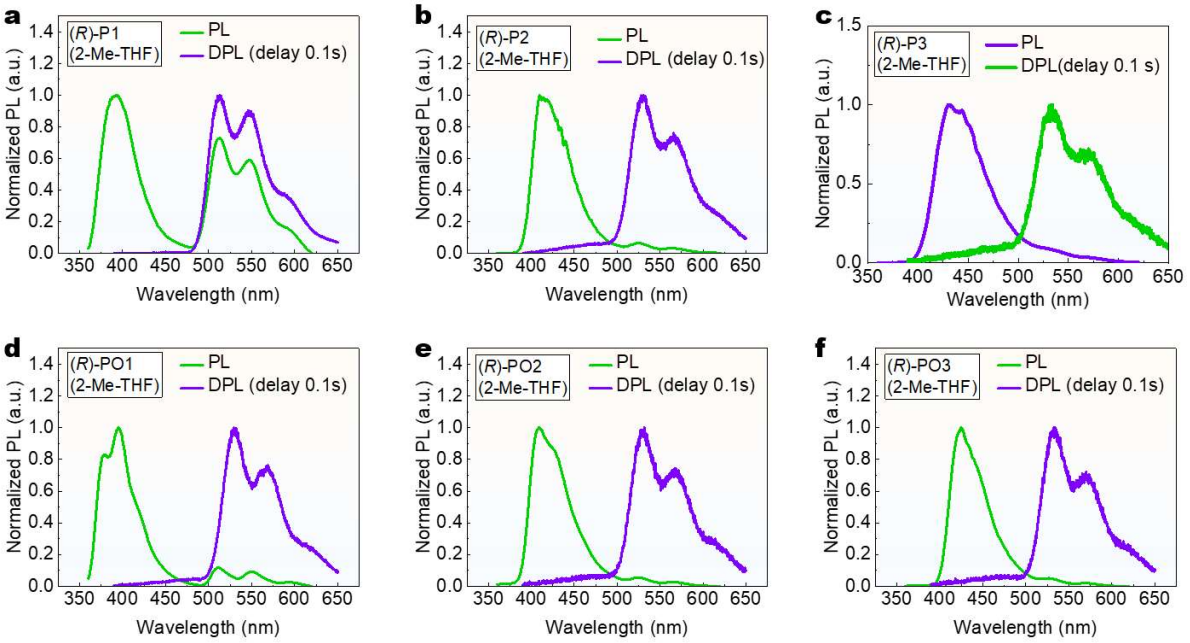

Figure S29. (a-f) PL and delayed PL spectra of six emitters in 2-Me-THF at 77 K.

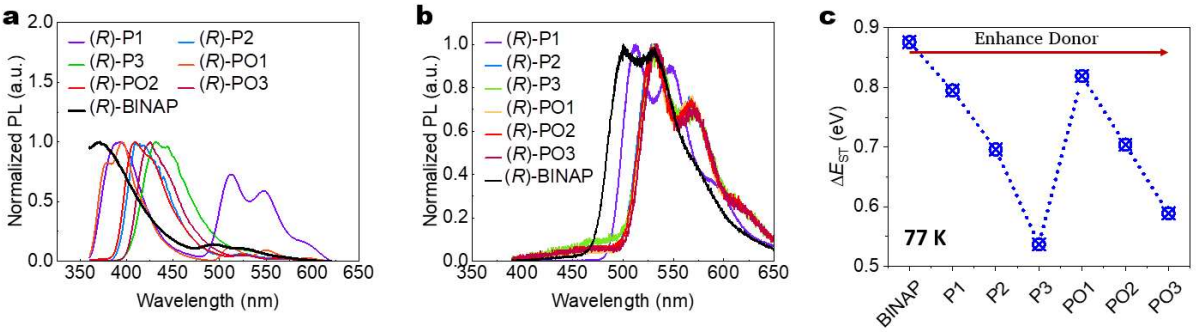

Figure S30. (a-b) PL and delayed PL emission comparison of six emitters in 2-Me-THF at 77 K. (c) Established ΔE_{ST} values by fluo. and phos. emission peaks.

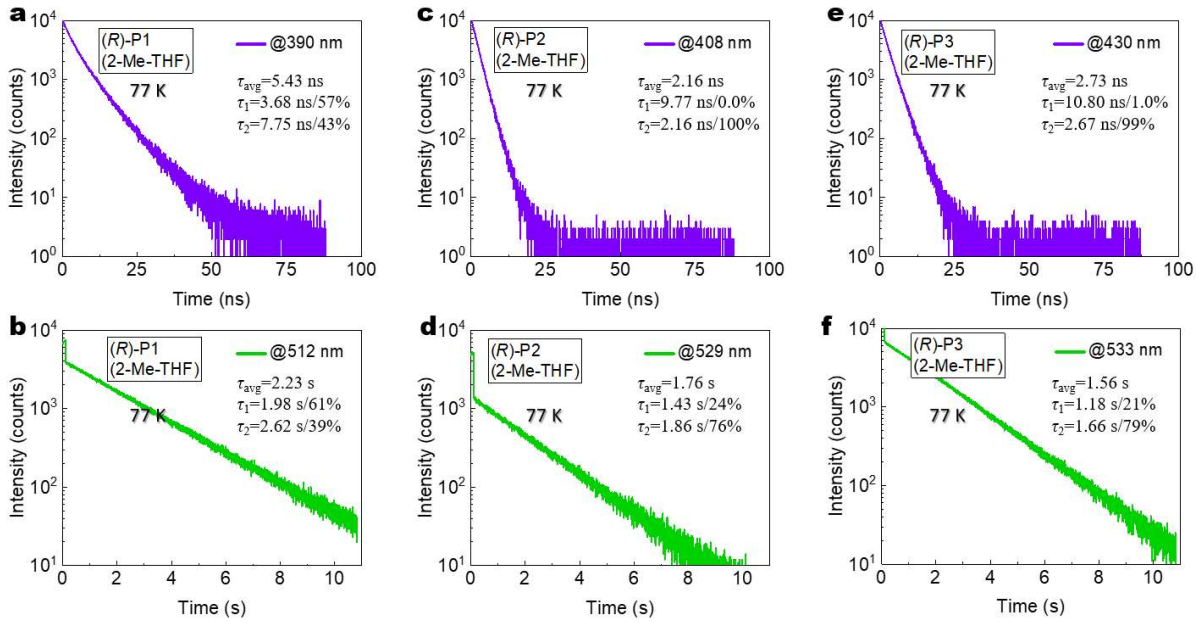

Figure S31. (a–f) Emission lifetimes of **P1–P3** emitters in 2-Me-THF at 77 K.

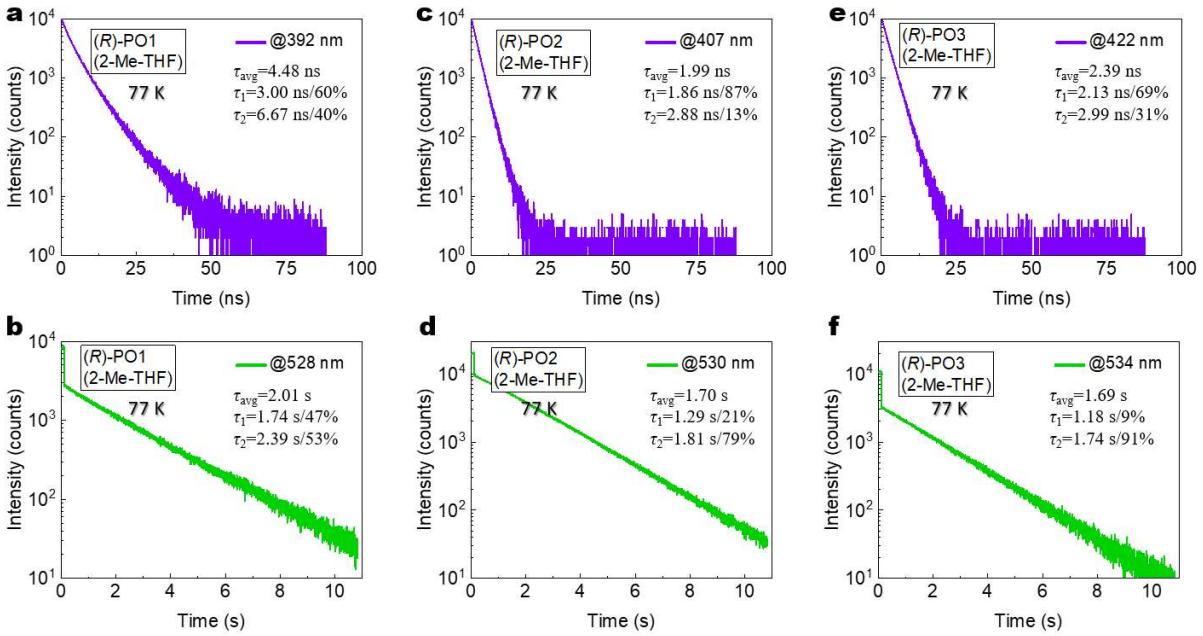

Figure S32. (a–f) Emission lifetimes of **PO1–PO3** emitters in 2-Me-THF at 77 K.

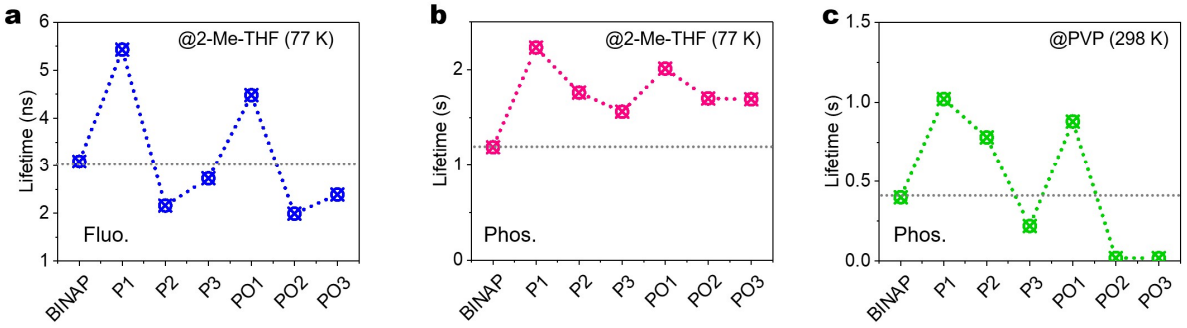

Figure S32. (a−c) Lifetime comparisons between BINAP and BINAPs/BINAPOs emitters in different mediums.

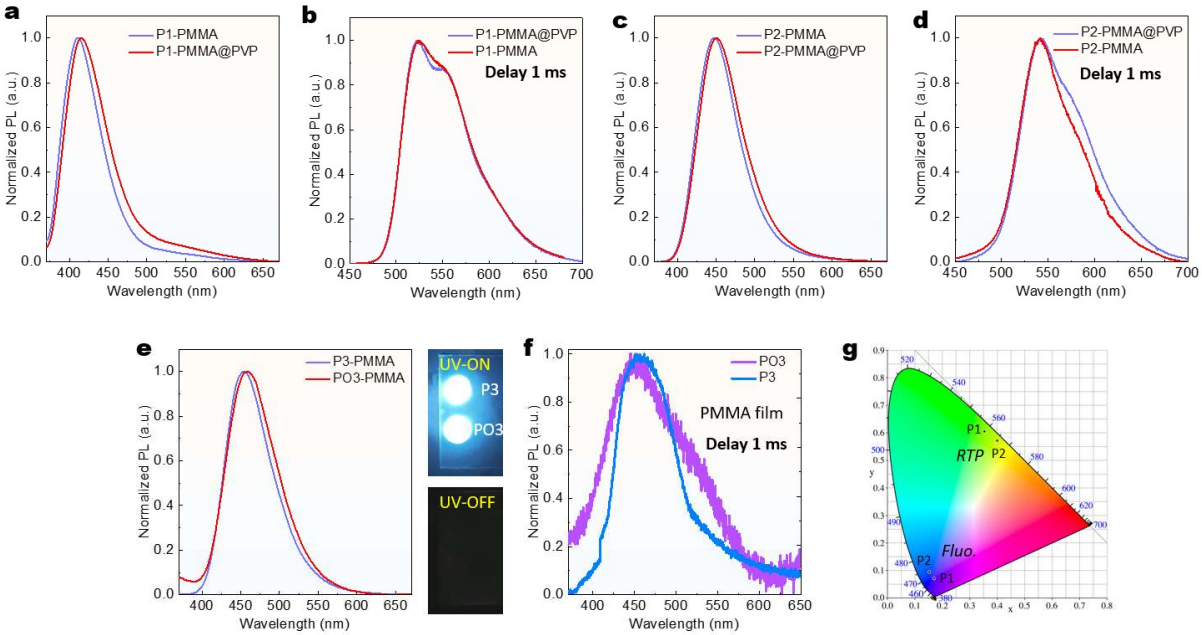

Figure S33. (a-f) PL spectra of **P1−P3** emitters in a PMMA matrix (0.5 wt%). (g) CIE 1931 chromaticity coordinates. *The phosphorescence is decreased from **P1** to **PO3**. The phosphorescence is decreased in PMMA.

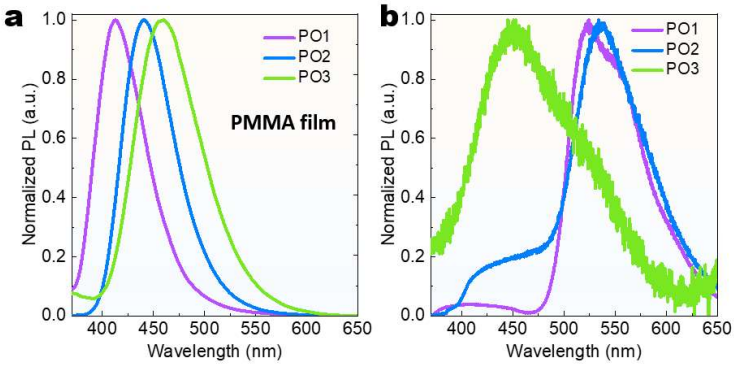

Figure S34. (a) PL and (b) delayed PL spectra (0.1 ms) of **PO1-PO3** emitters in PMMA@PVP matrices (0.5 wt%).

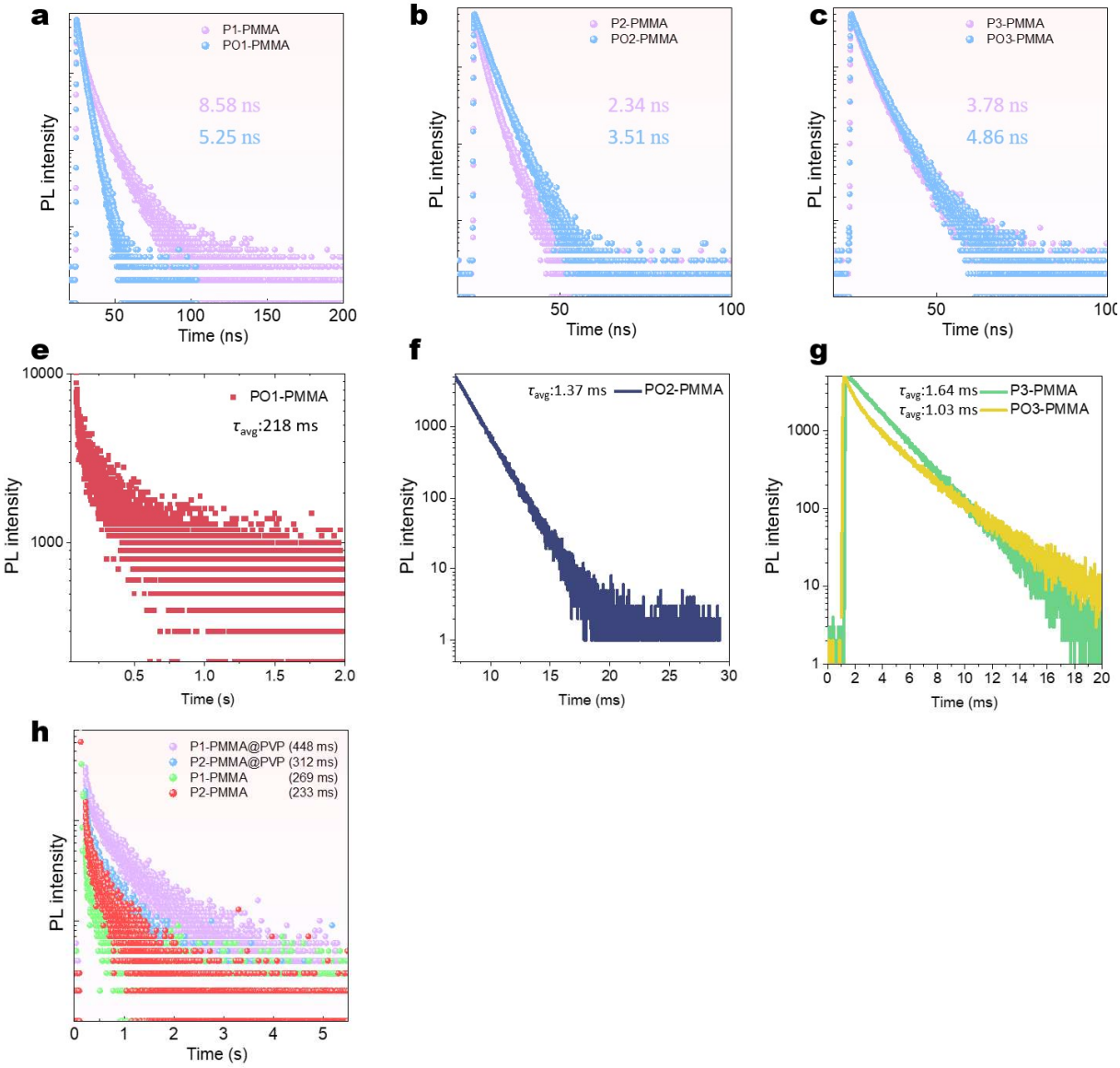

Figure S35. (a–c) Lifetime profiles of **P1**–**P3** and **PO1**–**PO3** emitters in PMMA at 298 K (at fluo. peaks). (e) Lifetime profiles spectra of **PO1** (at phos. peak) and (f,g) **PO2,** and **P3**/**PO3** emitters in PMMA at 298 K (at fluo. peak). (h) Lifetime profiles spectra of **P1** and **P2** in PMMA at 298 K (at phos. peak).

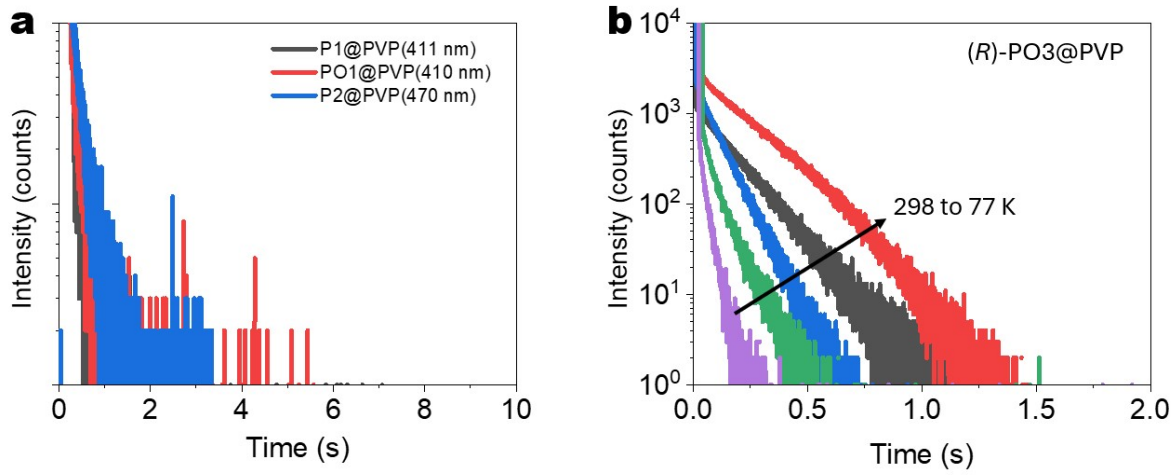

Figure S36. (a) Emission lifetimes of **P1@PVP, PO1@PVP,** and **P2@PVP** at 298 K. (b) Emission lifetimes of **PO3@PVP** at different temperatures.

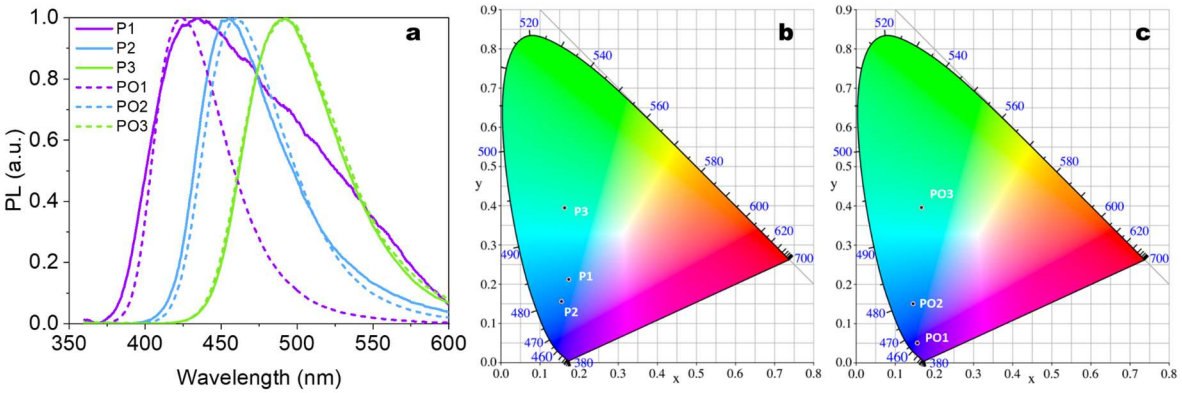

Figure S37. (a) PL spectra of six emitters at drop-cast amorphous solid states (Ex at 350 nm, 298 K). (b,c) CIE 1931 chromaticity coordinates of six emitters (amorphous powder, 298 K).

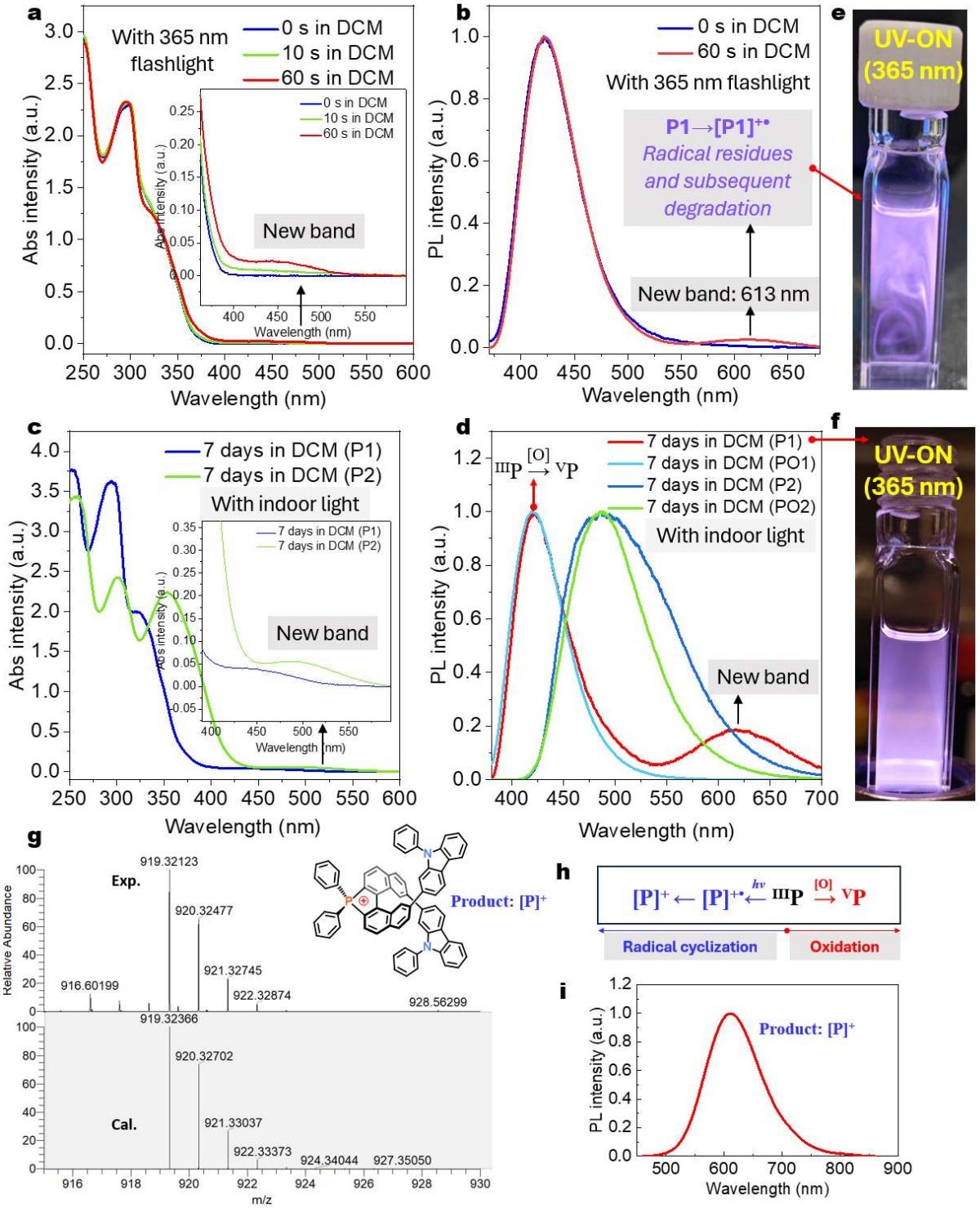

Figure S38. (a,b) UV-vis absorption and emission of **P1** before and after continuous 365 nm UV irradiation. (c,d) UV-vis absorption and emission of **P1** and **P2** before and after continuous white light irradiation. (e,f) Pictures of **P1@DCM** solution with UV-light. (g) A small amount of product obtained by separation and its HRMS data. (h) Reaction paths of phosphines in air with light irradiation. (i) PL spectra of pure product $[P1]^+[Cl]^-$ in DCM.

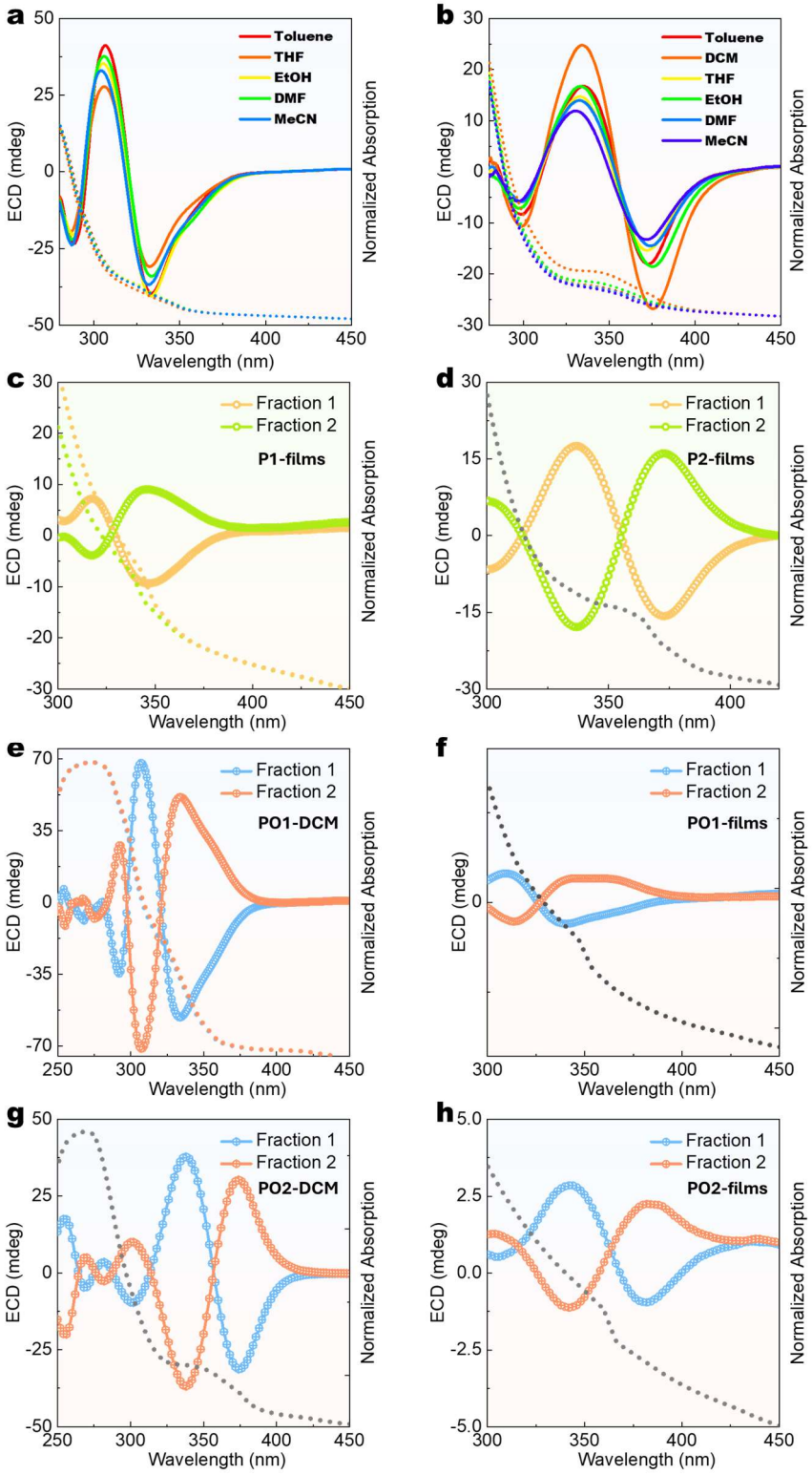

Figure S39. (a–b) ECD and UV-vis spectra of **(*R*)-PO1** and **(*R*)-PO2** in different solvents. (c–h) ECD and UV-vis spectra of **PO1** and **PO2** enantiomers in DCM and in the solid state.

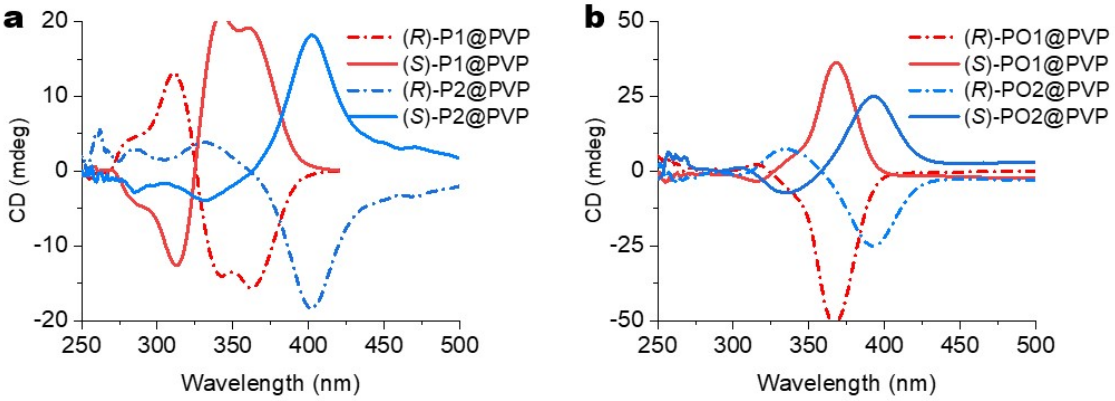

Figure S40. (a–b) ECD spectra of four chiral emitters in PVP at 298 K (0.5 wt%).

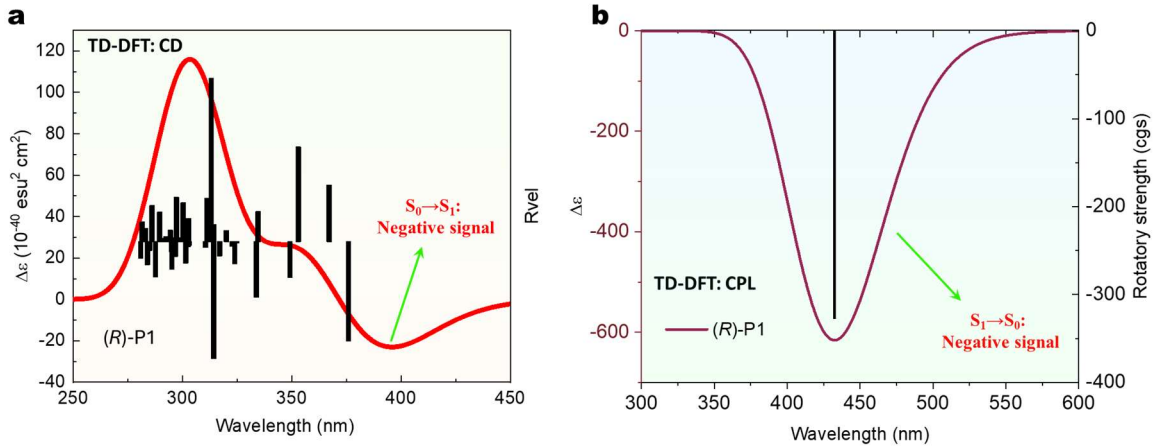

Figure S41. (a) TD-DFT simulative ECD and (b) CPL spectra of **(*R*)-P1**.

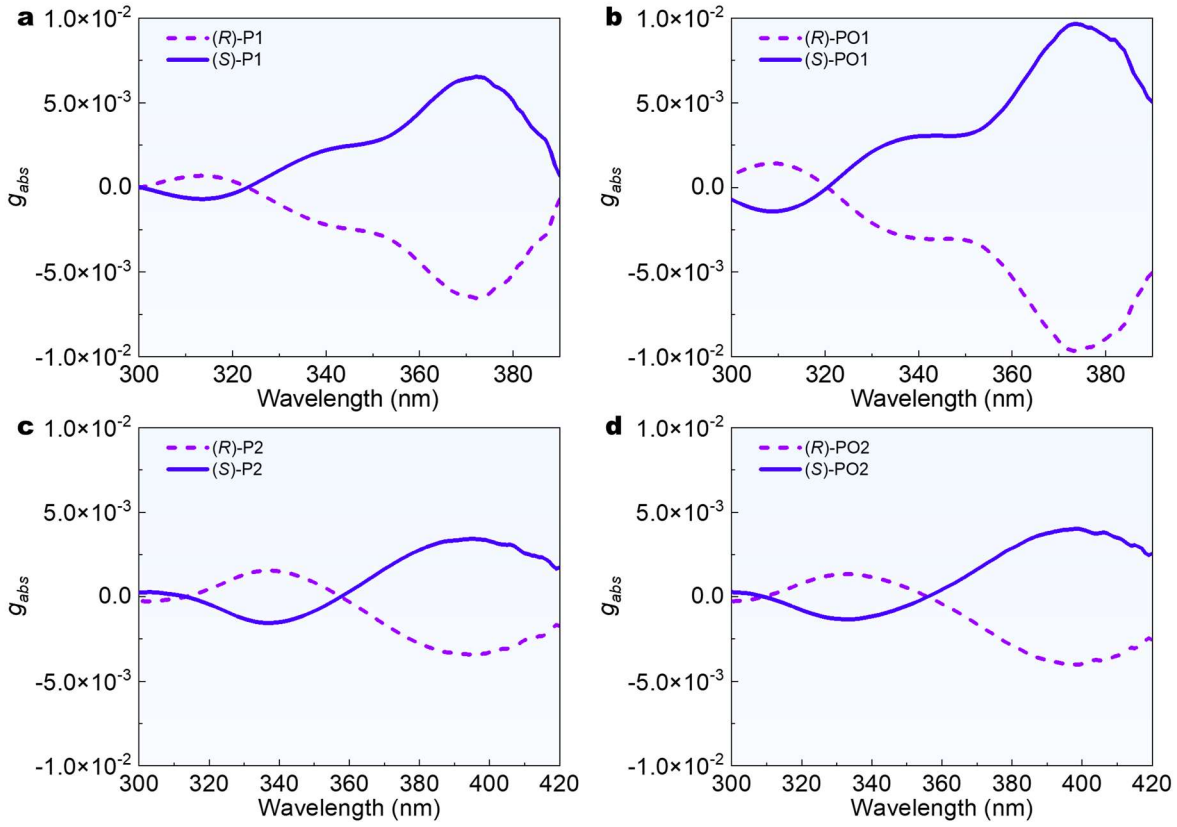

Figure S42. The g_{abs} spectra of eight emitters in DCM (2.0×10^{-4} M).

a

Ex. states (P1)	μ_e	μ_m	cosθ	g_{abs}
1	3.76×10^{-18}	8.05×10^{-21}	-0.9344	-8.00×10^{-3}
2	1.58×10^{-18}	1.01×10^{-20}	1.0000	25.40×10^{-3}
3	1.65×10^{-18}	1.63×10^{-20}	1.0000	39.60×10^{-3}
4	2.19×10^{-18}	4.74×10^{-21}	-0.9855	8.50×10^{-3}

b

Ex. states (PO1)	μ_e	μ_m	cosθ	g_{abs}
1	2.51×10^{-18}	5.98×10^{-21}	-0.9910	-9.40×10^{-3}
2	1.31×10^{-18}	-	0.0000	-
3	2.22×10^{-18}	4.74×10^{-21}	-0.9970	8.53×10^{-3}
4	1.58×10^{-18}	-	0.0000	-

c

Ex. states (P2)	μ_e	μ_m	cosθ	g_{abs}
1	5.71×10^{-18}	-1.30×10^{-20}	-0.8851	-8.14×10^{-3}
2	3.36×10^{-18}	1.03×10^{-20}	0.8475	10.43×10^{-3}
3	4.35×10^{-18}	1.44×10^{-20}	0.4718	-5.30×10^{-3}
4	1.27×10^{-18}	8.11×10^{-21}	-0.2873	4.07×10^{-3}

d

Ex. states (PO2)	μ_e	μ_m	cosθ	g_{abs}
1	6.62×10^{-18}	1.10×10^{-20}	-0.9983	-6.50×10^{-3}
2	3.99×10^{-18}	1.54×10^{-20}	1	15.00×10^{-3}
3	7.90×10^{-20}	-	0	-
4	1.21×10^{-18}	3.65×10^{-21}	-0.9635	11.58×10^{-3}

Figure S43. TD-DFT simulative transition electric-magnetic dipole moments and their angles, g_{abs} values for (*R*)-isomer (S_0 to S_n states).

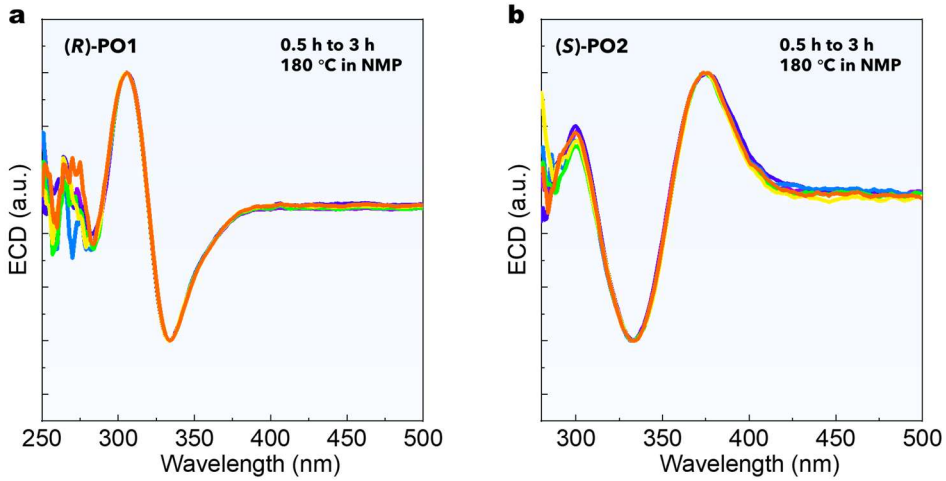

Figure S44. VT−ECD spectra of **(*R*)-PO1**, **(*R*)-PO2** after heating in *N*-methylpyrrolidone (NMP). ECD was tested at 25 °C.

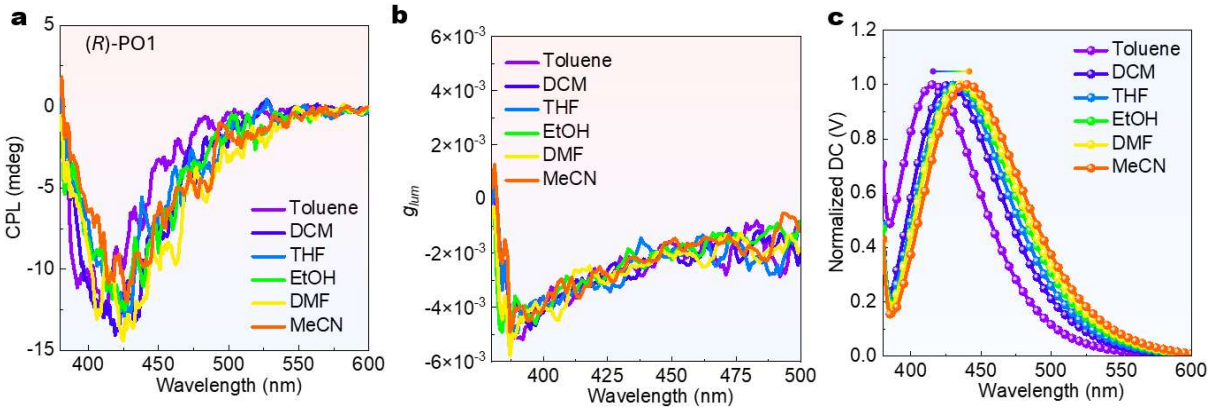

Figure S45. (a−c) Solvatochromic CPL, g_{lum}, DC spectra of **(*R*)-PO1** in solvents at 25 °C.

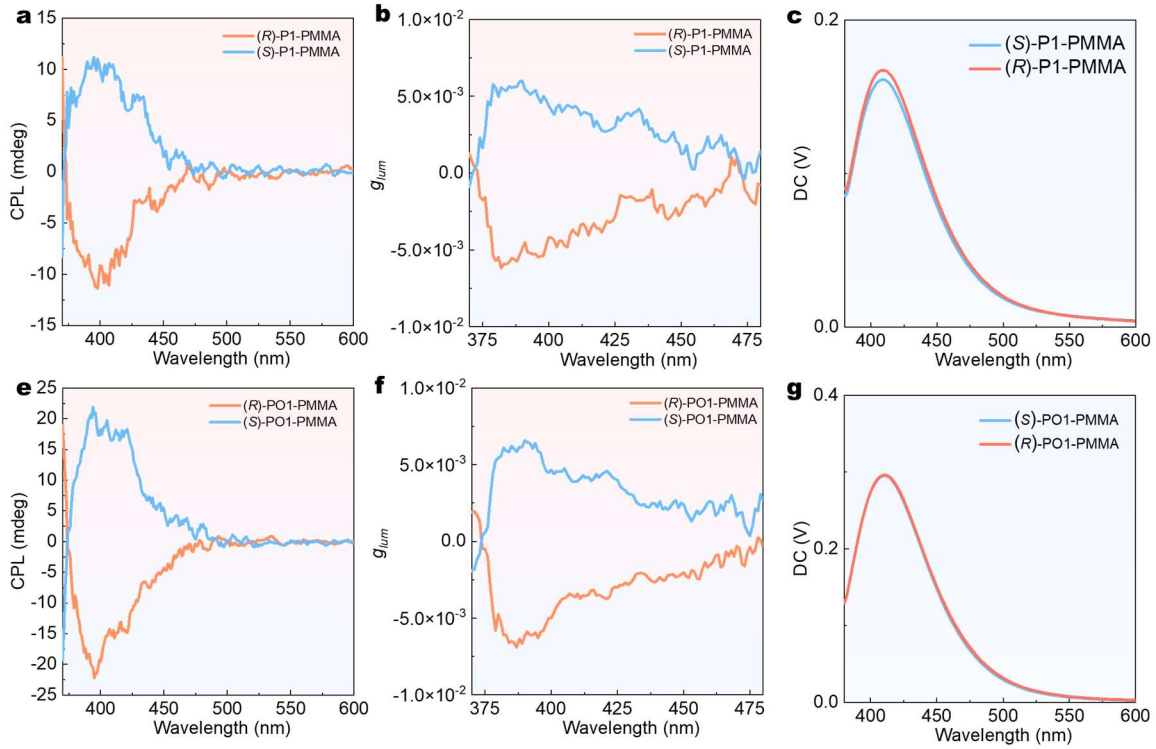

Figure S46. (a–g) CPL, g_{lum}, and DC spectra of **P1** and **PO1** enantiomers in doped PMMA films at 298 K (Ex. 340 nm, 0.5 wt%).

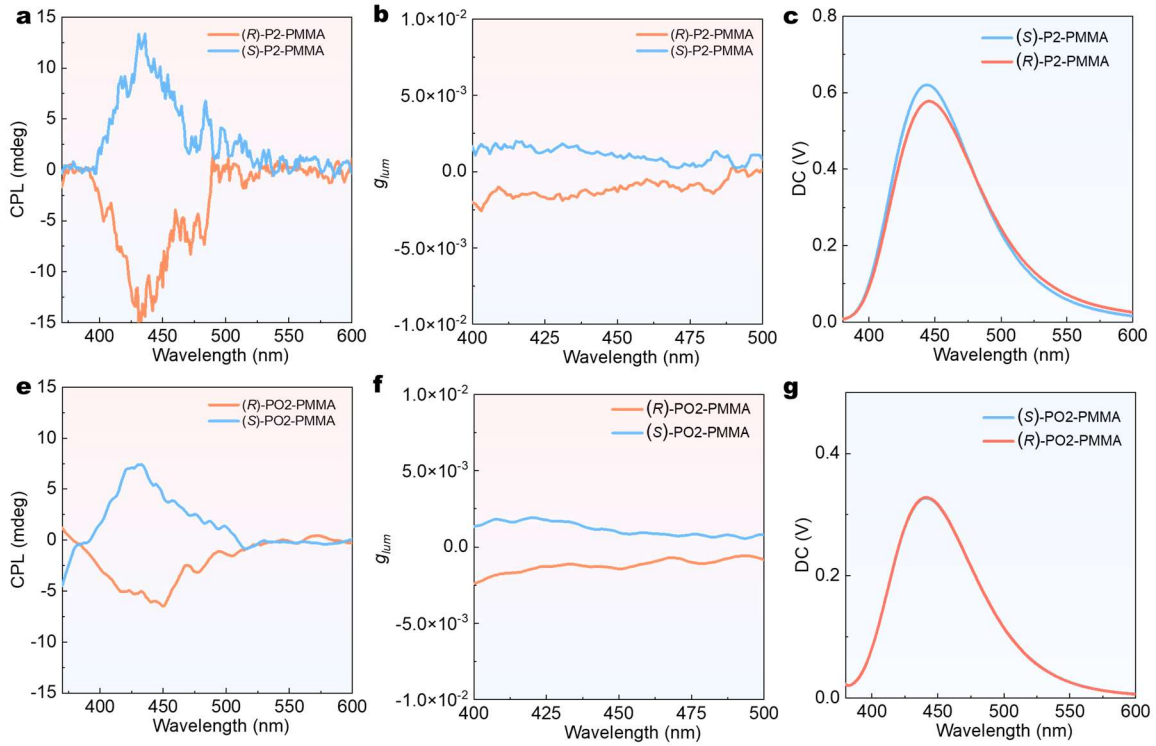

Figure S47. (a–g) CPL, g_{lum}, and DC spectra of **P2** and **PO2** enantiomers in doped PMMA films at 298 K (Ex. 340 nm, 0.5 wt%).

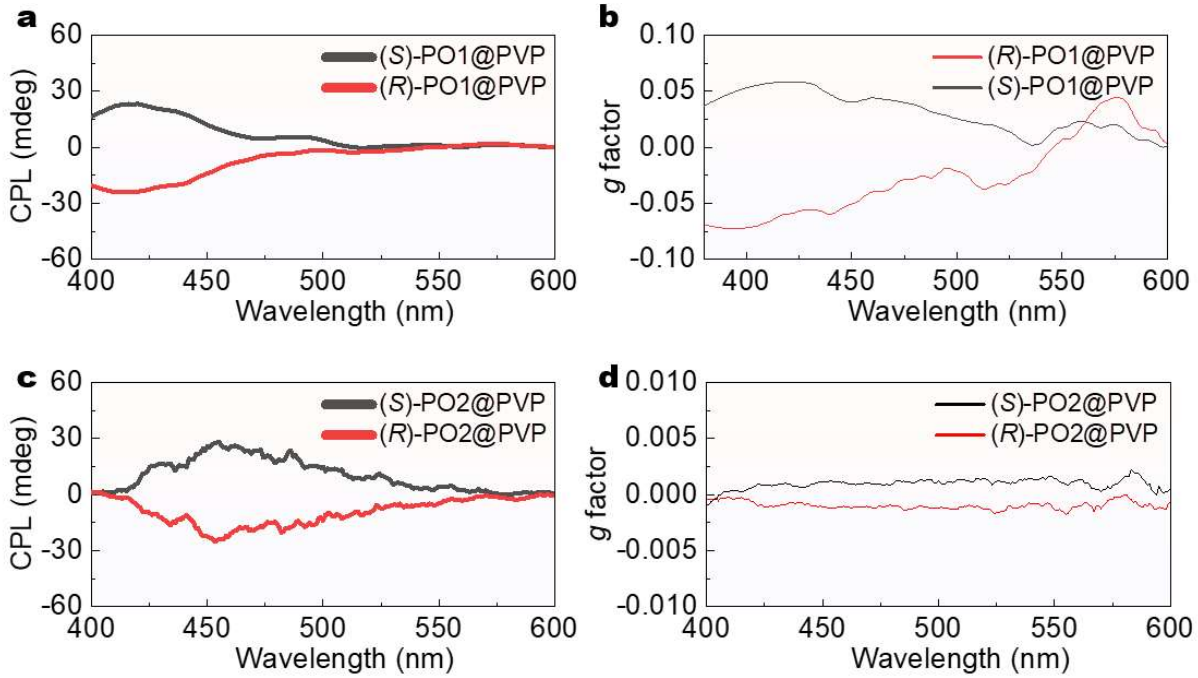

Figure S48. (a–d) CPL and g_{lum} spectra of **PO1** and **PO2** enantiomers in doped PVP films at 298 K (Ex. 330 nm, 0.5 wt%).

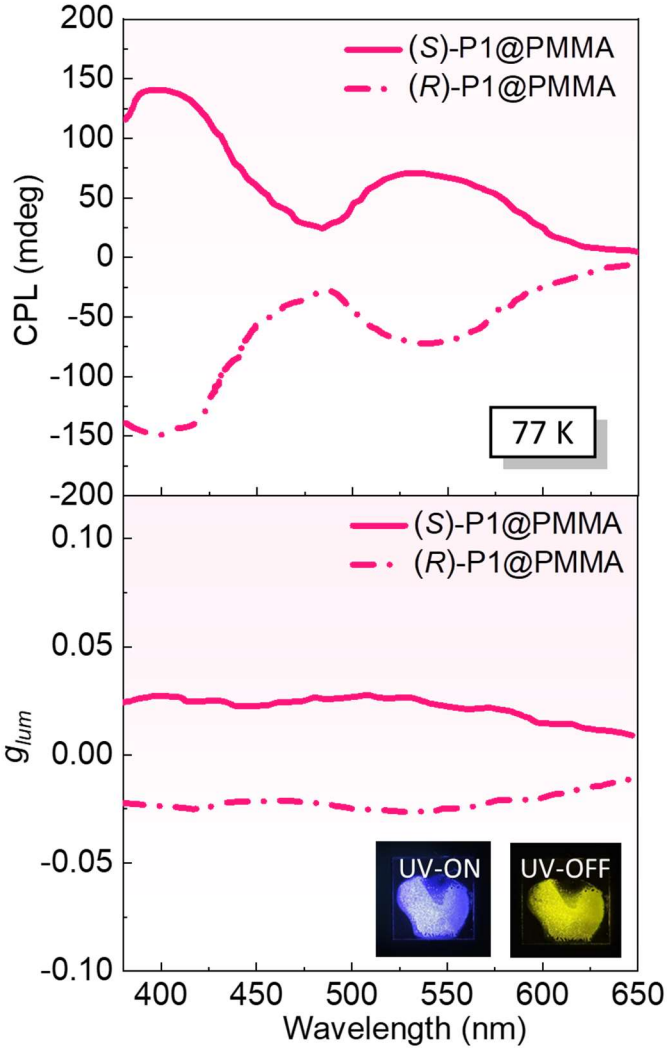

Figure S49. CPL and g_{lum} spectra of **P1** enantiomers in doped PMMA (0.5 wt%) at 77 K (λ_{ex} = 330 nm).

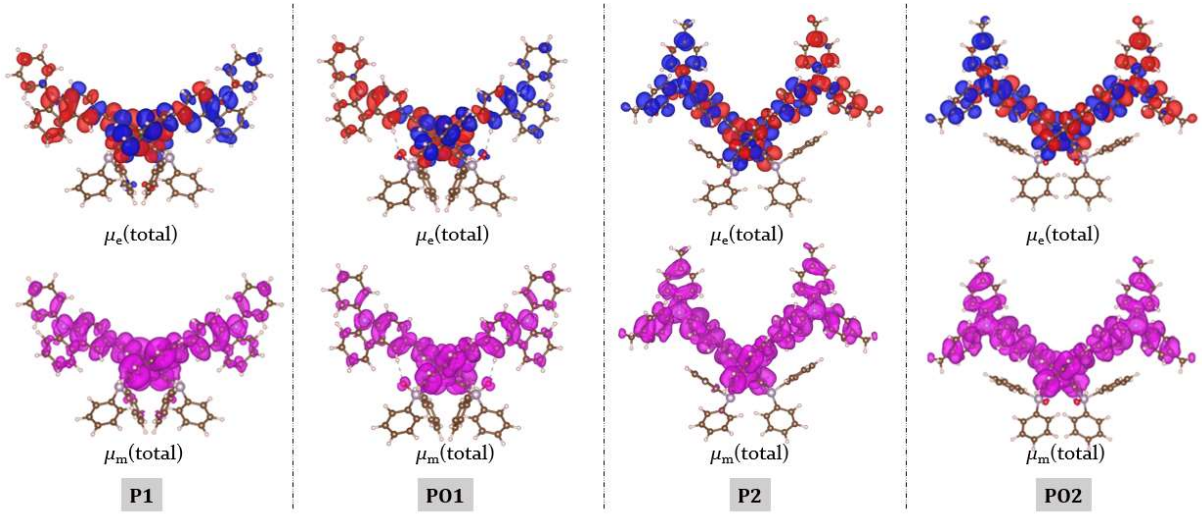

Figure S50. Transition electric dipole moment density and magnetic dipole moment density calculated at B3LYP/6-31G(d) level of theory (S_0 to S_1), displayed with an isosurface value of 0.002 au.

Ground to excited state transition electric dipole moments (Au):

state	X	Y	Z	Dip. S.	Osc.
1	-1.4420	-0.0002	-0.3287	2.1875	0.1767
2	-0.0004	0.6227	-0.0002	0.3877	0.0321
3	0.0008	0.6474	0.0001	0.4191	0.0361
4	0.8605	-0.0004	-0.0054	0.7406	0.0644
5	-0.0028	-0.6368	0.0003	0.4055	0.0368
6	1.3260	-0.0009	0.0160	1.7586	0.1600
7	0.6993	0.0000	-0.0383	0.4904	0.0459
8	-0.0001	0.5388	-0.0001	0.2903	0.0272
9	-0.4921	0.0004	0.1444	0.2630	0.0247
10	0.0022	-0.1985	-0.0007	0.0394	0.0037
11	-1.2789	0.0003	-0.4428	1.8315	0.1755
12	-0.0162	-0.4196	-0.0009	0.1763	0.0170
13	1.6447	0.0016	0.0524	2.7077	0.2617
14	-0.0112	1.1101	-0.0002	1.2324	0.1195
15	-0.0038	-0.9183	0.0003	0.8433	0.0823
16	0.6128	-0.0009	-0.1496	0.3979	0.0389
17	-0.3629	0.0092	-0.3445	0.2505	0.0251
18	-0.0124	-0.6695	0.0017	0.4484	0.0450
19	-0.1930	0.0163	0.2324	0.0915	0.0092
20	-1.5189	0.0052	0.2869	2.3894	0.2408
21	-0.0051	-1.0135	0.0009	1.0271	0.1039
22	-0.0003	0.3349	0.0005	0.1121	0.0114
23	-0.0828	0.0003	0.3574	0.1346	0.0138
24	0.0014	0.1266	-0.0023	0.0160	0.0016
25	-0.4532	-0.0002	-0.2077	0.2485	0.0255
26	-0.0079	0.0145	-0.0037	0.0003	0.0000
27	-0.2382	0.0033	-0.1861	0.0914	0.0094
28	-0.0038	-0.1272	-0.0032	0.0162	0.0017
29	-0.3151	-0.0006	-0.2793	0.1773	0.0183
30	-0.0013	0.2468	0.0010	0.0609	0.0063
31	-0.0006	-0.6965	-0.0001	0.4852	0.0504
32	-0.6893	0.0004	-0.2694	0.5477	0.0572
33	0.0052	0.2092	0.0003	0.0438	0.0046
34	-0.8054	-0.0010	0.0297	0.6496	0.0686
35	0.0038	-0.6103	-0.0002	0.3724	0.0395
36	-0.5621	-0.0013	0.1100	0.3280	0.0350
37	-0.6991	0.0005	0.1311	0.5059	0.0541
38	-0.0045	-0.1982	0.0009	0.0393	0.0042
39	-0.0016	-0.1689	0.0009	0.0285	0.0031
40	-0.5981	0.0006	0.2220	0.4071	0.0440

Rotatory Strengths (R) in cgs (10**-40 erg-esu-cm/Gauss)

state	XX	YY	ZZ	R(velocity)	E-M Angle
1	69.3446	-460.0356	-457.3801	-282.6904	159.14
2	232.7368	-0.0001	244.8830	159.2066	0.07
3	410.1199	-0.0001	394.5772	268.2323	0.07
4	-0.3059	-204.6765	-101.7171	-102.2332	170.25
5	99.6202	-0.0006	153.8181	84.4792	0.37
6	29.6038	-153.8757	-352.3007	-158.8575	174.33
7	-47.3058	65.8350	-32.4355	-4.6355	91.82
8	-165.7931	0.0000	-22.4153	-62.7362	90.00
9	1.1716	-0.9067	-41.6346	-13.7899	105.55
10	38.4569	0.0002	53.7161	30.7244	0.82
11	394.5664	-226.0437	-293.3879	-41.6217	99.30
12	63.8557	-0.0647	78.2375	47.3428	3.29
13	10.1421	-618.2894	-391.7183	-333.2885	154.99
14	653.8991	-0.0257	735.7824	463.2186	0.77
15	107.7471	-0.0010	259.8380	122.5280	0.32
16	-1.2406	-8.0305	-41.7111	-16.9941	144.42
17	159.7797	-167.3697	-26.9137	-11.5013	103.71
18	-70.0673	0.0596	266.1305	65.3743	2.31
19	-75.8540	35.1204	-4.2691	-15.0009	115.94
20	-408.8857	421.2474	-194.7703	-60.8029	99.02
21	-39.2943	0.0066	368.5685	109.7603	0.85
22	-19.0753	0.0004	49.0539	9.9930	1.08
23	526.1227	-145.1260	-5.7077	125.0963	23.95
24	-95.7840	-0.0083	-33.7934	-43.1952	178.36
25	-27.5560	36.2850	8.1318	5.6202	79.14
26	-1.7926	0.0089	0.4856	-0.4327	148.37
27	-178.8188	-62.8098	3.3692	-79.4198	130.98
28	42.8453	-0.0451	-10.4480	10.7841	8.32
29	-138.2744	51.4186	0.3857	-28.8234	131.33
30	56.4430	-0.0012	40.6534	32.3651	0.54
31	-50.7219	0.0001	88.6509	12.6431	90.00
32	84.6139	0.3227	-60.0394	8.2991	77.19
33	149.1788	-0.0030	98.2012	82.4590	1.32
34	2.5116	-182.5717	-123.4979	-101.1860	126.66
35	138.1419	0.0007	165.7645	101.3024	0.44
36	-6.2887	44.4872	-115.6484	-25.8166	156.30
37	-6.2741	-125.0746	-66.8589	-66.0692	137.35
38	82.4573	-0.0066	29.6787	37.3764	1.56
39	119.9225	-0.0004	46.2690	55.3970	0.62
40	9.0694	-91.5272	-60.9730	-47.8103	122.48

Figure S51. TD-DFT simulative transition electric dipole moments and their angles for **(*R*)-P1** (S_0 to S_1−S_{40}).

Ground to excited state transition electric dipole moments (Au):

state	X	Y	Z	Dip. S.	Osc.
1	-0.9540	-0.0000	-0.2568	0.9760	0.0739
2	0.0003	0.5151	0.0000	0.2653	0.0203
3	-0.8670	0.0009	-0.1003	0.7617	0.0604
4	0.0007	0.6226	0.0000	0.3876	0.0308
5	-0.1463	0.0000	-0.2228	0.0710	0.0062
6	-0.0003	-0.0959	-0.0002	0.0092	0.0008
7	-0.0001	-0.4277	0.0001	0.1829	0.0163
8	0.7747	0.0010	-0.0030	0.6002	0.0535
9	1.8790	-0.0002	-0.1042	3.5413	0.3191
10	0.0000	-0.9954	0.0000	0.9909	0.0901
11	-0.0005	0.7640	-0.0000	0.5837	0.0532
12	-0.5630	0.0002	0.0446	0.3190	0.0292
13	0.4894	0.0000	-0.4136	0.4106	0.0385
14	0.3099	0.0003	-0.0177	0.0963	0.0091
15	-0.0002	-0.0331	0.0004	0.0011	0.0001
16	-0.0003	-0.0636	0.0000	0.0040	0.0004
17	-0.5993	-0.0001	-0.1713	0.3884	0.0373
18	0.0001	-0.7168	0.0001	0.5137	0.0493
19	0.0001	-1.0424	0.0000	1.0866	0.1061
20	1.0789	-0.0003	-0.0616	1.1678	0.1145
21	-0.0012	0.2620	0.0003	0.0686	0.0068
22	0.6638	-0.0000	-0.3385	0.5552	0.0548
23	-0.5556	-0.0001	0.0538	0.3116	0.0310
24	0.0007	0.6056	-0.0000	0.3668	0.0366
25	0.0000	-0.4174	0.0000	0.1742	0.0176
26	0.3321	0.0006	0.0725	0.1156	0.0117
27	0.0881	-0.0006	0.0523	0.0105	0.0011
28	0.0003	-0.9993	0.0001	0.9986	0.1016
29	0.5760	0.0007	0.3211	0.4350	0.0444
30	-0.1647	-0.0233	-0.1056	0.0388	0.0040
31	0.0272	-0.1413	0.0174	0.0210	0.0022
32	0.0001	-0.6174	0.0000	0.3812	0.0392
33	0.0006	0.5779	-0.0001	0.3340	0.0347
34	0.7897	-0.0002	0.0185	0.6240	0.0650
35	0.2421	0.0010	-0.0733	0.0640	0.0067
36	0.0005	-0.1390	-0.0002	0.0193	0.0020
37	0.2102	-0.0008	-0.0460	0.0463	0.0049
38	0.0044	0.2186	-0.0015	0.0478	0.0050
39	0.8237	-0.0018	-0.2803	0.7571	0.0799
40	-0.0009	-0.3993	0.0004	0.1595	0.0169

Rotatory Strengths (R) in cgs (10**-40 erg-esu-cm/Gauss)

state	XX	YY	ZZ	R(velocity)	E-M Angl
1	50.2367	-269.3697	-227.2242	-148.7857	172.31
2	122.3696	-0.0000	128.5303	83.6333	90.00
3	30.7288	-153.8401	-191.6742	-104.9285	175.84
4	146.0889	-0.0001	147.8523	97.9804	90.00
5	3.5764	-25.3792	-6.9145	-9.5724	159.84
6	2.1834	-0.0000	5.0095	2.3976	90.00
7	70.3396	0.0000	90.7364	53.6920	90.00
8	2.0466	-128.7808	-139.1854	-88.6399	176.75
9	-84.7876	-304.0513	-711.2719	-366.7036	176.45
10	403.3837	-0.0000	500.9463	301.4433	90.00
11	232.6844	-0.0000	263.6647	165.4497	90.00
12	-3.7873	-27.8395	-81.7688	-37.7985	169.99
13	-57.4919	-21.4620	-44.3946	-41.1162	174.56
14	-1.0709	-16.9302	-12.6476	-10.2162	134.15
15	-2.4381	-0.0001	-1.4325	-1.2902	90.00
16	3.6526	-0.0000	5.3413	2.9980	90.00
17	191.9014	11.7040	-63.6327	46.6575	75.79
18	-131.6822	-0.0000	-52.0217	-61.2347	90.00
19	258.6823	-0.0000	532.2504	263.6442	90.00
20	-28.5971	-86.4819	-230.2982	-115.1257	140.94
21	9.8880	0.0000	-0.5234	3.1215	90.00
22	-134.4390	-4.7430	-25.8852	-55.0224	148.39
23	-45.6390	19.4552	-68.7079	-31.6306	115.22
24	1.7737	0.0000	110.2726	37.3488	90.00
25	-12.6619	-0.0000	25.7396	4.3592	90.00
26	44.1726	-15.1618	-13.4024	5.2028	83.77
27	37.3198	2.6588	9.1211	16.3666	50.82
28	-471.3308	0.0000	147.0679	-108.0876	90.00
29	495.3133	-35.0904	-70.7861	129.8122	58.36
30	-95.1102	-59.4423	-0.0128	-51.5218	130.03
31	37.0035	-1.6261	-11.4451	7.9774	52.41
32	-31.5139	-0.0000	48.9791	5.8217	90.00
33	-29.1573	-0.0001	69.3982	13.4136	90.00
34	1.2829	-43.0727	-139.6374	-60.4757	128.68
35	-5.1321	2.2135	-3.2291	-2.0492	162.44
36	9.6309	0.0000	12.9383	7.5231	90.00
37	2.1777	-16.5050	-21.4350	-11.9207	141.07
38	39.2944	-0.0028	32.8964	24.0627	1.52
39	29.7914	-87.1096	-177.3124	-78.2102	126.76
40	105.5323	-0.0001	79.6193	61.7172	0.21

Figure S52. TD-DFT simulative transition electric dipole moments and their angles for **(*R*)-PO1** (S_0 to S_1–S_{40}).

Ground to excited state transition electric dipole moments (Au):

state	X	Y	Z	Dip. S.	Osc.
1	2.2343	-0.2343	-0.0522	5.0499	0.3797
2	0.3625	-1.2711	-0.0563	1.7502	0.1335
3	-0.9499	-1.4229	0.0402	2.9285	0.2269
4	0.3026	-0.3954	-0.0105	0.2480	0.0195
5	-1.1388	-0.2155	0.2035	1.3847	0.1160
6	-1.0215	1.3216	0.1926	2.8272	0.2384
7	-0.3842	0.2215	0.1634	0.2234	0.0191
8	-0.7763	0.1051	0.2837	0.6942	0.0613
9	-1.2241	-0.7221	0.1215	2.0346	0.1844
10	0.5493	-0.5718	0.0477	0.6310	0.0574
11	0.3721	0.2608	-0.3837	0.3537	0.0324
12	-0.2729	0.3988	0.2918	0.3187	0.0294
13	-0.1666	0.0568	-0.4457	0.2296	0.0214
14	0.1600	0.1324	0.0139	0.0433	0.0041
15	-0.4590	0.3004	0.5195	0.5709	0.0543
16	0.1687	-0.6448	-0.2573	0.5104	0.0487
17	-0.4224	-0.1950	0.1419	0.2366	0.0227
18	0.3525	0.5444	-0.2626	0.4896	0.0471
19	0.9094	-0.4325	-0.3992	1.1734	0.1141
20	-0.2108	-1.7542	0.4362	3.3119	0.3225
21	-0.0399	0.5414	-0.2439	0.3542	0.0347
22	-0.2047	-0.1727	0.1057	0.0829	0.0082
23	-0.0808	0.3636	0.0206	0.1391	0.0138
24	0.0023	0.2804	-0.1266	0.0946	0.0095
25	-0.0083	0.3936	-0.0220	0.1555	0.0157
26	-0.0828	0.0105	0.0337	0.0081	0.0008
27	0.1177	-0.6007	-0.1890	0.4104	0.0419
28	-0.6930	-0.4242	-0.3547	0.7861	0.0810
29	0.0620	-0.0090	-0.0048	0.0040	0.0004
30	0.0041	0.1231	0.0597	0.0187	0.0019
31	-0.5577	-0.5465	-0.2025	0.6506	0.0675
32	-0.2643	-0.2505	0.2676	0.2042	0.0212
33	-0.3246	-0.0626	0.1693	0.1379	0.0144
34	0.0665	-0.4394	0.1009	0.2077	0.0218
35	-0.3811	-0.1866	0.0135	0.1802	0.0189
36	0.0220	0.0464	-0.0226	0.0031	0.0003
37	-0.5319	-0.5415	0.1826	0.6095	0.0644
38	0.2391	-0.3478	-0.0734	0.1835	0.0194
39	-0.0979	-0.0375	0.0733	0.0164	0.0017
40	-0.4379	0.5666	0.0833	0.5197	0.0552

Rotatory Strengths (R) in cgs (10**-40 erg-esu-cm/Gauss)

state	XX	YY	ZZ	R(velocity)	E-M Angle
1	1.9133	-933.0740	-1061.0066	-664.0557	152.27
2	516.0249	-22.3914	391.1468	294.9268	32.06
3	603.5287	-188.5293	337.4022	250.8005	61.85
4	62.8276	-30.3058	16.4320	16.3179	73.30
5	-85.3740	31.7929	-202.0680	-85.2164	157.50
6	394.6951	-76.4879	159.4195	159.2089	69.40
7	17.6546	31.6208	18.0508	22.4420	66.35
8	-14.2496	3.7185	-89.5533	-33.3615	120.47
9	119.8165	-124.3673	-127.1880	-43.9129	99.58
10	13.4132	-76.7292	-17.6023	-26.9728	103.57
11	-34.6062	-267.5273	49.1206	-84.3376	109.33
12	-40.6516	-166.0734	46.7619	-53.3211	102.59
13	41.5705	-17.2362	-25.9873	-0.5510	90.36
14	-12.5379	9.2106	-0.8170	-1.3815	96.61
15	-117.5993	-119.3090	28.3947	-69.5045	114.51
16	84.2901	0.1383	37.2502	40.5595	78.69
17	13.1886	28.6486	-40.4867	0.4502	89.25
18	-74.3302	-58.7241	25.9490	-35.7018	103.65
19	1206.5708	67.8019	136.8932	470.4220	67.60
20	-1328.1728	-44.0214	361.2826	-336.9705	124.14
21	35.5239	-1.9253	121.0656	51.5547	42.58
22	5.1295	6.4762	5.5832	5.7296	58.81
23	-20.3656	-3.8314	-3.8028	-9.3333	100.26
24	79.5201	-33.7138	25.1287	23.6450	13.65
25	38.2624	1.3150	70.6505	36.7426	28.74
26	0.4394	0.1149	-1.9860	-0.4772	105.54
27	61.5013	35.5313	83.3515	60.1280	33.43
28	0.3138	-147.2418	-211.7509	-119.5596	122.17
29	-0.2694	-5.0238	0.8388	-1.4848	165.66
30	-0.5158	-0.3206	1.4084	0.1907	86.54
31	72.7842	-136.4378	-50.1131	-37.9223	108.27
32	101.0150	57.5513	14.8697	57.8120	60.00
33	-62.2910	3.8567	-22.3724	-26.9356	133.85
34	42.0296	-24.0251	0.2945	6.0996	86.90
35	7.7332	79.7480	-35.4850	17.3321	67.44
36	-0.4660	0.5442	0.3684	0.1489	90.00
37	-67.0851	69.9477	23.3581	8.7402	82.42
38	-4.7928	16.2051	37.1556	16.1893	73.46
39	-19.0041	12.0833	10.5780	1.2191	84.65
40	134.0868	24.0535	54.0741	70.7381	47.69

Figure S53. TD-DFT simulative transition electric dipole moments and their angles for **(*R*)-P2** (S_0 to S_1−S_{40}).

Ground to excited state transition electric dipole moments (Au):

state	X	Y	Z	Dip. S.	Osc.
1	2.6052	0.0004	-0.0659	6.7913	0.5142
2	-0.0007	1.5694	-0.0001	2.4630	0.1898
3	-0.0073	0.0302	0.0013	0.0010	0.0001
4	0.4701	0.0006	-0.0843	0.2281	0.0177
5	-1.4057	0.0013	0.2630	2.0451	0.1679
6	-0.0032	-0.7914	0.0007	0.6263	0.0518
7	0.0252	1.0309	-0.0086	1.0634	0.0959
8	1.6685	-0.0201	-0.4036	2.9472	0.2666
9	0.0147	-0.1504	0.0170	0.0231	0.0021
10	-0.4334	-0.0201	-0.3417	0.3050	0.0279
11	-0.4348	-0.0010	0.4559	0.3969	0.0369
12	0.0028	0.1185	-0.0026	0.0141	0.0013
13	-0.0147	0.8474	0.0180	0.7186	0.0684
14	-0.3435	-0.0306	0.4705	0.3404	0.0325
15	-0.0972	-0.0000	0.8301	0.6985	0.0673
16	0.0114	0.0142	-0.0300	0.0012	0.0001
17	-0.0073	-2.1045	0.0029	4.4290	0.4327
18	-0.6793	0.0211	0.1082	0.4736	0.0464
19	0.0050	-0.2044	-0.0003	0.0418	0.0041
20	0.2072	-0.0002	-0.1532	0.0664	0.0066
21	0.0004	-0.1173	0.0000	0.0138	0.0014
22	-0.0008	-0.0857	0.0006	0.0073	0.0007
23	-0.4318	0.0035	0.1917	0.2232	0.0222
24	0.0028	0.1554	-0.0010	0.0242	0.0024
25	-0.1825	0.0135	0.0628	0.0374	0.0038
26	-0.0191	-0.1328	0.0065	0.0180	0.0018
27	0.0002	-0.2716	-0.0001	0.0738	0.0075
28	-0.0804	-0.0026	0.0110	0.0066	0.0007
29	-0.1953	0.1012	0.0691	0.0531	0.0055
30	-0.1003	-0.2059	0.0350	0.0537	0.0056
31	-0.1223	0.2060	0.0106	0.0575	0.0060
32	0.3483	0.0744	-0.0295	0.1277	0.0134
33	0.0009	-0.7742	-0.0001	0.5994	0.0631
34	1.4229	0.0021	-0.1507	2.0473	0.2164
35	0.0230	-0.2255	0.0053	0.0514	0.0055
36	0.0456	0.0855	0.0166	0.0097	0.0010
37	-0.0016	-0.1594	0.0007	0.0254	0.0027
38	0.4094	-0.0020	-0.1234	0.1828	0.0195
39	-0.2843	0.0100	0.0739	0.0864	0.0092
40	-0.0102	-0.3311	0.0026	0.1098	0.0117

Rotatory Strengths (R) in cgs (10**-40 erg-esu-cm/Gauss)

state	XX	YY	ZZ	R(velocity)	E-M Angle
1	-30.5130	-1005.8153	-1103.7955	-713.3746	176.74
2	996.5761	-0.0001	845.3645	613.9802	0.05
3	-0.1564	-0.0064	-0.2035	-0.1221	90.00
4	-8.2008	-27.6133	-42.6646	-26.1596	164.48
5	-88.1696	17.0344	-262.2287	-111.1213	148.12
6	181.1829	-0.0007	193.8647	125.0156	0.40
7	840.3652	-0.1037	442.7733	427.6782	1.91
8	-331.4703	-281.3593	-255.4459	-289.4252	147.90
9	-115.4883	-0.7755	5.7581	-36.8352	174.01
10	-205.2083	-319.2157	-97.8183	-207.4141	140.12
11	-64.2506	75.5734	-14.6631	-1.1134	96.53
12	-19.6620	0.0027	-4.5225	-8.0606	178.42
13	-489.6373	-0.0239	97.5400	-130.7070	169.97
14	804.2138	-52.7970	62.1088	271.1752	32.19
15	-148.8009	-239.9608	23.2304	-121.8438	127.29
16	-43.8759	-7.1485	0.0598	-16.9882	145.58
17	-562.4027	-0.0081	483.0119	-26.4663	152.33
18	283.0805	41.4376	-33.4423	97.0253	81.71
19	-18.6116	0.0025	-20.0809	-12.8966	172.61
20	-14.1605	15.8335	8.5448	3.4060	61.02
21	-10.3175	0.0001	-8.7618	-6.3597	90.00
22	-4.3904	-0.0000	-7.8741	-4.0882	90.00
23	-5.6448	33.2731	7.4667	11.6983	63.63
24	7.7857	0.0015	-5.5121	0.7584	15.23
25	-1.7643	8.8385	-1.6270	1.8157	73.70
26	8.0583	0.0964	3.5087	3.8878	10.02
27	2.1958	0.0000	-11.2949	-3.0330	174.77
28	-5.0453	-3.1781	-2.6456	-3.6230	111.15
29	-17.8940	-4.8487	-1.0673	-7.9367	116.34
30	4.6469	-1.3309	5.9409	3.0856	73.72
31	19.1492	-9.2339	23.2861	11.0671	57.82
32	7.5129	-75.4107	-40.2318	-36.0432	147.63
33	257.0094	-0.0032	252.8616	169.9559	0.66
34	-123.7427	12.1370	-356.6642	-156.0900	137.52
35	22.6363	0.0347	12.7493	11.8068	38.05
36	-0.5979	0.2513	1.3228	0.3254	88.27
37	-17.2394	0.0012	-6.6602	-7.9662	90.00
38	62.1973	95.0020	54.5247	70.5746	64.93
39	-19.3751	10.7421	9.2755	0.2141	88.43
40	60.1599	0.0144	37.2567	32.4770	1.86

Figure S54. TD-DFT simulative transition electric dipole moments and their angles for **(*R*)-PO2** (S_0 to S_1−S_{40}).

Name	μ_e	μ_m	θ	$\lvert g_{lum} \rvert$
P1	4.1×10^{-18}	9.7×10^{-21}	147.2	7.9×10^{-3}
PO1	5.9×10^{-19}	2.3×10^{-21}	108.3	4.8×10^{-3}
P2	5.1×10^{-19}	7.8×10^{-22}	69.1	2.2×10^{-3}
PO2	4.8×10^{-18}	1.1×10^{-21}	94.1	0.66×10^{-3}

Figure S55. TD-DFT simulative transition electric-magnetic dipole moments and their angles, g_{lum} values for four emitters ($S_1 \rightarrow S_0$ states).

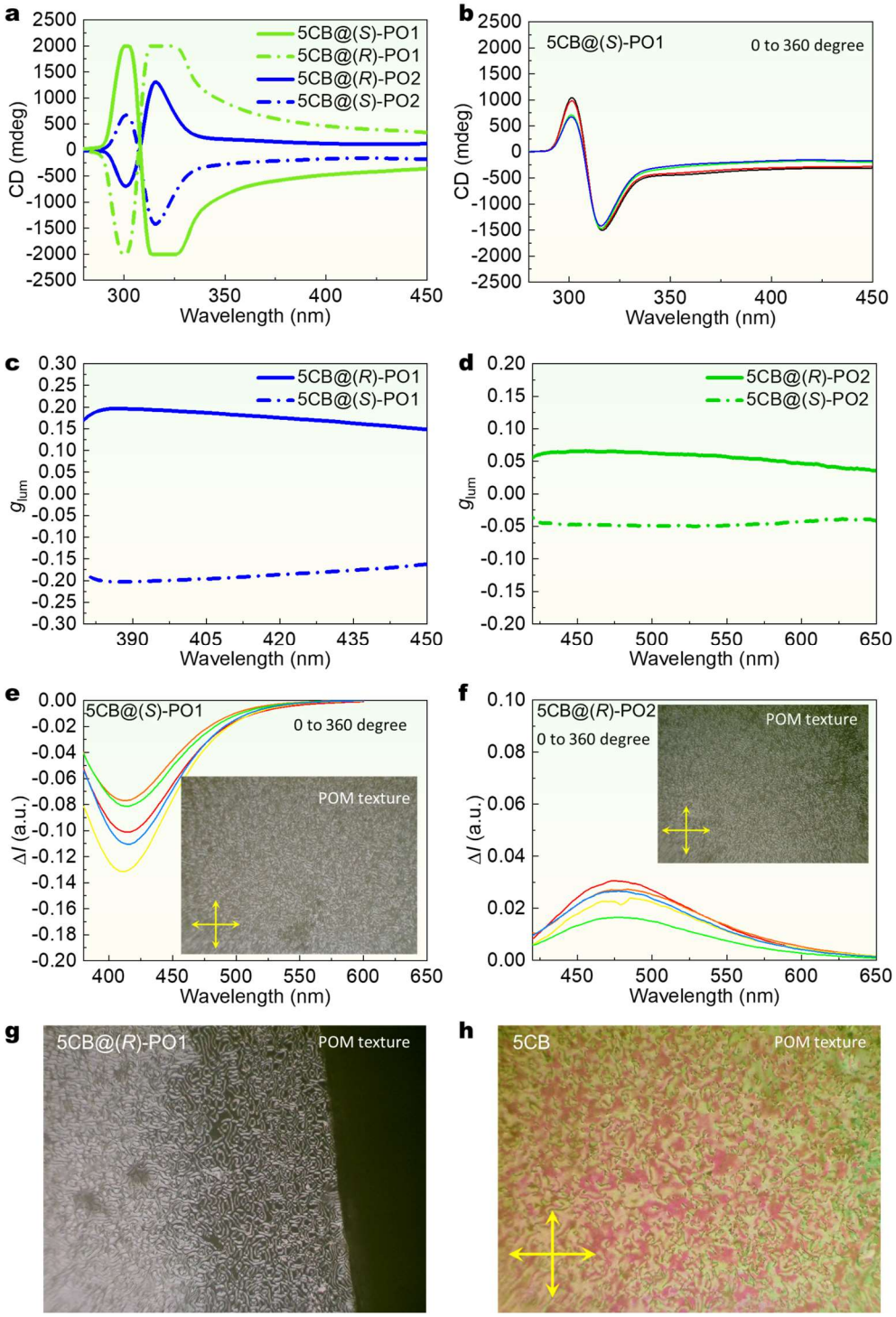

Figure S56. (a) CD and (b) angle-dependent CD spectra of chiral LC film at 25 °C. (c,d) g_{lum} spectra of chiral LC film at 25 °C. (e,f) Angle-dependent CPL spectra of chiral LC film at 25 °C. (g,h) POM textures of doped chiral LC (N* mesophase) film and achiral 5CB (N mesophase) at 25 °C.

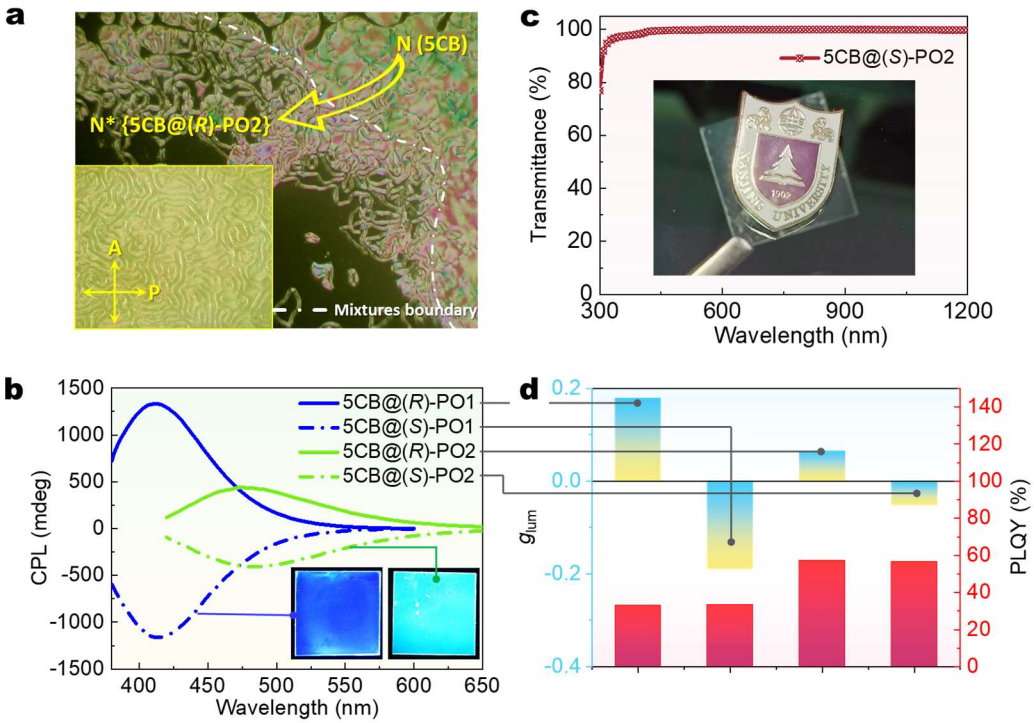

Figure S57. (a) Polarized optical microscope (POM) textures for mixtures of pure 5CB and emitter-doped 5CB at liquid crystal phase (inserted POM picture is **5CB@(*R*)-PO2** film in N* mesophase; 0.2% wt doping concentration; 25 °C). (b) CPL spectra and emission images of chiral LC films at 25 °C (Ex = 330 nm). (g) g_{lum} and PLQY value comparisons for LC films. (c) Transmission spectra of **5CB@(*R*)-PO2** film at 25 °C (inserted picture is corresponding transparent LC film under daylight). (d) g_{lum} and PLQY values of LCs films.

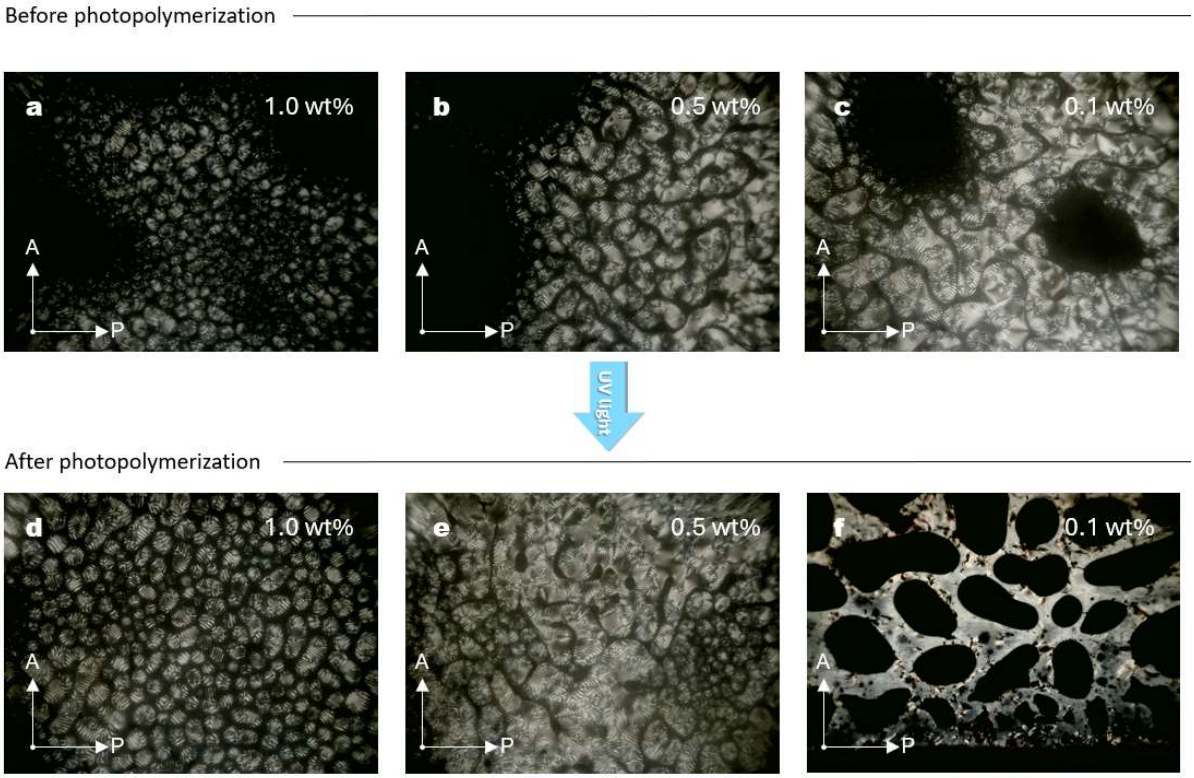

Figure S58. (a–c) Polarized optical microscope (POM) textures for mixtures of RM257, IRG651, and ***(S)*-PO1** at liquid crystal phase (100 °C, before photopolymerization). (d–f) Polarized optical microscope (POM) textures for polymeric liquid crystals (25 °C, after photopolymerization).

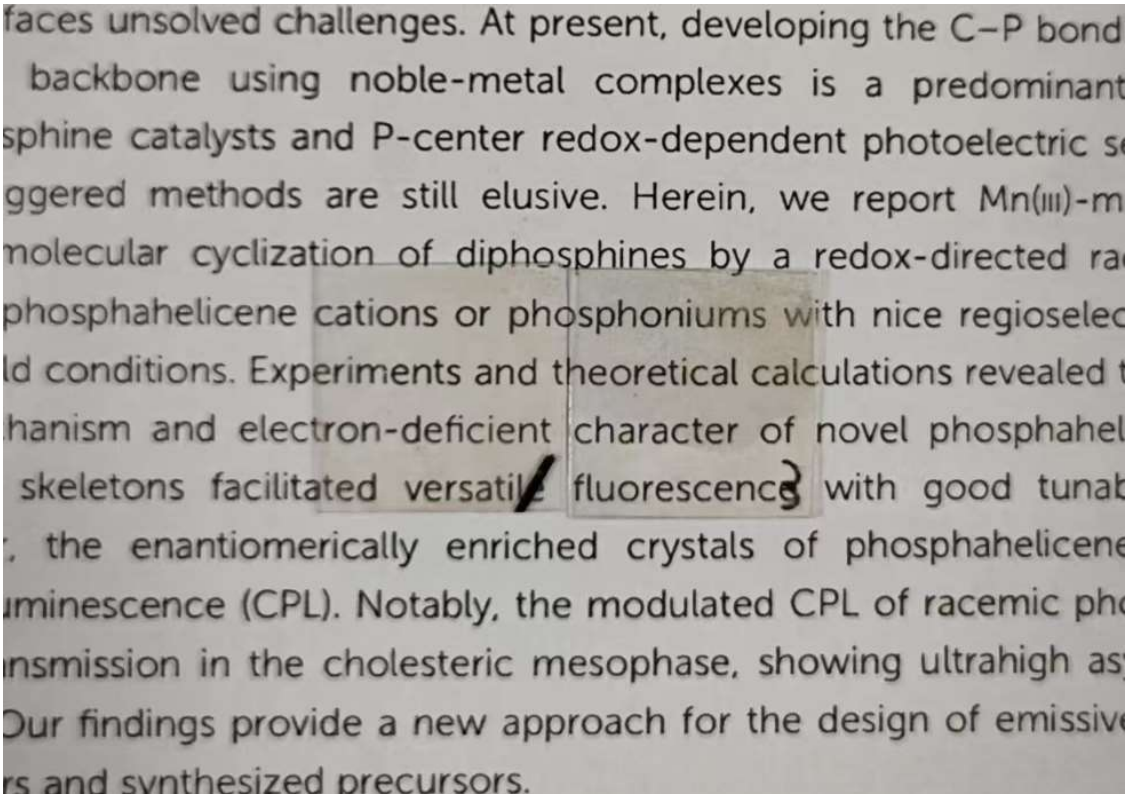

Figure S59. Photograph of transparent **PLC@PO1** films under daylight.

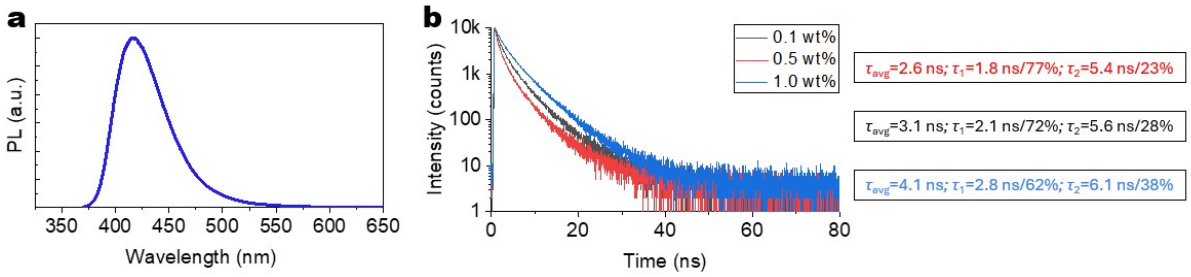

Figure S60. (a) PL spectra of mixtures of RM257, IRG651, and **(*S*)-PO1** at quenched liquid crystal phase (before photopolymerization, 25 °C). (b) Lifetime decay of the polymeric liquid crystal films (after photopolymerization, 25 °C).

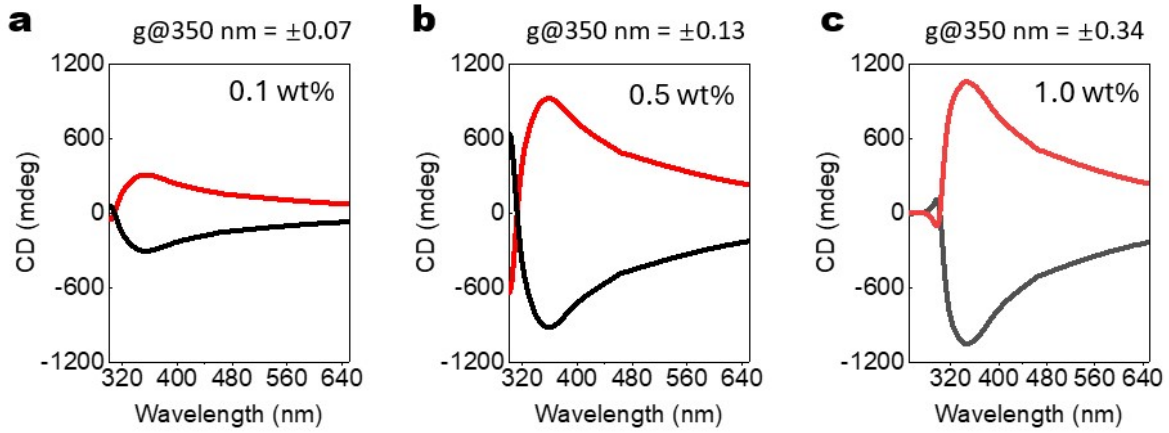

Figure S61. (a–c) CD spectra of the polymeric liquid crystal films (25 °C, after photopolymerization). Red line: **PLC@(*R*)-PO1**; Black line: **PLC@(*S*)-PO1**.

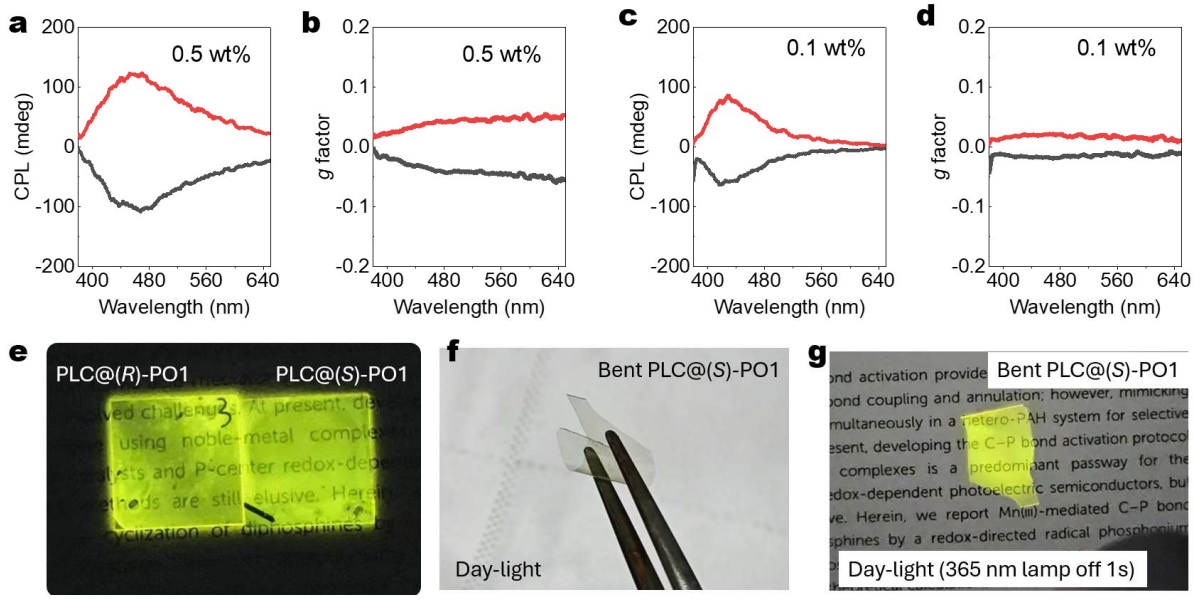

Figure S62. (a–d) CPL spectra of mixtures of the polymeric liquid crystal films (25 °C, after photopolymerization). (e) CP-OURTP emissive observation without polarized glasses, no obvious brightness difference. (f) Photograph of bent **PLC@PO1** films under daylight. (g) Photograph of transparent **PLC@PO1** films under daylight (365 nm off 1 s).

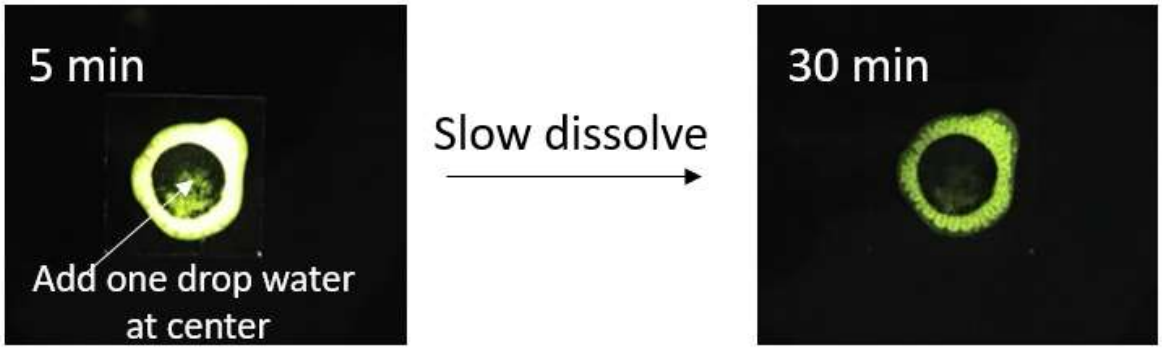

Figure S63. RTP quenching phenomenon of **PO1@PVP** in water. The central sample is slowly dissolved.

Table S5. Summary of the TD-DFT calculations for **(*R*)-P1**			
States (S_n)	Energy (eV)	*f*	Contribution
1	3.2976	0.17670	H -> L 95.1%
2	3.3776	0.03210	H-1 -> L 94.9%
3	3.5121	0.03610	H-2 -> L 80.3%, H -> L+1 11.9%
4	3.5506	0.06440	H-3 -> L 81.8%
5	3.7053	0.03680	H -> L+1 82.9%, H-2 -> L 10.9%
6	3.7144	0.16000	H-1 -> L+1 90.9%
7	3.8177	0.04590	H-4 -> L 31.5%, H -> L+3 16.9%, H -> L+5 14.3%, H-1 -> L+4 13.9%
8	3.8275	0.02720	H -> L+4 30.1%, H-5 -> L 27.2%, H-1 -> L+5 23.2%
9	3.8414	0.02470	H-2 -> L+1 35.2%, H -> L+5 17.9%, H -> L+3 16.3%, H-1 -> L+4 13.1%
10	3.8733	0.00370	H-3 -> L+1 24.6%, H-1 -> L+3 17.3%, H -> L+4 10.1%, H -> L+2 9.3%, H-1 -> L+5 9.0%, H-2 -> L+3 5.9%
H (HOMO), L (LUMO). Only MO transitions with absolute contribution ≥ 5.0 % are shown above.			

Table S6. Summary of the TD-DFT calculations for **(*R*)-PO1(syn)**			
States (S_n)	Energy (eV)	*f*	Contribution
1	3.0905	0.07390	H -> L 96.9%
2	3.1229	0.02030	H-1 -> L 97.1%
3	3.2376	0.06040	H-1 -> L+1 96.8%
4	3.2397	0.03080	H -> L+1 96.7%
5	3.5914	0.00620	H-2 -> L 94.3%
6	3.6067	0.00080	H-3 -> L 89.6%
7	3.6277	0.01630	H -> L+2 90.4%
8	3.6406	0.05350	H-1 -> L+2 94.1%
9	3.6780	0.31910	H -> L+3 85.1%
10	3.7113	0.09010	H-1 -> L+3 60.4%, H-2 -> L+1 29.8%
H (HOMO), L (LUMO). Only MO transitions with absolute contribution ≥ 5.0 % are shown above.			

Table S7. Summary of the TD-DFT calculations for **(*R*)-P2**			
States (S_n)	Energy (eV)	*f*	Contribution
1	3.0687	0.37970	H -> L 51.3%, H-1 -> L 35.7%, H -> L+1 7.6%
2	3.1135	0.13350	H-1 -> L 56.9%, H -> L 40.4%
3	3.1625	0.22690	H -> L+1 83.5%, H -> L 5.2%
4	3.2116	0.01950	H-1 -> L+1 90.2%
5	3.4206	0.11600	H -> L+2 86.7%
6	3.4425	0.23840	H-1 -> L+2 87.5%
7	3.4933	0.01910	H-2 -> L 84.5%
8	3.6042	0.06130	H-2 -> L+1 83.3%
9	3.6997	3.6997	H -> L+3 77.3%, H-1 -> L+3 9.1%
10	3.7139	0.05740	H-1 -> L+3 58.7%, H-1 -> L+6 13.0%, H -> L+3 9.3%, H-1 -> L+5 6.5%
H (HOMO), L (LUMO). Only MO transitions with absolute contribution ≥ 5.0 % are shown above.			

Table S8. Summary of the TD-DFT calculations for **(*R*)-PO2**			
States (S_n)	Energy (eV)	*f*	Contribution
1	3.0903	0.51420	H -> L 69.4%, H-1 -> L+1 27.5%
2	3.1459	0.18980	H-1 -> L 55.8%, H -> L+1 41.7%
3	3.1732	0.00010	H -> L+1 54.1%, H-1 -> L 41.9%
4	3.1758	0.01770	H-1 -> L+1 67.5%, H -> L 28.0%
5	3.3510	0.16790	H -> L+2 90.4%
6	3.3747	0.05180	H-1 -> L+2 91.6%
7	3.6826	0.09590	H -> L+3 84.4%, H-1 -> L+7 5.9%
8	3.6925	0.26660	H-1 -> L+3 77.0%, H -> L+7 7.8%
9	3.7286	0.00210	H -> L+4 33.9%, H-1 -> L+7 18.5%, H -> L+8 16.9%, H-1 -> L+9 9.5%, H -> L+3 6.2%
10	3.7316	0.02790	H-1 -> L+4 30.2%, H -> L+7 18.9%, H-1 -> L+8 17.2%, H -> L+9 10.6%, H-1 -> L+3 7.7%
H (HOMO), L (LUMO). Only MO transitions with absolute contribution ≥ 5.0 % are shown above.			

Table S9. Summary of the TD-DFT calculations for **(*R*)-P3**			
States (S_n)	Energy (eV)	*f*	Contribution
1	3.0021	0.44080	H -> L 84.8%, H-1 -> L+1 13.1%
2	3.0518	0.16320	H-1 -> L 91.1%, H -> L+1 7.4%
3	3.1078	0.05760	H -> L+1 88.9%, H-1 -> L 7.2%
4	3.1114	0.09200	H-1 -> L+1 81.4%, H -> L 13.3%
5	3.2286	0.16170	H -> L+2 91.0%
6	3.2516	0.06990	H-1 -> L+2 93.2%
7	3.5510	0.00320	H-1 -> L+5 36.4%, H -> L+4 29.3%, H -> L+6 22.6%, H-1 -> L+7 7.4%
8	3.5520	0.02560	H -> L+5 38.8%, H-1 -> L+4 27.0%, H-1 -> L+6 22.2%, H -> L+7 7.8%
9	3.6243	0.00660	H-2 -> L 77.2%, H -> L+3 8.5%, H-3 -> L+1 5.5%
10	3.6580	0.11690	0.11690
H (HOMO), L (LUMO). Only MO transitions with absolute contribution ≥ 5.0 % are shown above.			

Table S10. Summary of the TD-DFT calculations for **(*R*)-PO3**			
States (S_n)	Energy (eV)	*f*	Contribution
1	3.0035	0.47760	H -> L 71.0%, H-1 -> L+1 26.5%
2	3.0548	0.17390	H-1 -> L 64.6%, H -> L+1 33.7%
3	3.0741	0.00290	H -> L+1 63.1%, H-1 -> L 33.5%
4	3.0765	0.02200	H-1 -> L+1 69.2%, H -> L 27.0%
5	3.2574	0.18780	H -> L+2 91.6%
6	3.2795	0.06380	H-1 -> L+2 92.8%
7	3.5469	0.01710	H -> L+4 28.0%, H-1 -> L+5 25.7%, H -> L+8 16.7%, H-1 -> L+6 14.8%, H -> L+3 10.3%
8	3.5483	0.05770	H -> L+5 27.5%, H-1 -> L+4 27.1%, H-1 -> L+8 16.7%, H -> L+6 15.9%, H-1 -> L+3 8.3%
9	3.6121	0.11050	H -> L+3 81.9%, H -> L+4 6.5%
10	3.6186	0.30470	H-1 -> L+3 80.9%, H-1 -> L+4 5.4%
H (HOMO), L (LUMO). Only MO transitions with absolute contribution ≥ 5.0 % are shown above.			

F: NMR spectra data, HRMS, and cartesian coordinates

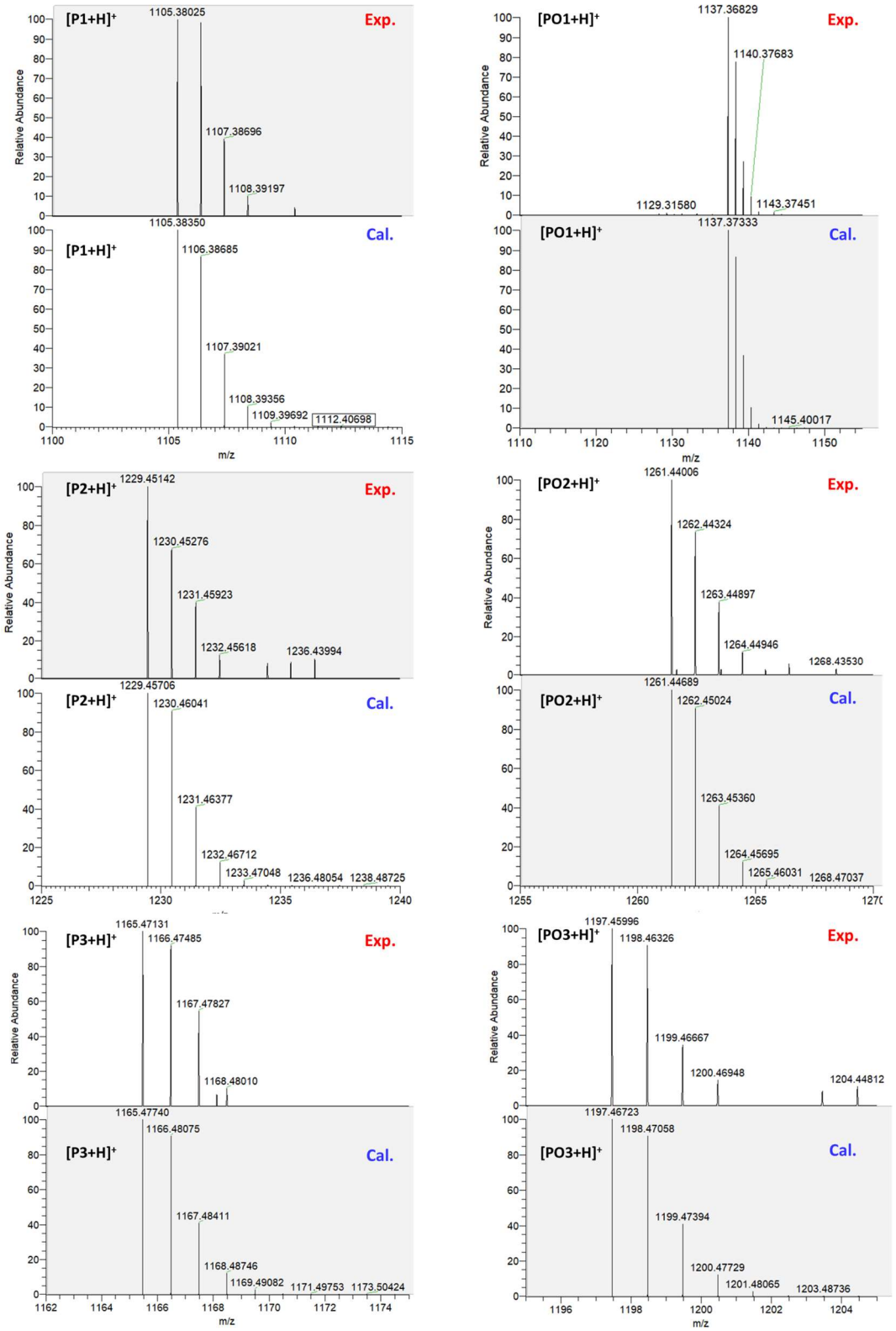

Figure S64. ESI-HRMS data for all compounds.

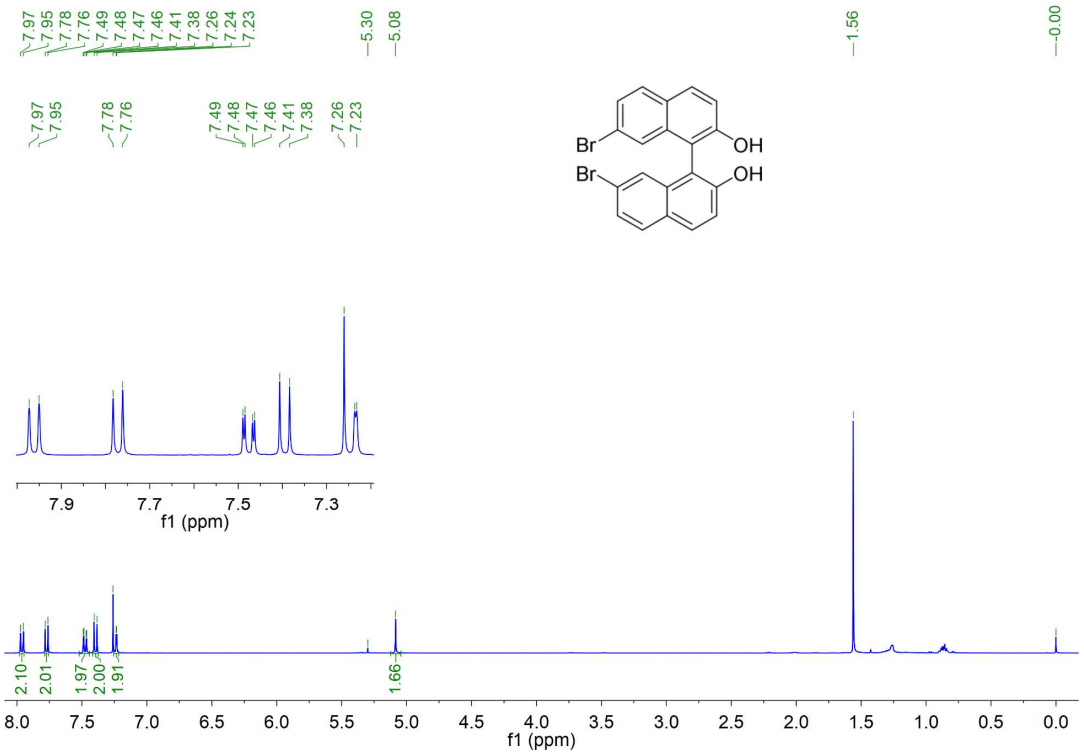

^{1}H NMR (400 MHz, $CDCl_3$) δ 7.96 (d, J = 8.9 Hz, 2H), 7.77 (d, J = 8.7 Hz, 2H), 7.48 (dd, J = 8.7, 1.9 Hz, 2H), 7.39 (d, J = 8.9 Hz, 2H), 7.23 (d, J = 1.8 Hz, 2H), 5.08 (s, 2H). *1.56–0.8 ppm denote trace grease from PE or H_2O from $CDCl_3$.

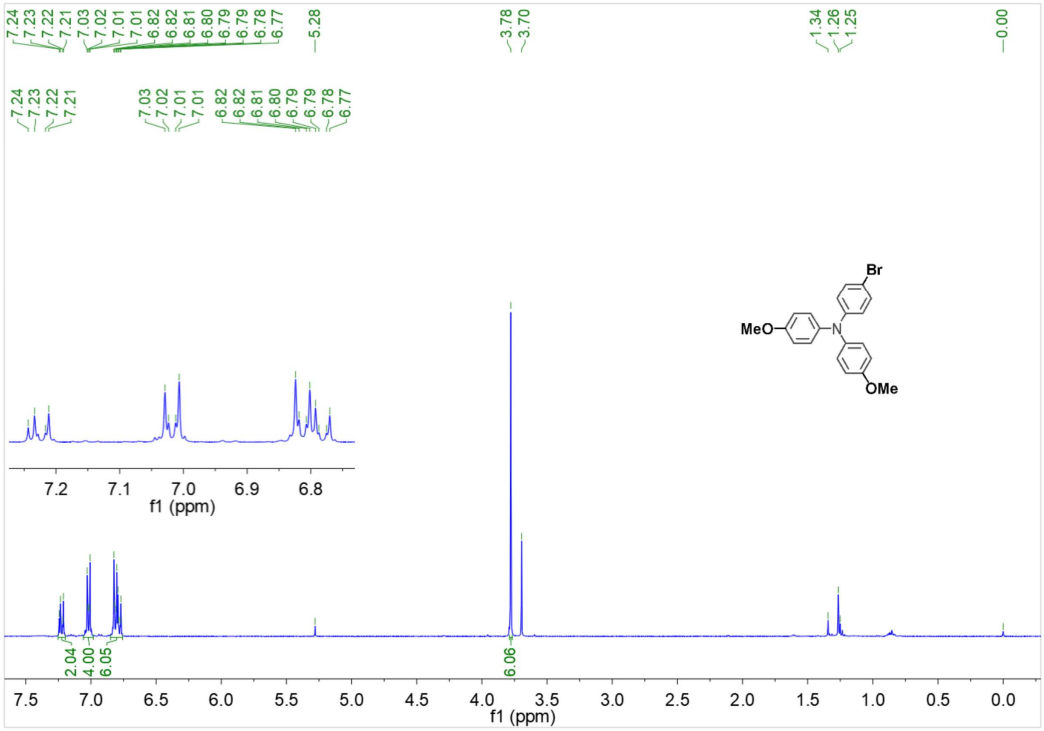

^{1}H NMR (400 MHz, $CDCl_3$) δ 7.23 (dd, *J* = 9.9, 3.0 Hz, 2H), 7.13 – 6.93 (m, 4H), 6.91 – 6.70 (m, 6H), 3.78 (s, 6H). *1.56–0.8 ppm denote trace grease from PE or H_2O from $CDCl_3$.

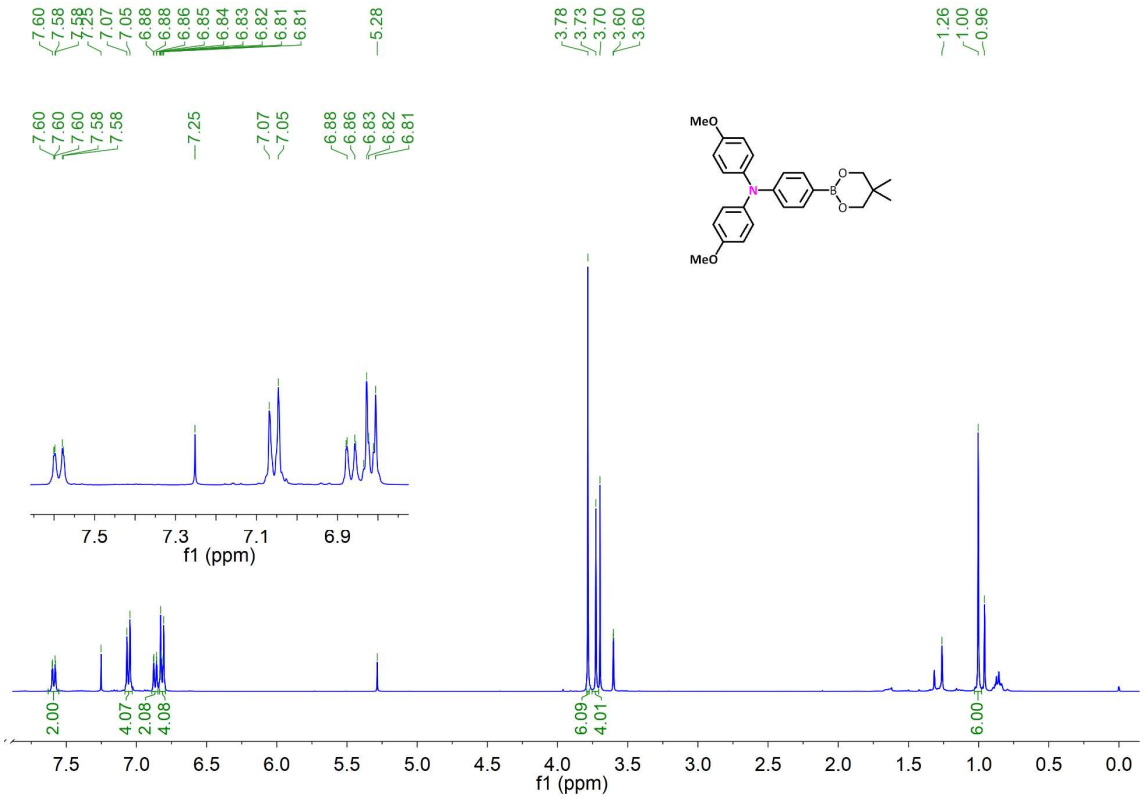

^{1}H NMR (400 MHz, $CDCl_3$) δ 7.64 – 7.50 (m, 2H), 7.06 (d, J = 8.9 Hz, 4H), 6.93 – 6.83 (m, 2H), 6.86 – 6.69 (m, 6H), 3.78 (s, 6H), 3.71 (d, J = 11.8 Hz, 6H), 1.00 (s, 6H). *1.56–0.8 ppm denote trace grease from PE or H_2O from $CDCl_3$.

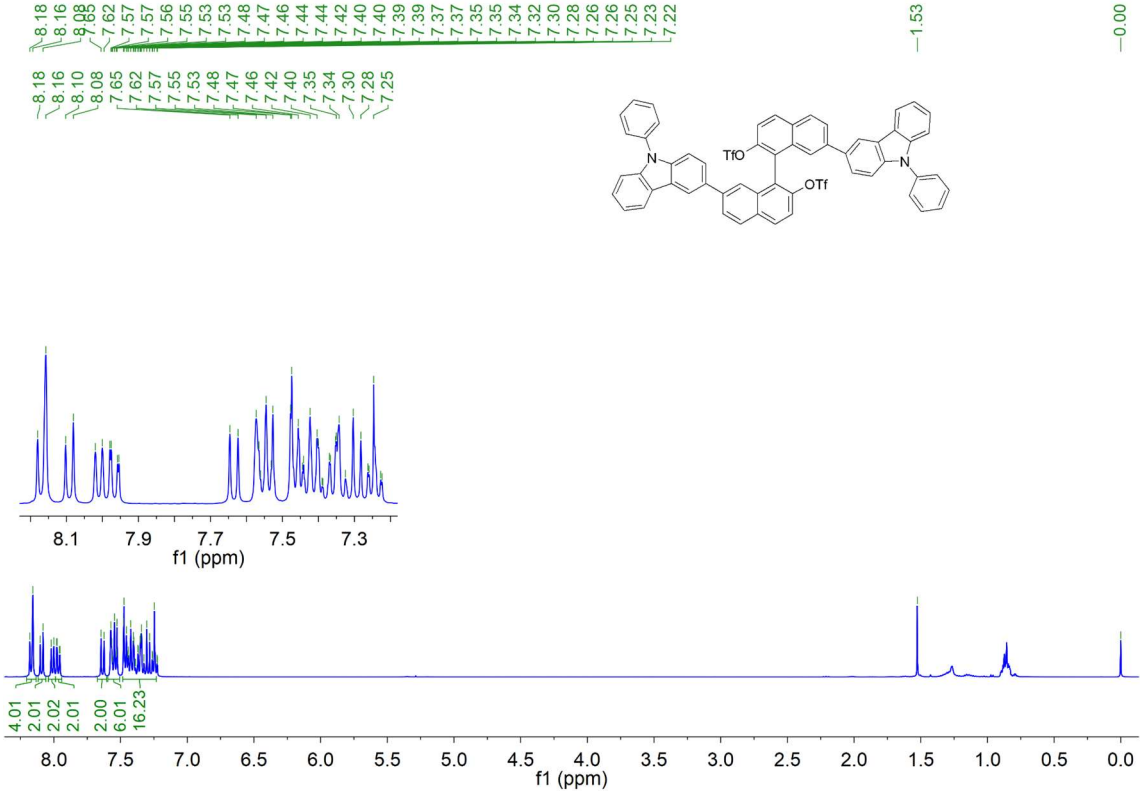

^{1}H NMR (400 MHz, $CDCl_3$) δ 8.17 (d, *J* = 9.1 Hz, 4H), 8.09 (d, *J* = 8.6 Hz, 2H), 8.01 (d, *J* = 7.8 Hz, 2H), 7.97 (dd, *J* = 8.5, 1.6 Hz, 2H), 7.63 (d, *J* = 9.1 Hz, 2H), 7.60 – 7.51 (m, 6H), 7.48 – 7.23 (m, 16H). *1.56–0.8 ppm denote trace grease from PE or H_2O from $CDCl_3$.

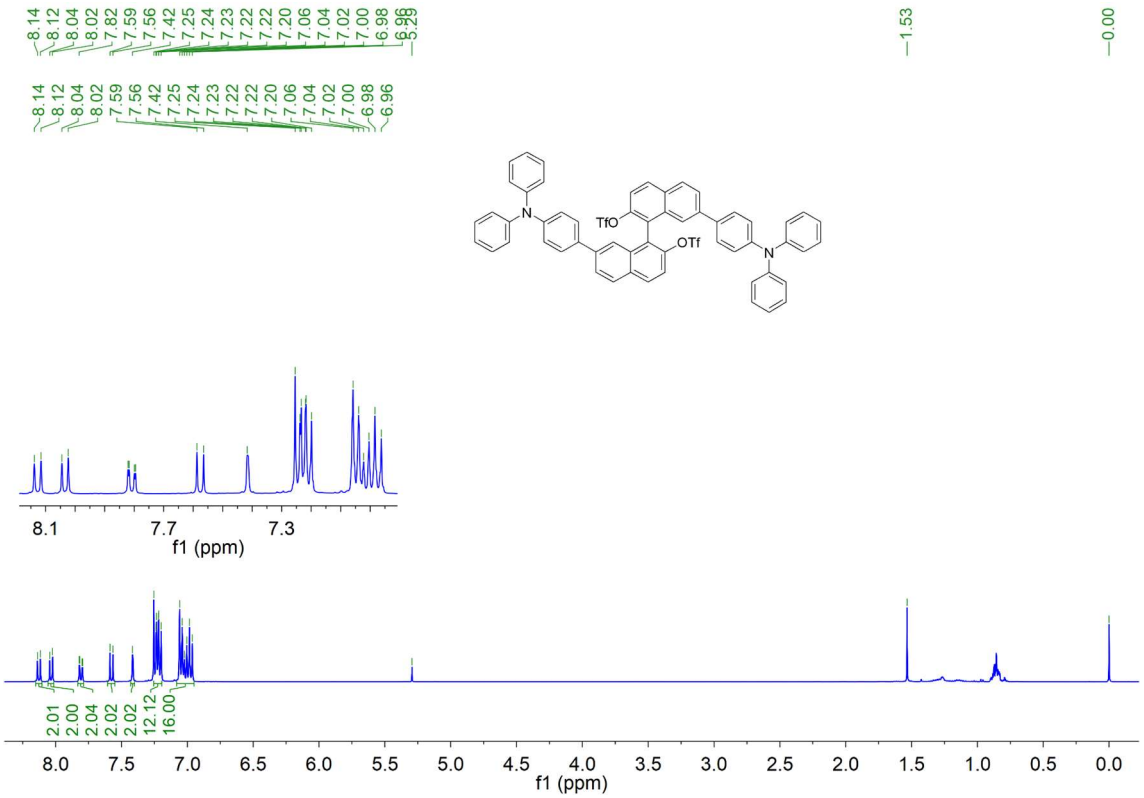

^{1}H NMR (400 MHz, $CDCl_3$) δ 8.13 (d, *J* = 9.1 Hz, 2H), 8.03 (d, *J* = 8.6 Hz, 2H), 7.81 (dd, *J* = 8.6, 1.7 Hz, 2H), 7.58 (d, *J* = 9.0 Hz, 2H), 7.42 (s, 2H), 7.32 – 7.12 (m, 12H), 7.12 – 6.86 (m, 16H).*1.56–0.8 ppm denote trace grease from PE or H_2O from $CDCl_3$.

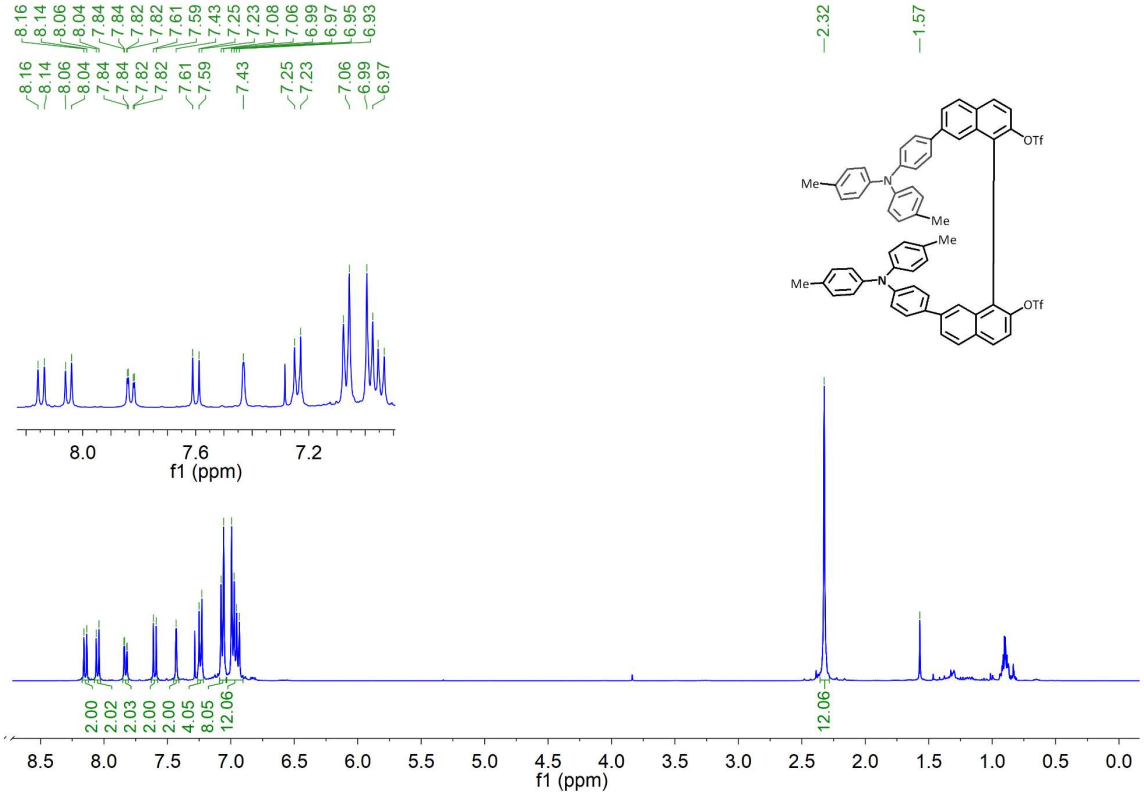

^{1}H NMR (400 MHz, $CDCl_3$) δ 8.15 (d, *J* = 9.0 Hz, 2H), 8.05 (d, *J* = 8.6 Hz, 2H), 7.83 (dd, *J* = 8.6, 1.6 Hz, 2H), 7.60 (d, *J* = 9.0 Hz, 2H), 7.43 (s, 2H), 7.24 (d, *J* = 8.7 Hz, 4H), 7.07 (d, *J* = 8.3 Hz, 8H), 6.96 (dd, *J* = 16.1, 8.5 Hz, 12H), 2.32 (s, 12H). *1.56–0.8 ppm denote trace grease from PE or H_2O from $CDCl_3$.

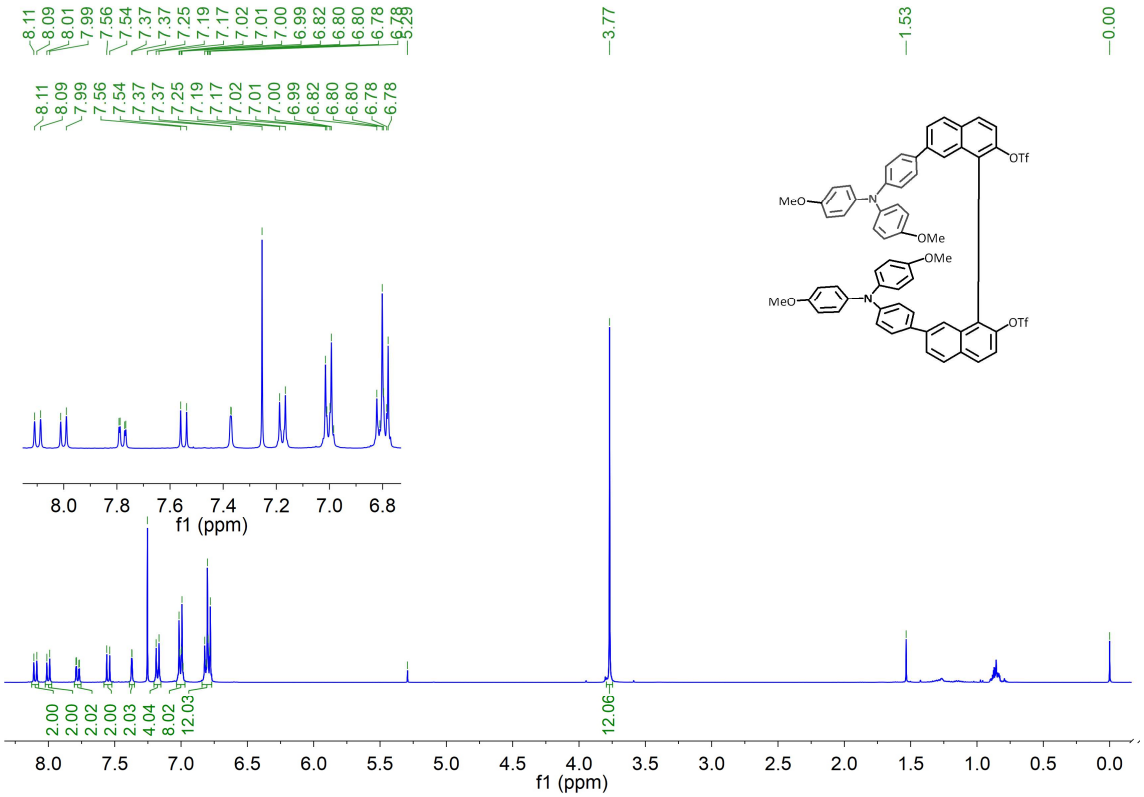

^{1}H NMR (400 MHz, $CDCl_3$) δ 8.10 (d, *J* = 9.0 Hz, 2H), 8.00 (d, *J* = 8.6 Hz, 2H), 7.78 (dd, *J* = 8.6, 1.7 Hz, 2H), 7.55 (d, *J* = 9.0 Hz, 2H), 7.37 (d, *J* = 0.7 Hz, 2H), 7.18 (d, *J* = 8.8 Hz, 4H), 7.03 – 6.97 (m, 8H), 6.84 – 6.77 (m, 12H), 3.77 (s, 12H). *1.56–0.8 ppm denote trace grease from PE or H_2O from $CDCl_3$.

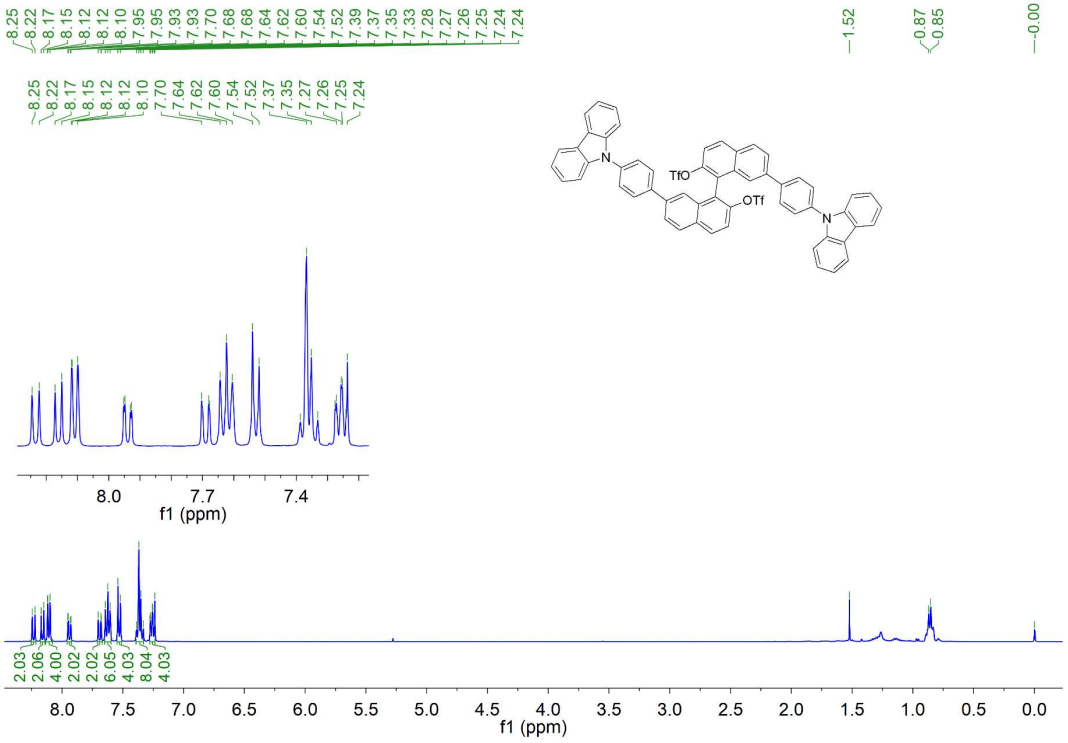

^{1}H NMR (400 MHz, $CDCl_3$) δ 8.23 (d, *J* = 9.1 Hz, 2H), 8.16 (d, *J* = 8.6 Hz, 2H), 8.13 – 8.08 (m, 4H), 7.94 (dd, *J* = 8.5, 1.6 Hz, 2H), 7.71 – 7.67 (m, 2H), 7.62 (t, *J* = 7.8 Hz, 6H), 7.53 (d, *J* = 8.4 Hz, 4H), 7.39 – 7.33 (m, 8H), 7.28 – 7.24 (m, 4H). *1.56–0.8 ppm denote trace grease from PE or H_2O from $CDCl_3$.

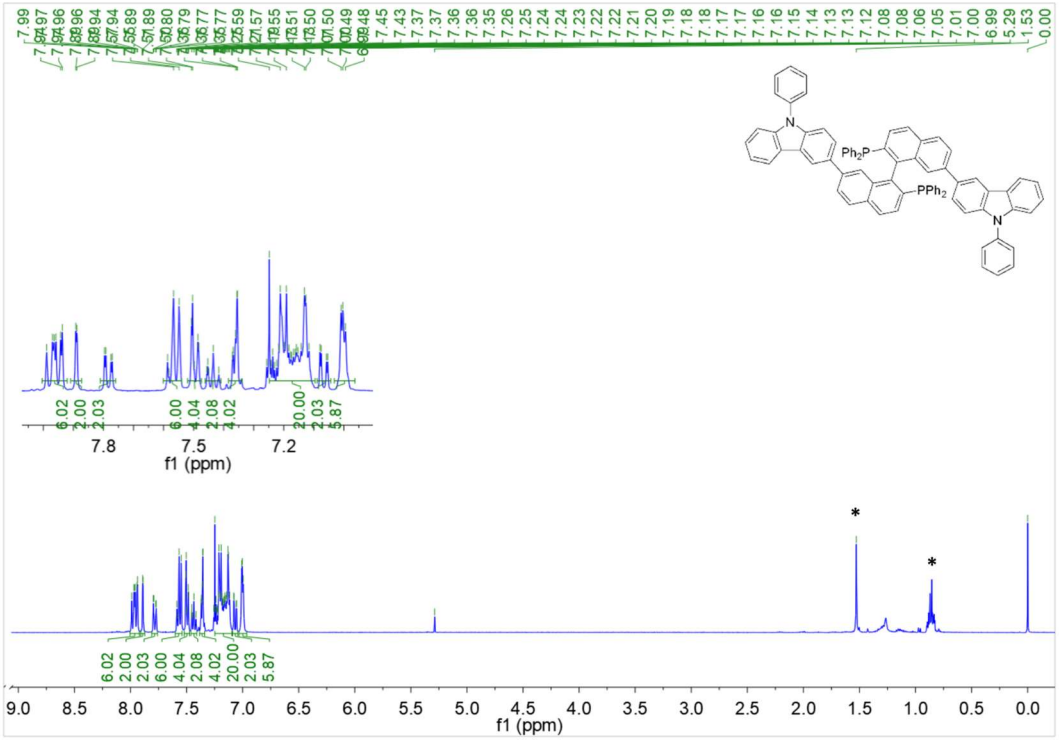

^{1}H NMR (400 MHz, $CDCl_3$) δ 8.00 – 7.92 (m, 6H), 7.89 (d, *J* = 1.4 Hz, 2H), 7.78 (dd, *J* = 8.5, 1.7 Hz, 2H), 7.57 (dd, *J* = 10.8, 4.5 Hz, 6H), 7.52 – 7.47 (m, 4H), 7.46 – 7.41 (m, 2H), 7.38 – 7.34 (m, 4H), 7.25 – 7.10 (m, 20H), 7.07 (dd, *J* = 8.6, 1.8 Hz, 2H), 7.03 – 6.96 (m, 6H). *denote trace grease from PE or H_2O from $CDCl_3$.

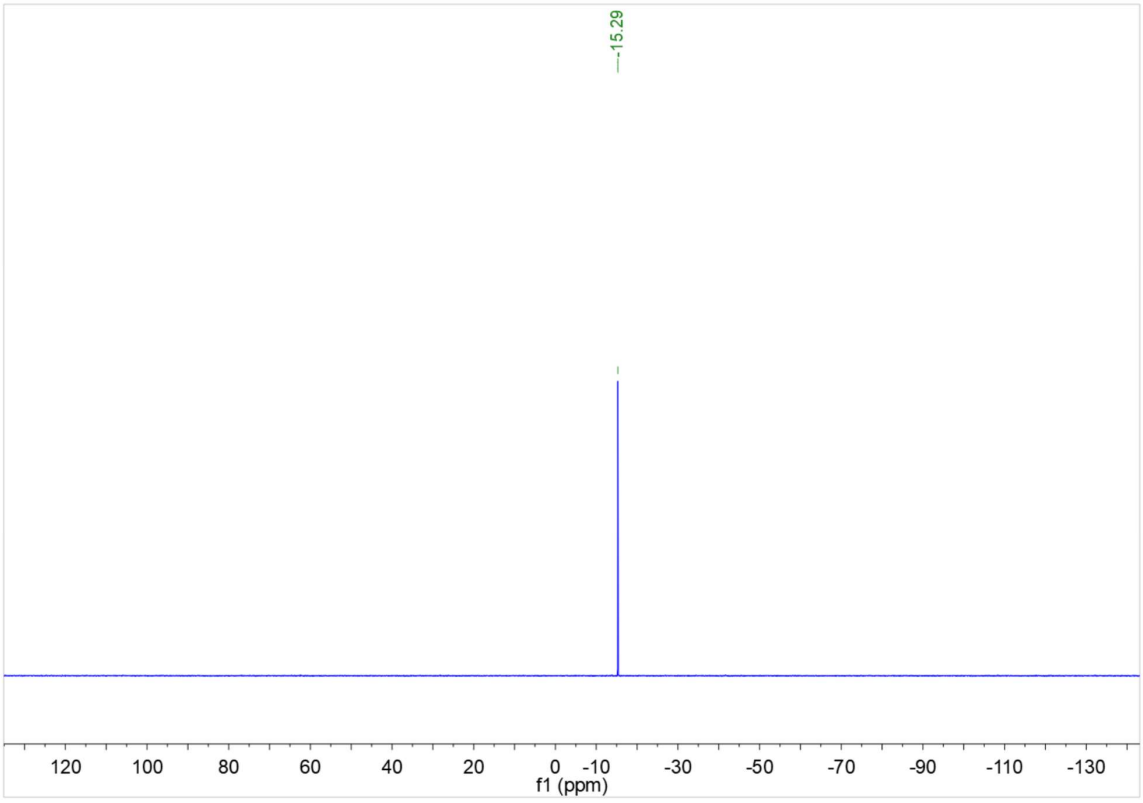

^{31}P NMR (162 MHz, $CDCl_3$) δ -15.29 (s).

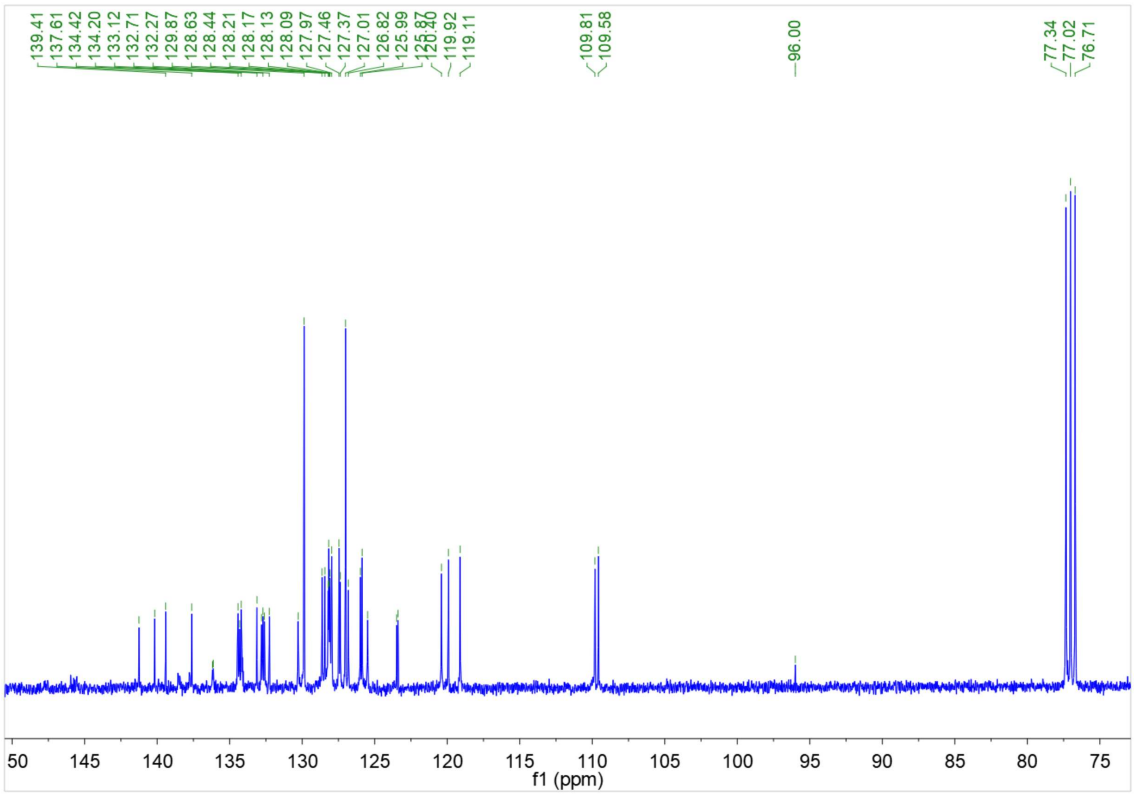

^{13}C NMR (101 MHz, $CDCl_3$) δ 141.25 (s), 140.17 (s), 139.41 (s), 137.61 (s), 136.16 (d, *J* = 5.4 Hz), 134.81 – 133.81 (m), 133.12 (s), 132.93 – 132.44 (m), 132.27 (s), 130.28 (s), 129.87 (s), 128.53 (d, *J* = 19.5 Hz), 128.30 – 127.89 (m), 127.42 (d, *J* = 9.0 Hz), 127.01 (s), 126.82 (s), 125.93 (d, *J* = 12.0 Hz), 125.49 (s), 123.44 (d, *J* = 9.5 Hz), 120.40 (s), 119.92 (s), 119.11 (s), 96.00 (s).

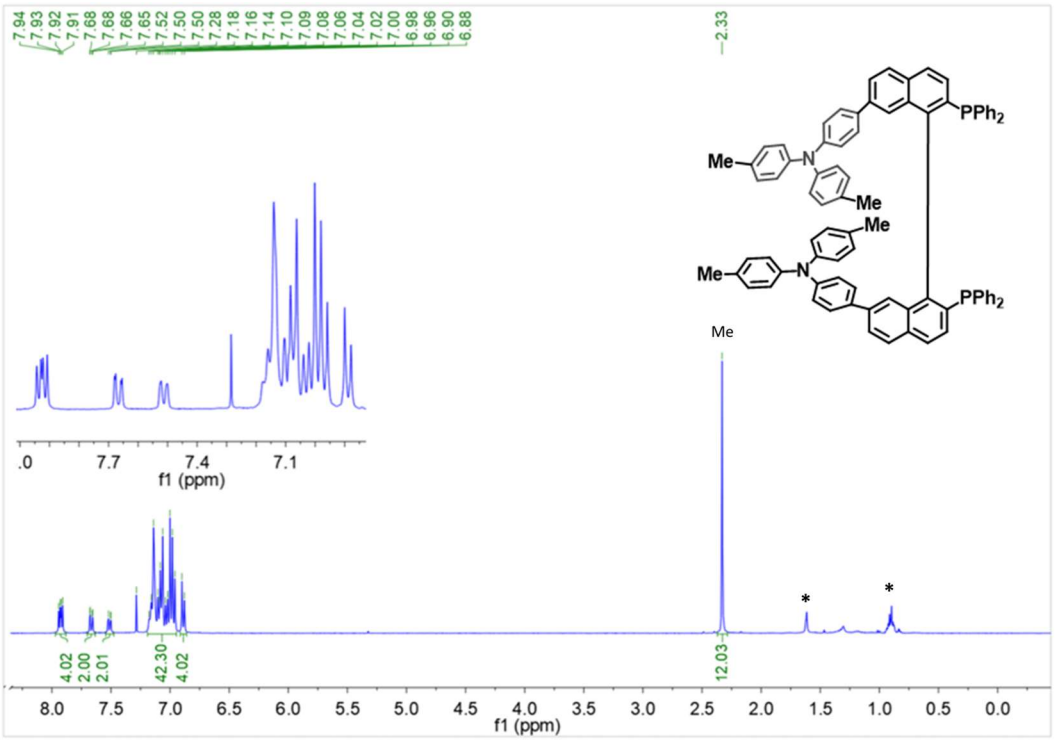

^{1}H NMR (400 MHz, $CDCl_3$) δ 7.93 (dd, *J* = 8.5, 5.5 Hz, 4H), 7.67 (dd, *J* = 8.5, 1.6 Hz, 2H), 7.54 – 7.48 (m, 2H), 7.19 – 6.95 (m, 42H), 6.89 (d, *J* = 8.6 Hz, 4H), 2.33 (s, 12H). *denote trace grease from PE or H_2O from $CDCl_3$.

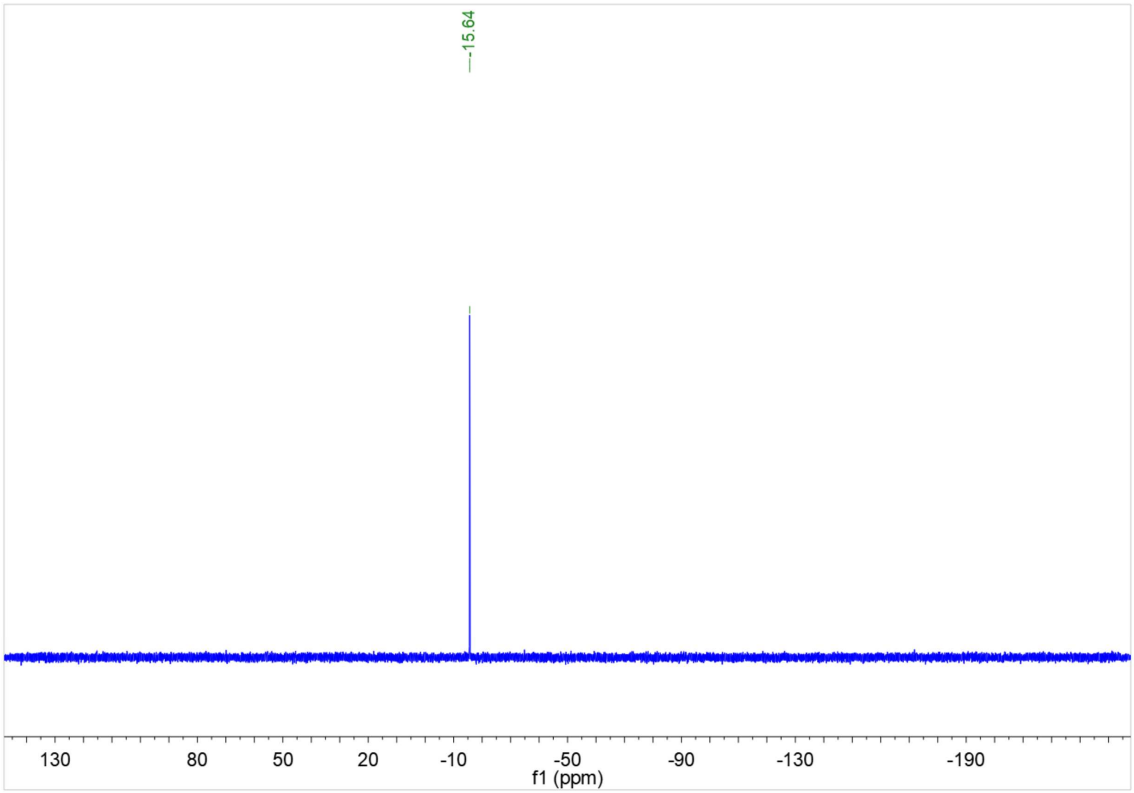

^{31}P NMR (162 MHz, $CDCl_3$) δ -15.64 (s).

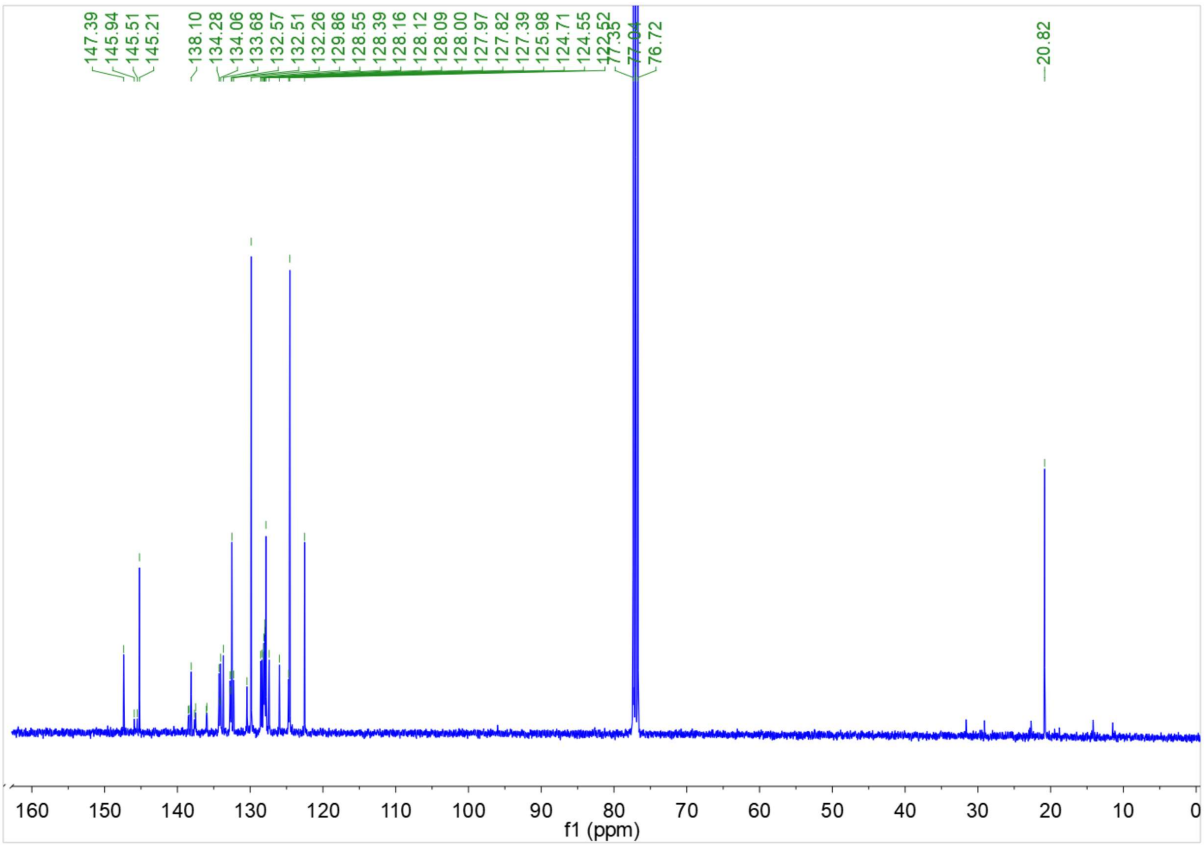

^{13}C NMR (101 MHz, $CDCl_3$) δ 147.39 (s), 145.94 (s), 145.51 (s), 145.21 (s), 138.44 (d, *J* = 12.1 Hz), 137.87 (d, *J* = 47.0 Hz), 137.50 (s), 135.98 (d, *J* = 7.3 Hz), 134.22 (d, *J* = 11.0 Hz), 134.07 – 132.39 (m), 132.36 – 129.63 (m), 129.86 (s), 129.86 (s), 128.47 (d, *J* = 16.8 Hz), 128.26 – 127.93 (m), 127.97 – 127.93 (m), 127.61 (d, *J* = 43.5 Hz), 127.97 – 124.37 (m), 122.52 (s), 77.35 (s), 77.04 (s), 76.72 (s), 20.82 (s). Weak signals at high-field (~10, 30 ppm) denote trace grease from PE.

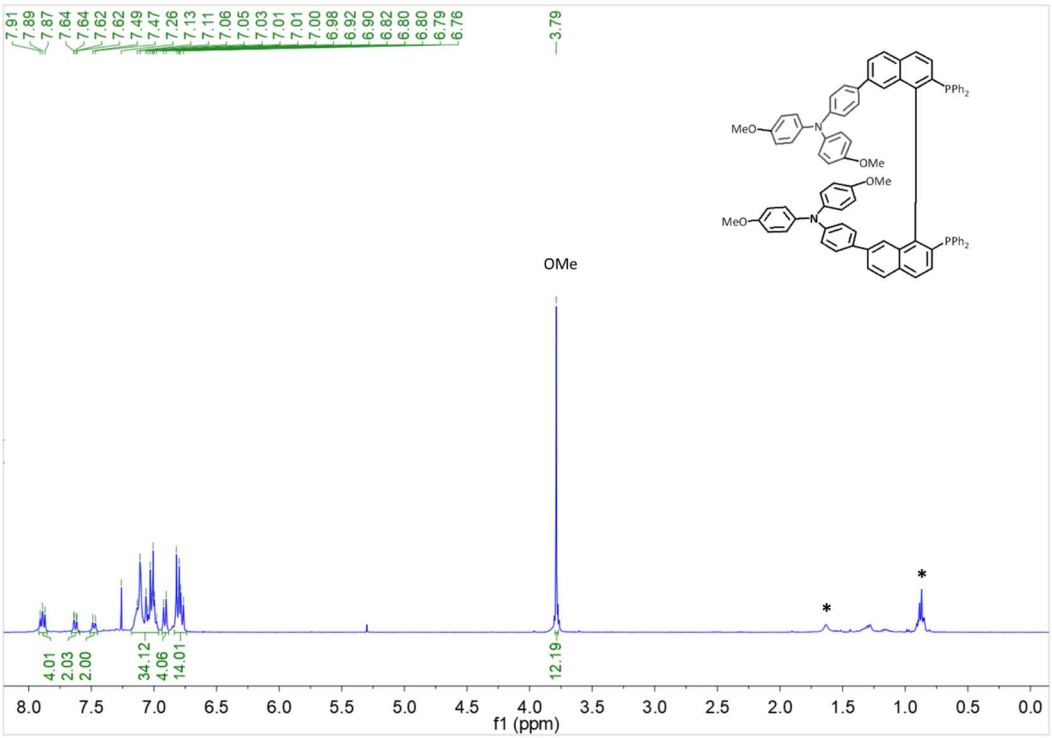

^{1}H NMR (400 MHz, $CDCl_3$) δ 7.92 – 7.85 (m, 4H), 7.63 (dd, *J* = 8.5, 1.4 Hz, 2H), 7.48 (d, *J* = 8.3 Hz, 2H), 7.04 (tt, *J* = 11.2, 8.1 Hz, 34H), 6.91 (d, *J* = 8.6 Hz, 4H), 6.84 – 6.74 (m, 14H), 3.79 (s, 12H).*denote trace grease from PE or H_2O from $CDCl_3$.

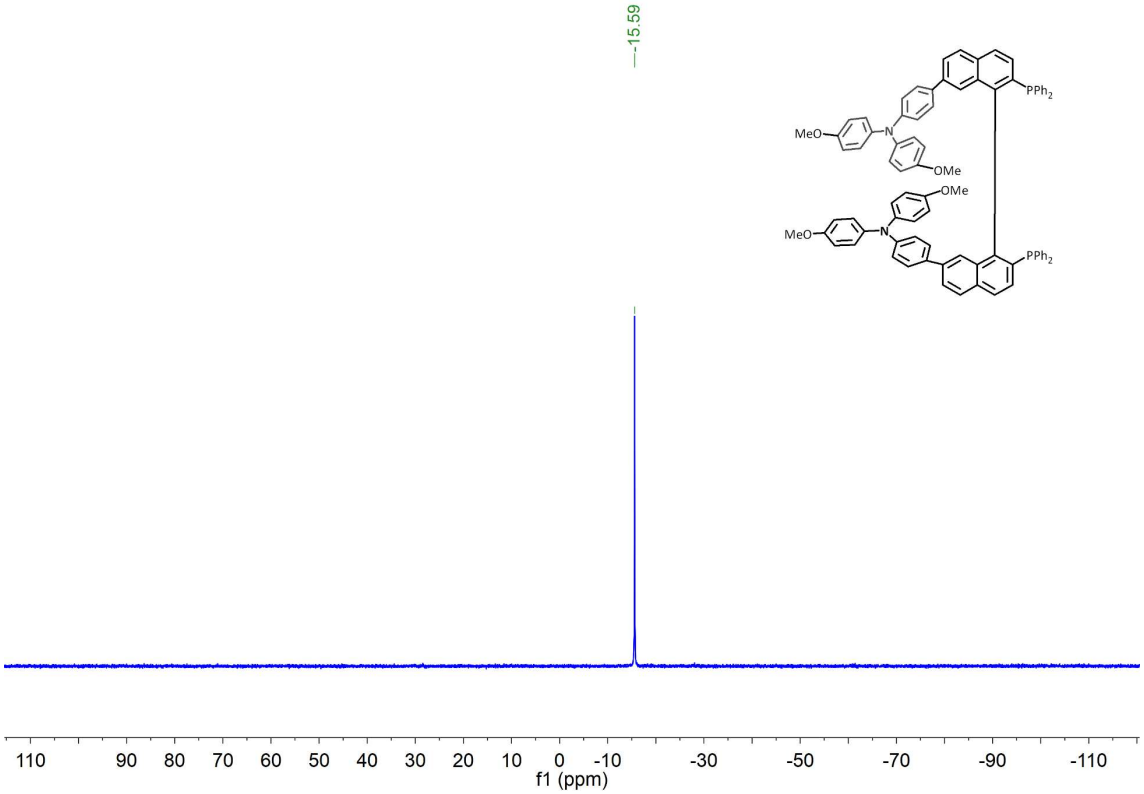

^{31}P NMR (162 MHz, $CDCl_3$) δ -15.59 (s).

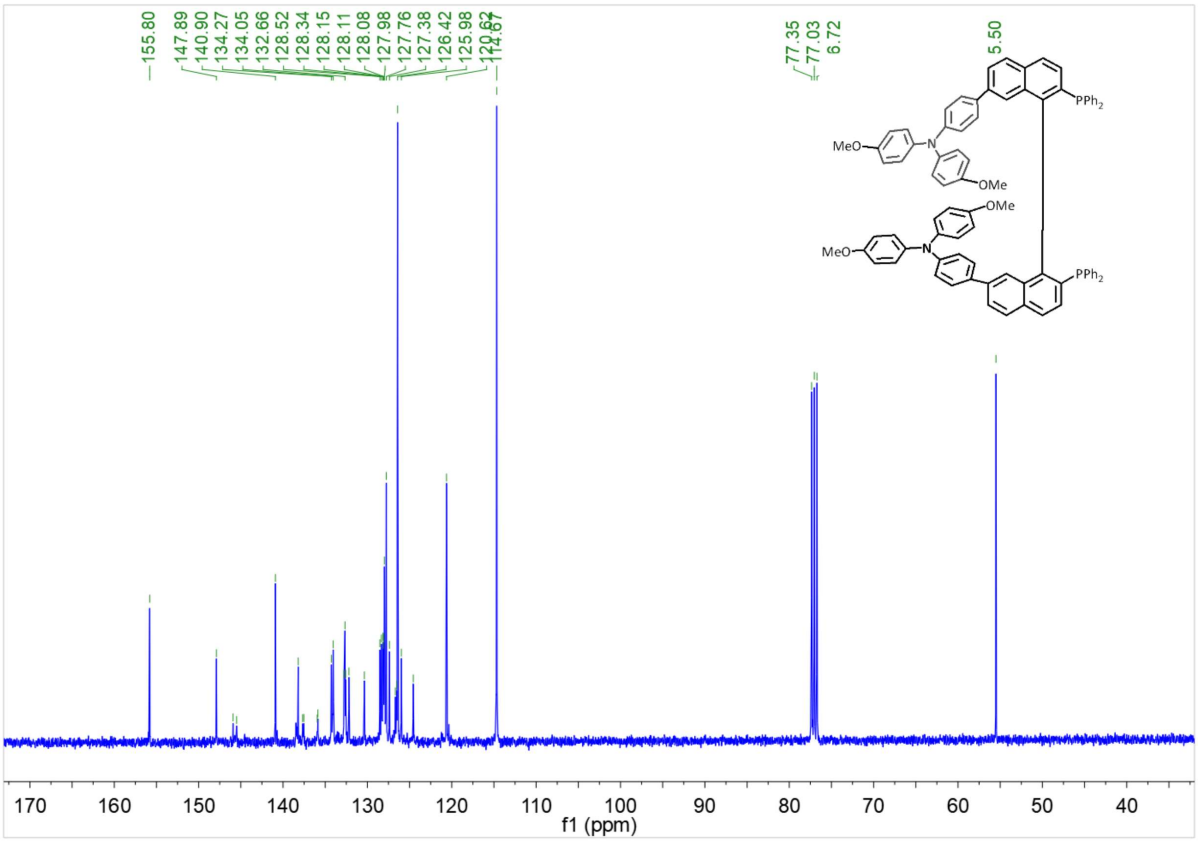

^{13}C NMR (101 MHz, $CDCl_3$) δ 155.80 (s), 147.89 (s), 145.50 (s), 140.90 (s), 138.20 (s), 137.61 (d, *J* = 13.6 Hz), 135.90 (d, *J* = 7.0 Hz), 134.16 (d, *J* = 21.6 Hz), 132.67 (t, *J* = 9.8 Hz), 132.19 (s), 130.36 (s), 128.81 – 127.95 (m), 127.76 (s), 127.38 (s), 127.08 – 126.30 (m), 125.98 (s), 124.56 (s), 120.62 (s), 114.67 (s), 77.35 (s), 77.03 (s), 76.72 (s), 55.50 (s).

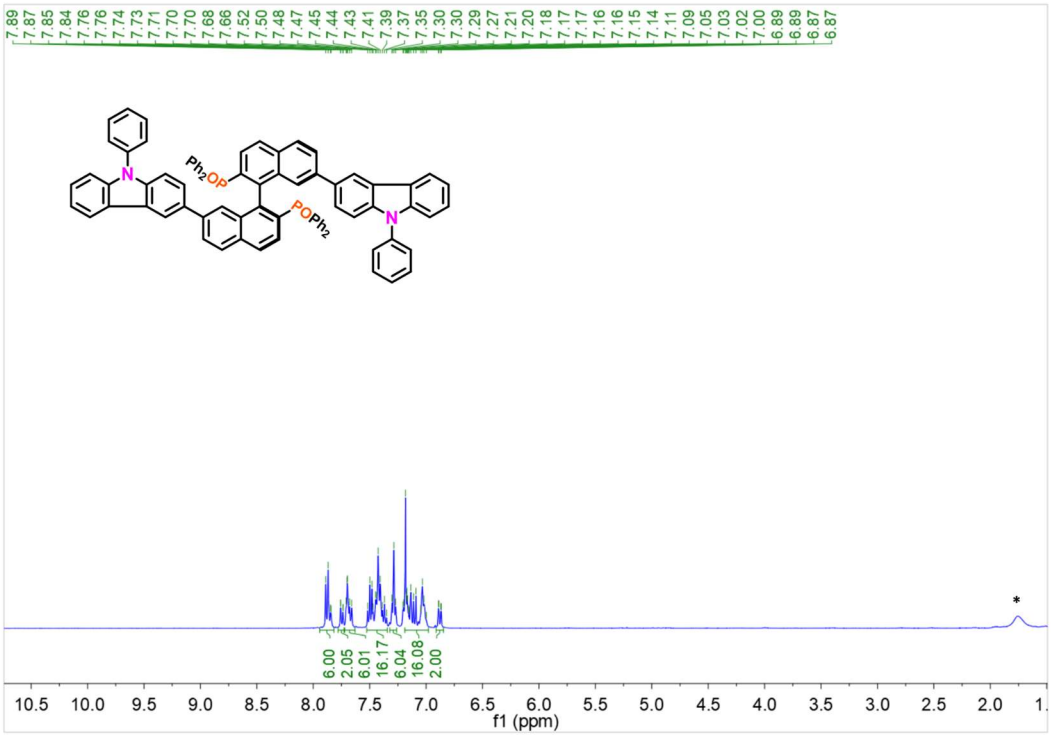

^{1}H NMR (400 MHz, $CDCl_3$) δ 7.86 (dd, *J* = 13.9, 5.2 Hz, 6H), 7.75 (dd, *J* = 8.5, 1.4 Hz, 2H), 7.73 – 7.63 (m, 6H), 7.53 – 7.34 (m, 16H), 7.29 (dd, *J* = 9.7, 3.6 Hz, 6H), 7.19 – 6.98 (m, 16H), 6.88 (dd, *J* = 8.6, 1.5 Hz, 2H). *denote trace H_2O from $CDCl_3$.

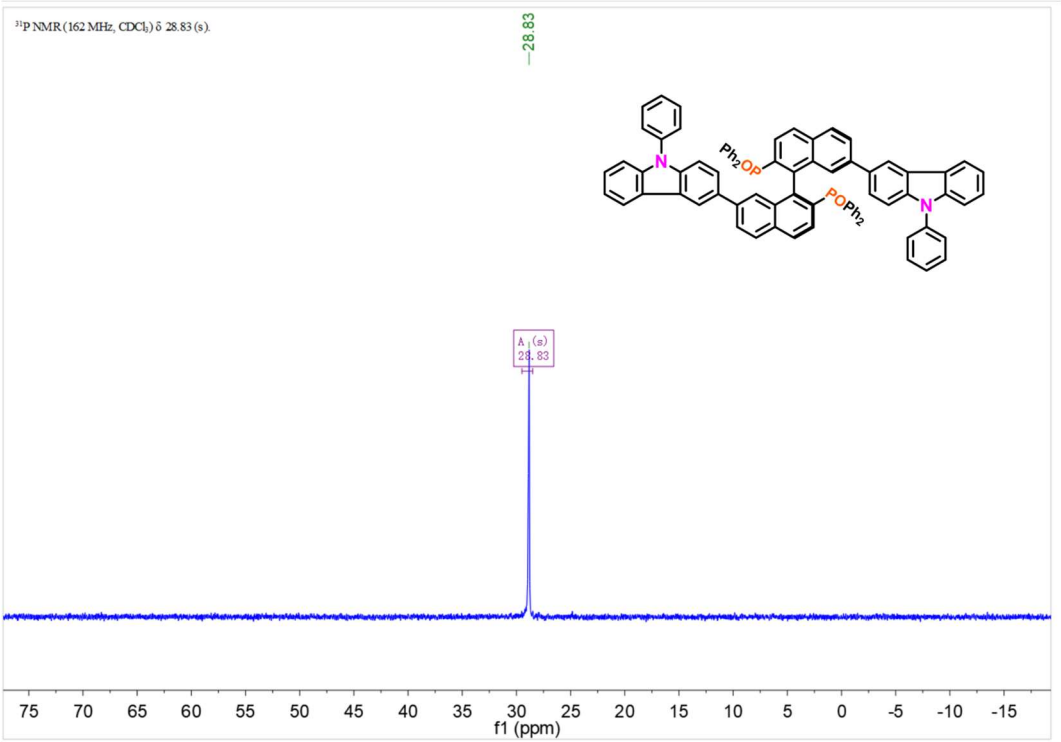

^{31}P NMR (162 MHz, $CDCl_3$) δ 28.83 (s).

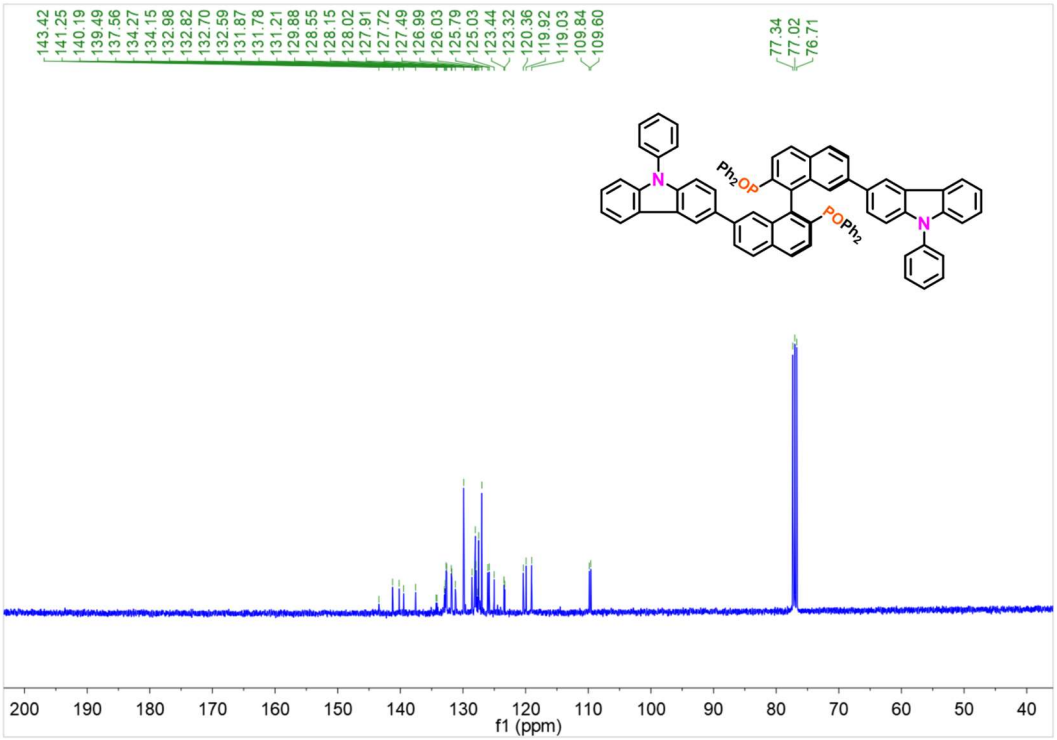

^{13}C NMR (101 MHz, $CDCl_3$) δ 143.42, 141.25, 140.19, 139.49, 137.56, 134.27, 134.15, 132.98, 132.82, 132.70, 132.59, 131.87, 131.78, 131.21, 129.88, 128.55, 128.15, 128.02, 127.91, 127.72, 127.49, 126.99, 126.03, 125.79, 125.03, 123.44, 123.32, 120.36, 119.92, 119.03, 109.84, 109.60, 77.34, 77.02, 76.71.

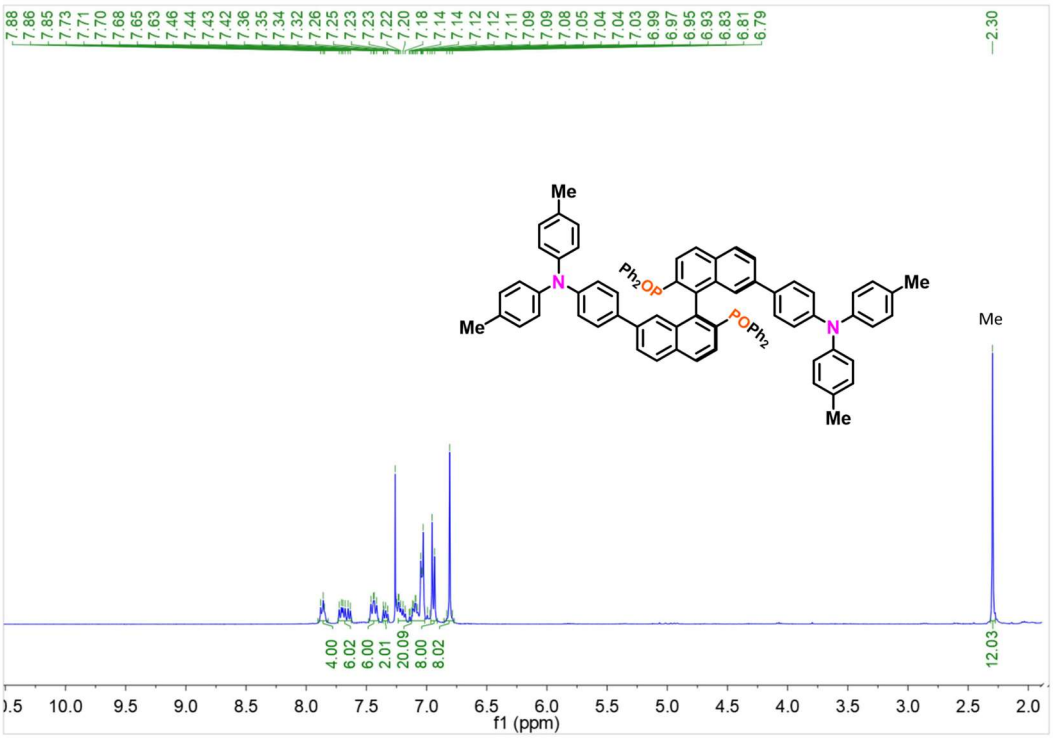

^{1}H NMR (400 MHz, $CDCl_3$) δ 7.79 (t, *J* = 6.1 Hz, 4H), 7.69 – 7.54 (m, 6H), 7.36 (dd, *J* = 10.7, 8.0 Hz, 6H), 7.27 (dd, *J* = 10.1, 4.6 Hz, 2H), 7.17 – 6.91 (m, 20H), 6.87 (d, *J* = 8.3 Hz, 8H), 6.73 (s, 2H), 2.22 (s, 12H).

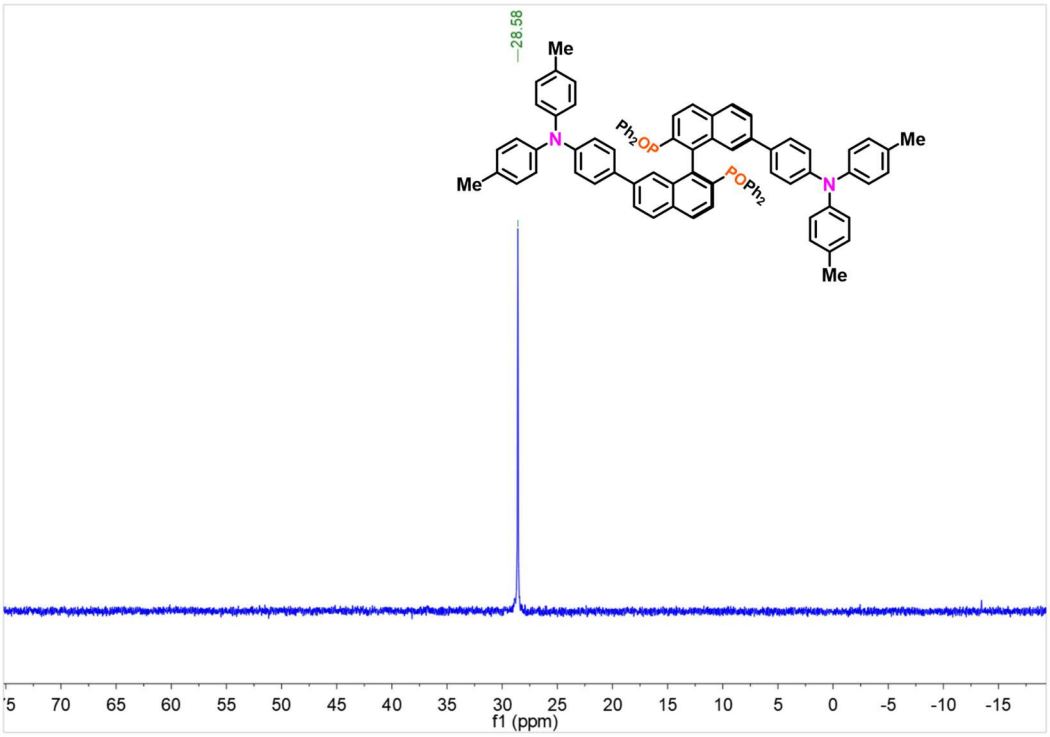

^{31}P NMR (162 MHz, $CDCl_3$) δ 28.58 (s).

^{13}C

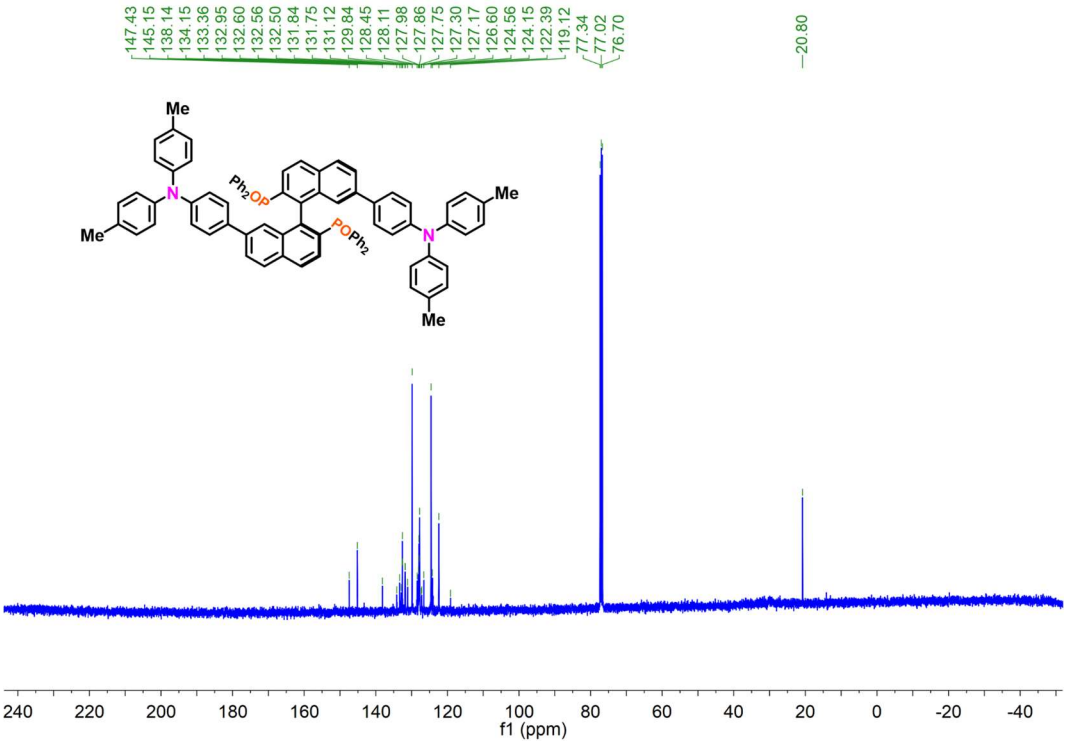

NMR (101 MHz, $CDCl_3$) δ 147.43, 145.15, 138.14, 134.15, 133.36, 132.95, 132.60, 132.56, 132.50, 131.84, 131.75, 131.15, 131.12, 131.08, 131.06, 129.84, 128.45, 128.11, 127.98, 127.86, 127.75, 127.30, 127.27, 127.17, 126.60, 124.56, 124.15, 122.39, 119.12, 77.34, 77.02, 76.70, 29.71, 20.80.

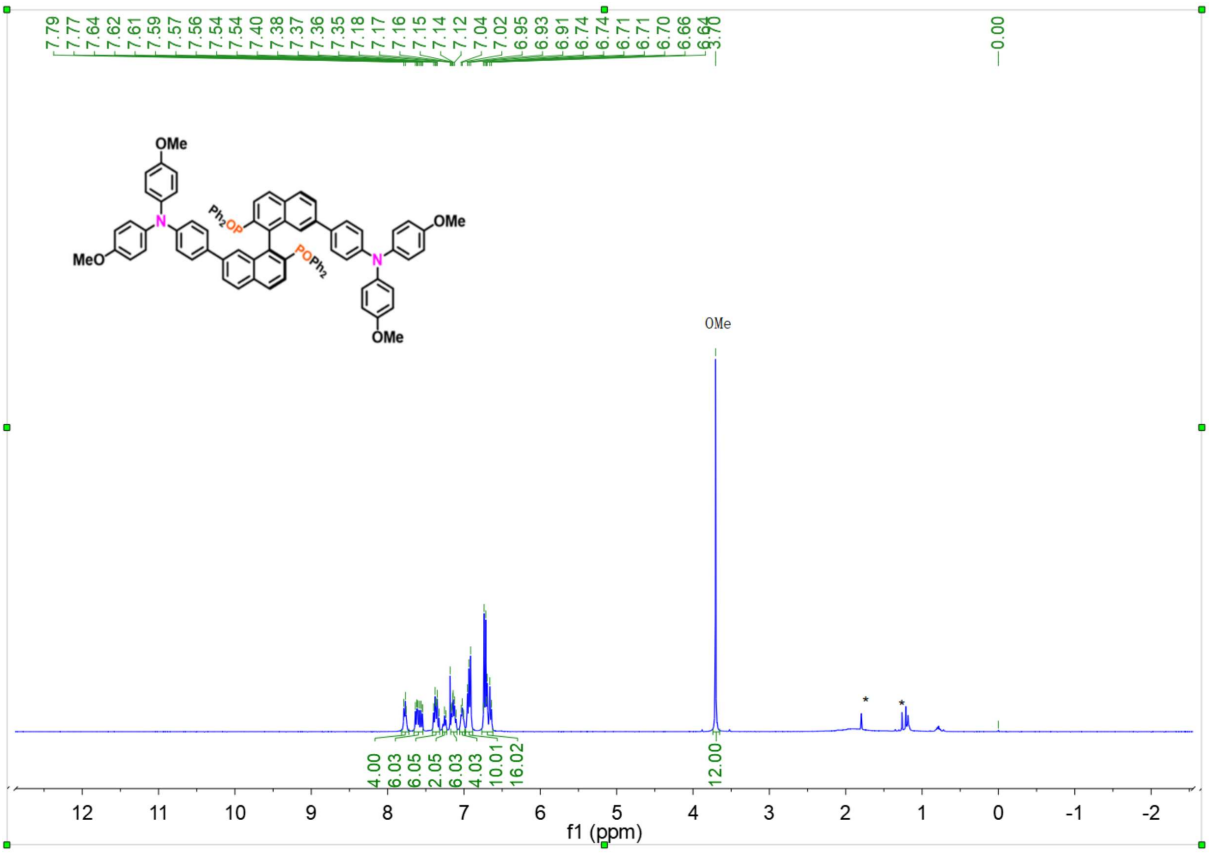

^{1}H NMR (400 MHz, $CDCl_3$) δ 7.77 (t, *J* = 6.0 Hz, 4H), 7.71 – 7.52 (m, 6H), 7.36 (dt, *J* = 11.5, 8.3 Hz, 6H), 7.25 (d, *J* = 7.0 Hz, 2H), 7.17 – 7.08 (m, 6H), 7.02 (t, *J* = 6.2 Hz, 4H), 6.98 – 6.85 (m, 10H), 6.78 – 6.61 (m, 16H), 3.70 (s, 12H). *denote trace grease from PE or H_2O from $CDCl_3$.

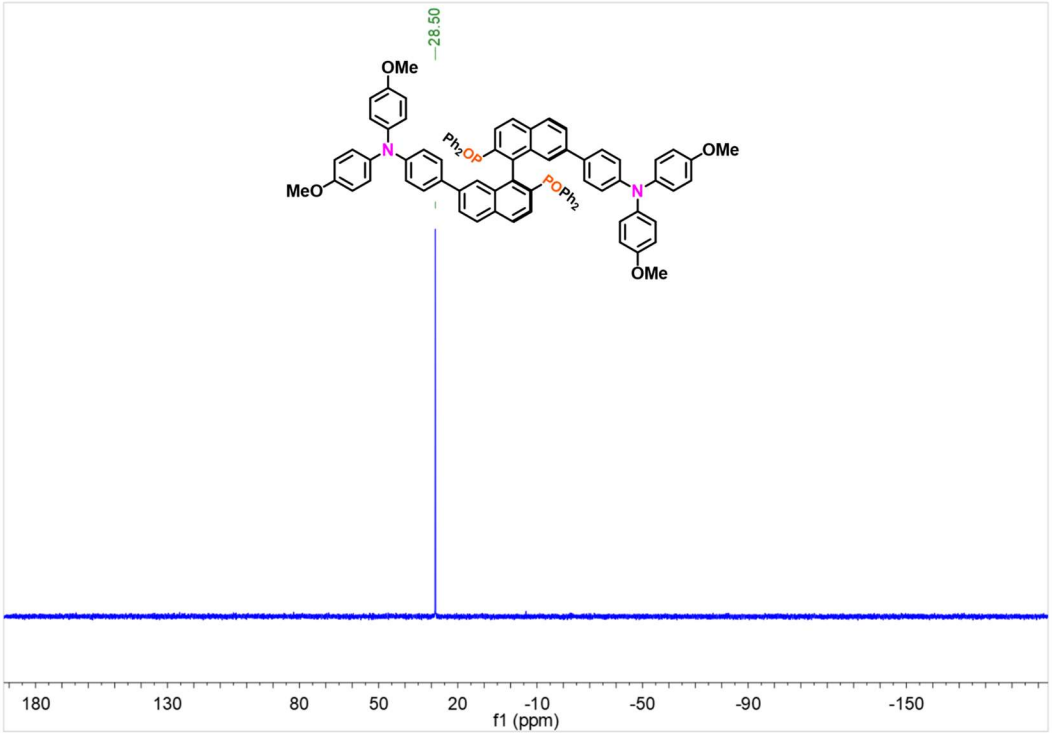

^{31}P NMR (162 MHz, $CDCl_3$) δ 28.50.

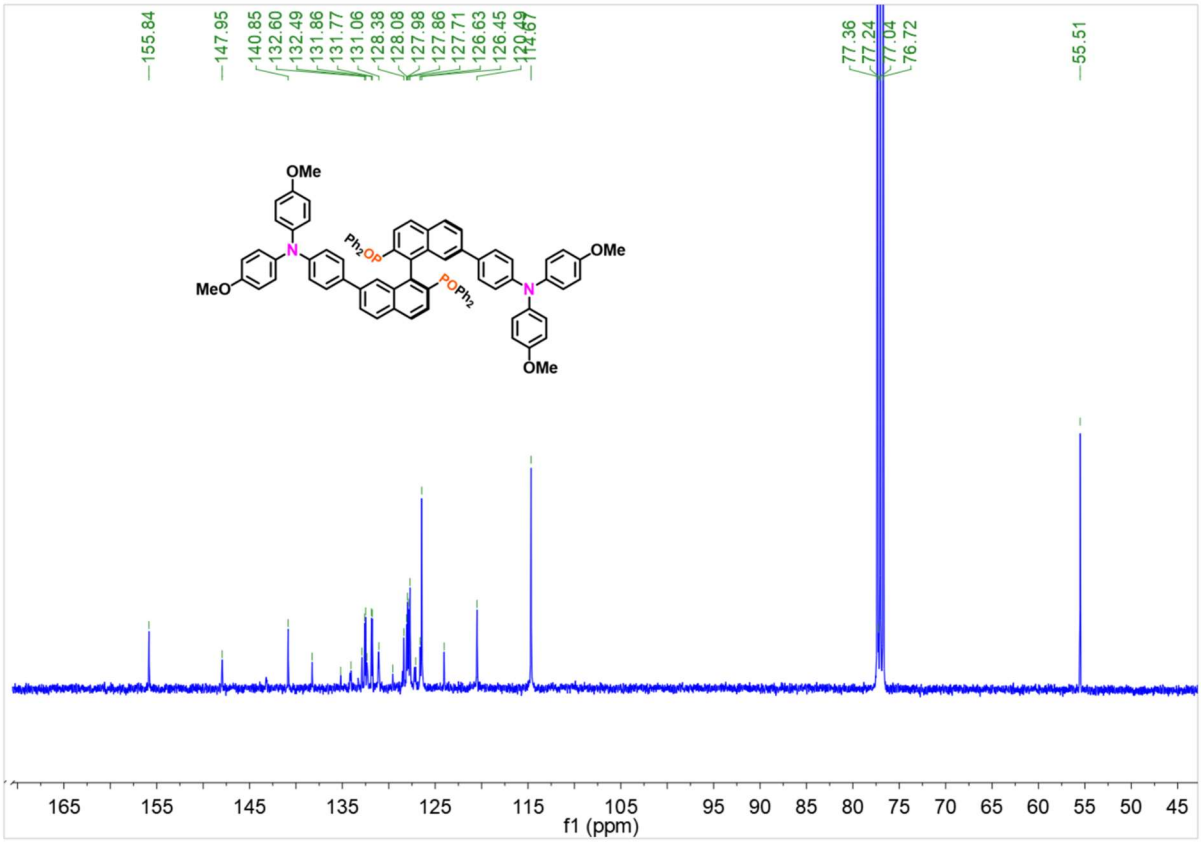

^{13}C NMR (101 MHz, $CDCl_3$) δ 155.84, 147.95, 140.85, 138.26, 135.18, 134.07, 132.89, 132.60, 132.49, 132.36, 131.86, 131.77, 131.06, 129.57, 128.38, 128.08, 127.98, 127.86, 127.71, 127.11, 126.63, 126.45, 124.04, 120.49, 114.67, 77.36, 77.24, 77.04, 76.72, 55.51.

Table S11. Coordinates (Å) for the optimized structure (B3LYP-D3/6-31G(d)) in the ground state of **(*R*)-P1**

Atoms	X	Y	Z	Atoms	X	Y	Z
C	-1.37895	1.376986	-1.15397	C	3.203269	5.236194	2.796173
C	-0.22081	0.734094	-0.71507	C	2.607981	4.218403	2.054113
C	0.220349	0.733946	0.715012	P	-2.67569	2.138154	-0.06151
C	1.378589	1.376619	1.154035	C	-3.3593	3.474251	-1.13453
C	-0.55691	-0.04647	1.640249	C	-2.60477	4.219816	-2.0536
C	-0.17018	-0.12487	3.014083	C	-3.19826	5.238891	-2.79533
C	1.018267	0.52415	3.420604	C	-4.55503	5.529736	-2.63151
C	1.76968	1.233074	2.520067	C	-5.3168	4.790459	-1.72662
C	-1.77012	1.233696	-2.52002	C	-4.72283	3.765719	-0.98726
C	-1.01882	0.524857	-3.42071	C	-1.85114	3.138236	1.258386
C	0.169569	-0.12438	-3.01432	C	-1.90718	2.639029	2.567924
C	0.556289	-0.04632	-1.64046	C	-1.37594	3.367291	3.631545
C	-1.73808	-0.72167	1.2446	C	-0.81789	4.625871	3.407059
C	-2.56733	-1.35968	2.15269	C	-0.78967	5.148246	2.111908
C	-2.16945	-1.41697	3.516332	C	-1.29845	4.408025	1.045377
C	-0.99452	-0.83228	3.925875	H	1.332334	0.453158	4.459045
C	0.993823	-0.83171	-3.92624	H	2.684873	1.704329	2.858759
C	2.16867	-1.41667	-3.51681	H	-2.68526	1.705158	-2.85859
C	2.56652	-1.35975	-2.15315	H	-1.33292	0.454056	-4.45916
C	1.73732	-0.72183	-1.24494	H	-2.01133	-0.7303	0.198475
C	5.842405	-1.66656	-0.3316	H	-2.81672	-1.90603	4.23835
C	4.608027	-1.1832	-0.75639	H	-0.69265	-0.87916	4.969381
C	3.868798	-1.9009	-1.70499	H	0.691988	-0.8783	-4.96977
C	4.400667	-3.10021	-2.22775	H	2.815912	-1.90561	-4.23893
C	5.630844	-3.60558	-1.81498	H	2.010536	-0.73072	-0.19881
C	6.344102	-2.88507	-0.85406	H	4.235811	-0.23092	-0.39128
C	-5.8433	-1.66607	0.331162	H	3.822868	-3.65846	-2.95872
C	-4.60888	-1.1828	0.755974	H	6.019621	-4.52872	-2.23051
C	-3.86967	-1.90066	1.704474	H	-4.23664	-0.2305	0.390925
C	-4.40158	-3.10001	2.227087	H	-3.82377	-3.6584	2.957955
C	-5.63178	-3.60527	1.814303	H	-6.02057	-4.52846	2.229721
C	-6.34503	-2.88462	0.853488	H	9.835532	-2.62929	1.420231
N	7.600304	-3.13302	-0.28929	H	9.932783	-0.59746	2.840534
C	7.910534	-2.08343	0.587164	H	8.092633	1.058569	2.825916
C	6.839223	-1.1537	0.58386	H	6.087935	0.703343	1.395227
C	9.029762	-1.90376	1.401751	H	-6.0888	0.704022	-1.39539
C	9.071402	-0.76097	2.199076	H	-8.09349	1.059423	-2.82608
C	8.025912	0.17811	2.193694	H	-9.93367	-0.59657	-2.84086
C	6.904206	-0.01454	1.391948	H	-9.83646	-2.62853	-1.42075
C	-6.84011	-1.15309	-0.58424	H	6.863886	-5.67796	-0.14442
C	-7.91144	-2.0828	-0.58765	H	8.287493	-7.64955	-0.65412
N	-7.60123	-3.13249	0.288686	H	10.66564	-7.33128	-1.30854

C	-6.90508	-0.01384	-1.39221	H	11.59839	-5.0325	-1.482
C	-8.02678	0.178899	-2.19394	H	10.14819	-3.06535	-1.03469
C	-9.07229	-0.76015	-2.19942	H	-10.149	-3.0645	1.03428
C	-9.03067	-1.90302	-1.40221	H	-11.5995	-5.03148	1.481738
C	8.420468	-4.25429	-0.56047	H	-10.667	-7.33037	1.308197
C	7.894983	-5.54723	-0.45558	H	-8.28895	-7.64893	0.653567
C	8.701657	-6.64869	-0.73548	H	-6.86514	-5.67752	0.14374
C	10.03753	-6.47052	-1.09931	H	1.282402	4.828493	-0.04585
C	10.5618	-5.18017	-1.19295	H	0.368999	6.135276	-1.92776
C	9.756421	-4.07218	-0.93579	H	0.417281	5.2054	-4.23419
C	-8.42152	-4.25366	0.55993	H	1.408755	2.956342	-4.63433
C	-9.75741	-4.07138	0.935359	H	2.364268	1.675128	-2.75383
C	-10.5629	-5.17927	1.192592	H	5.322073	3.179245	0.289368
C	-10.0388	-6.46969	1.098916	H	6.378877	4.997357	1.600503
C	-8.70298	-6.64803	0.734958	H	5.023617	6.318006	3.212779
C	-7.8962	-5.54666	0.454986	H	2.60492	5.804065	3.504047
P	2.67544	2.137216	0.061302	H	1.558009	3.99357	2.199757
C	1.851144	3.138784	-1.25762	H	-1.55514	3.993405	-2.19911
C	1.299878	4.409053	-1.0437	H	-2.59884	5.806067	-3.50285
C	0.79149	5.150405	-2.10963	H	-5.01676	6.323892	-3.21174
C	0.818637	4.628699	-3.40507	H	-6.37442	5.004807	-1.60021
C	1.375148	3.369593	-3.63045	H	-5.32081	3.184452	-0.28963
C	1.906058	2.640193	-2.56743	H	-2.36643	1.674311	2.753601
C	3.361151	3.471959	1.134631	H	-1.41041	2.953552	4.635194
C	4.725145	3.761243	0.98729	H	-0.41625	5.20169	4.236651
C	5.320918	4.7847	1.726985	H	-0.36614	6.132804	1.930761
C	4.560489	5.524864	2.632268	H	-1.28013	4.827961	0.047752

Table S12. Coordinates (Å) for the optimized structure (B3LYP-D3/6-31G(d)) in the ground state of **(*R*)-PO1**							
Atoms	X	Y	Z	Atoms	X	Y	Z
C	1.372701	-1.79465	-1.14065	C	3.296673	-3.97619	-1.08471
C	0.238021	-1.10566	-0.71132	C	2.542741	-4.73759	-1.98594
C	-0.23805	-1.10568	0.711306	C	3.139476	-5.78265	-2.68884
C	-1.37269	-1.79471	1.140642	C	4.493498	-6.06877	-2.49991
C	0.458841	-0.24797	1.631139	C	5.251131	-5.30349	-1.61139
C	0.006436	-0.14164	2.985585	C	4.656338	-4.25812	-0.90452
C	-1.13238	-0.87492	3.388227	C	1.804296	-3.522	1.32989
C	-1.80516	-1.66492	2.493394	C	1.87327	-2.9266	2.596422
C	1.805211	-1.66477	-2.49338	C	1.367013	-3.59282	3.71056
C	1.132404	-0.87478	-3.38821	C	0.827119	-4.873	3.576201
C	-0.00647	-0.14159	-2.98558	C	0.787316	-5.4841	2.320878
C	-0.45888	-0.24796	-1.63114	C	1.267198	-4.8088	1.199118
C	1.589449	0.512077	1.24164	H	-1.47969	-0.7914	4.41477
C	2.285494	1.308678	2.135554	H	-2.69388	-2.19304	2.817424
C	1.81962	1.399106	3.476012	H	2.693989	-2.1928	-2.81741
C	0.711893	0.697557	3.884826	H	1.47973	-0.79123	-4.41475
C	-0.71198	0.697563	-3.88483	H	1.930766	0.463517	0.217211
C	-1.81975	1.399044	-3.47601	H	2.369507	2.011265	4.184728
C	-2.28559	1.308617	-2.13555	H	0.364522	0.765892	4.912621
C	-1.58952	0.512049	-1.24164	H	-0.36462	0.76591	-4.91263
C	-5.56995	1.986462	-0.44559	H	-2.36969	2.011158	-4.18473
C	-4.4101	1.337279	-0.85925	H	-1.93083	0.46347	-0.21721
C	-3.51635	2.006014	-1.70464	H	-4.21813	0.307034	-0.57457
C	-3.81611	3.316024	-2.13898	H	-3.11516	3.830396	-2.79053
C	-4.96855	3.983319	-1.73145	H	-5.17888	4.990127	-2.0751
C	-5.83865	3.312086	-0.86894	H	4.21809	0.307119	0.574633
C	5.569878	1.986565	0.445665	H	3.114991	3.830507	2.790499
C	4.410019	1.337374	0.8593	H	5.178715	4.990255	2.075109
C	3.516239	2.006108	1.704658	H	-9.43369	3.444422	1.25626
C	3.815969	3.316128	2.138986	H	-9.92442	1.340305	2.475021
C	4.968412	3.983436	1.731476	H	-8.38173	-0.59085	2.361443
C	5.838545	3.3122	0.869006	H	-6.27521	-0.44695	1.023807
N	-7.06481	3.717084	-0.32784	H	6.275214	-0.44686	-1.02366
C	-7.58564	2.66155	0.436234	H	8.381782	-0.59076	-2.36122
C	-6.68191	1.570499	0.38118	H	9.924452	1.340417	-2.47479
C	-8.75591	2.600079	1.194486	H	9.43364	3.444555	-1.2561
C	-9.01885	1.41412	1.879257	H	-5.92453	6.081206	0.061147
C	-8.14109	0.318226	1.817968	H	-6.98061	8.299215	-0.30927
C	-6.9666	0.390252	1.073416	H	-9.35	8.441065	-1.0522
C	6.681866	1.5706	-0.38106	H	-10.6415	6.353844	-1.45341
C	7.585578	2.661668	-0.43611	H	-9.55576	4.140944	-1.14402
N	7.064705	3.717208	0.327929	H	9.555616	4.141156	1.144186

C	6.966603	0.390343	-1.07326	H	10.64132	6.354092	1.453532
C	8.141117	0.318323	-1.81778	H	9.349769	8.441269	1.052167
C	9.018857	1.41423	-1.87906	H	6.980421	8.299337	0.30914
C	8.755869	2.6002	-1.19433	H	5.924395	6.081289	-0.06122
C	-7.67602	4.978213	-0.52059	H	-1.24777	-5.29434	-0.23093
C	-6.94937	6.151778	-0.28773	H	-0.38165	-6.48612	-2.21511
C	-7.55084	7.392513	-0.49015	H	-0.44771	-5.39733	-4.44905
C	-8.88177	7.472581	-0.90357	H	-1.40874	-3.11542	-4.68548
C	-9.60745	6.300816	-1.12498	H	-2.33554	-1.95144	-2.69875
C	-9.00742	5.05577	-0.94581	H	-5.23416	-3.64688	0.218784
C	7.675886	4.978359	0.520646	H	-6.3063	-5.51895	1.471828
C	9.007258	5.055962	0.945916	H	-4.9583	-6.8821	3.050353
C	9.607257	6.301029	1.125057	H	-2.54796	-6.3664	3.389626
C	8.881565	7.472768	0.903558	H	-1.49818	-4.50305	2.153741
C	7.550661	7.392655	0.490081	H	1.498521	-4.50325	-2.15381
C	6.949215	6.151899	0.287701	H	2.548712	-6.36647	-3.38959
C	-1.80433	-3.5218	-1.33008	H	4.959106	-6.88172	-3.05017
C	-1.26715	-4.80859	-1.19952	H	6.30679	-5.51827	-1.47162
C	-0.78728	-5.48369	-2.32141	H	5.234246	-3.64635	-0.21871
C	-0.82716	-4.87239	-3.57664	H	2.335368	-1.95183	2.698827
C	-1.36712	-3.59223	-3.71077	H	1.408574	-3.11618	4.685344
C	-1.87337	-2.92621	-2.59651	H	0.447669	-5.39809	4.448522
C	-3.29648	-3.97636	1.084669	H	0.381736	-6.48653	2.214394
C	-4.6561	-4.25853	0.904589	H	1.247888	-5.29439	0.230442
C	-5.25067	-5.30398	1.611524	P	2.591922	-2.64266	-0.06082
C	-4.49285	-6.0691	2.500027	P	-2.59194	-2.64271	0.060806
C	-3.13887	-5.78272	2.68888	O	-3.67056	-1.71027	-0.43277
C	-2.54236	-4.73759	1.985903	O	3.670439	-1.7102	0.432962

Table S13. Coordinates (Å) for the optimized structure (B3LYP-D3/6-31G(d)) in the ground state of **(*R*)-P2**

Atoms	X	Y	Z	Atoms	X	Y	Z
C	1.120076	-3.29148	-1.20415	H	8.513011	7.489991	1.409741
C	0.204655	-2.34733	-0.74725	C	7.655994	5.592121	0.904602
C	-0.33619	-1.37437	-1.64075	H	8.586482	5.050596	1.038903
C	-1.30859	-0.4388	-1.21437	C	7.66501	2.925362	-0.37934
H	-1.59576	-0.44188	-0.17015	C	8.236144	3.559858	-1.49091
C	-1.90191	0.454132	-2.08957	H	7.813428	4.494176	-1.8451
C	-1.47084	0.453705	-3.44797	C	9.33312	2.995112	-2.13437
H	-1.9388	1.133782	-4.15283	H	9.759057	3.502459	-2.99691
C	-0.50689	-0.42063	-3.88768	C	9.885869	1.780391	-1.70975
H	-0.19896	-0.4157	-4.9304	C	9.298741	1.150496	-0.60546
C	0.079595	-1.36838	-3.00905	H	9.706409	0.206931	-0.25007
C	1.038653	-2.31896	-3.43515	C	8.214409	1.713263	0.061027
H	1.366632	-2.30681	-4.47188	H	7.780667	1.21406	0.921235
C	1.539264	-3.25603	-2.56124	C	3.068472	-3.7221	0.821612
H	2.254497	-3.99075	-2.91375	C	4.07635	-3.04358	0.11881
C	-0.20708	-2.34385	0.692275	H	4.073693	-3.05485	-0.9675
C	-1.25028	-3.1465	1.139835	C	5.071379	-2.34972	0.803892
C	-1.53089	-3.21885	2.531723	H	5.844073	-1.82197	0.252191
H	-2.31375	-3.88455	2.878457	C	5.056415	-2.30244	2.200074
C	-0.7979	-2.49522	3.441285	H	5.816014	-1.73598	2.731087
H	-1.01084	-2.57305	4.504871	C	4.054741	-2.96498	2.90709
C	0.243715	-1.63572	3.012983	H	4.028581	-2.91643	3.991625
C	1.028284	-0.87727	3.91943	C	3.070761	-3.67825	2.22059
H	0.82656	-0.96527	4.984204	H	2.278184	-4.17832	2.769664
C	2.035465	-0.05896	3.472682	C	2.510232	-5.79987	-1.12576
H	2.643586	0.478842	4.192696	C	3.870185	-6.12788	-1.0551
C	2.316887	0.076485	2.081755	H	4.516435	-5.60587	-0.35769
C	1.561747	-0.6647	1.189311	C	4.403854	-7.1221	-1.87838
H	1.738484	-0.57061	0.125596	H	5.46145	-7.36327	-1.8109
C	0.534779	-1.54061	1.617036	C	3.589576	-7.79872	-2.78524
C	-2.99404	1.340392	-1.63618	H	4.007864	-8.56879	-3.42739
C	-3.25991	2.577463	-2.24665	C	2.229564	-7.48561	-2.85796
H	-2.61333	2.93559	-3.04224	H	1.585025	-8.01187	-3.55681
C	-4.3406	3.361586	-1.85801	C	1.69332	-6.50482	-2.02806
H	-4.53789	4.305108	-2.35582	H	0.631786	-6.27418	-2.08235
C	-5.1887	2.935748	-0.82499	C	-2.7715	-5.53382	0.893223
C	-4.90723	1.723173	-0.18042	C	-1.77762	-6.33645	1.481717
H	-5.55422	1.379636	0.618931	H	-0.73237	-6.05137	1.38501
C	-3.83961	0.939152	-0.58877	C	-2.12199	-7.48421	2.190853
H	-3.68386	-0.01811	-0.10668	H	-1.34225	-8.08789	2.64772
C	-7.53546	3.009718	-0.1561	C	-3.46207	-7.86193	2.311526
C	-8.32945	3.394478	0.93192	H	-3.72977	-8.75946	2.862242

H	-8.01486	4.227693	1.551593	C	-4.45246	-7.08207	1.716154
C	-9.50783	2.709921	1.218101	H	-5.49726	-7.36916	1.801902
H	-10.1068	3.02237	2.070332	C	-4.11132	-5.92521	1.011651
C	-9.92624	1.617633	0.449117	H	-4.89292	-5.32356	0.559418
C	-9.12031	1.238364	-0.63269	C	-3.74568	-3.06733	-0.24815
H	-9.42267	0.399233	-1.25551	C	-4.17185	-2.69747	-1.53132
C	-7.95056	1.924826	-0.94276	H	-3.58327	-3.00001	-2.39282
H	-7.34371	1.619927	-1.7888	C	-5.33205	-1.94049	-1.70929
C	-6.26353	5.101395	-0.37985	H	-5.64062	-1.65323	-2.71039
C	-7.34534	5.889695	-0.79646	C	-6.08407	-1.54416	-0.60441
H	-8.23842	5.408814	-1.18127	H	-6.97954	-0.94365	-0.73494
C	-7.27782	7.277052	-0.70894	C	-5.66238	-1.89366	0.681145
H	-8.13073	7.868613	-1.03357	H	-6.238	-1.57533	1.546332
C	-6.13364	7.926349	-0.2299	C	-4.50017	-2.64343	0.858086
C	-5.05771	7.127787	0.177602	H	-4.18147	-2.90754	1.860988
H	-4.1594	7.601018	0.567449	N	-6.32715	3.689232	-0.45226
C	-5.11712	5.73917	0.11578	N	6.550119	3.496764	0.284627
H	-4.2779	5.139655	0.452341	P	1.673821	-4.59991	-0.00708
C	3.392938	0.975568	1.612179	P	-2.2136	-4.10267	-0.12606
C	3.809937	2.08458	2.367084	C	-11.2131	0.891594	0.754684
H	3.314063	2.315657	3.304559	H	-12.0462	1.282503	0.155118
C	4.842417	2.912111	1.94158	H	-11.1316	-0.17848	0.534973
H	5.149149	3.755836	2.550321	H	-11.4921	0.999858	1.807982
C	5.490421	2.670423	0.721503	C	-6.05143	9.432177	-0.1793
C	5.065122	1.582598	-0.05693	H	-5.4178	9.770692	0.647609
H	5.55111	1.385404	-1.00645	H	-5.62344	9.842073	-1.10416
C	4.046155	0.752712	0.387178	H	-7.04134	9.883083	-0.0527
H	3.76504	-0.09863	-0.22075	C	6.362019	9.173579	1.221707
C	6.505393	4.895416	0.511824	H	5.623582	9.667789	0.581158
C	5.310876	5.608576	0.338562	H	6.080354	9.383649	2.262374
H	4.416844	5.080813	0.023383	H	7.333112	9.648307	1.046386
C	5.27347	6.980375	0.567471	C	11.08832	1.186159	-2.40095
H	4.336971	7.514707	0.425171	H	12.02552	1.556845	-1.96429
C	6.417515	7.689439	0.955137	H	11.10043	0.094485	-2.31533
C	7.607358	6.967966	1.109818	H	11.10441	1.441825	-3.46586

Table S14. Coordinates (Å) for the optimized structure (B3LYP-D3/6-31G(d)) in the ground state of **(*R*)-PO2**							
Atoms	X	Y	Z	Atoms	X	Y	Z
C	1.251959	-2.50539	-1.18751	C	8.424423	5.376148	0.634087
C	0.203112	-1.7297	-0.71958	H	9.26678	4.778519	0.965998
C	-0.52317	-0.8905	-1.62315	C	8.216974	2.508335	-0.0386
C	-1.60989	-0.09687	-1.18624	C	9.00168	2.798445	-1.16243
H	-1.84943	-0.08954	-0.13068	H	8.765225	3.668903	-1.76547
C	-2.36922	0.659401	-2.06274	C	10.06987	1.973603	-1.50412
C	-2.00568	0.661802	-3.43932	H	10.66309	2.21383	-2.38338
H	-2.60444	1.228852	-4.14532	C	10.38325	0.832286	-0.75572
C	-0.93527	-0.07119	-3.89158	C	9.587738	0.549949	0.362295
H	-0.67576	-0.06585	-4.94726	H	9.812041	-0.32425	0.969707
C	-0.16888	-0.87266	-3.00709	C	8.528639	1.375619	0.727032
C	0.913155	-1.67219	-3.44955	H	7.927977	1.14523	1.600669
H	1.178591	-1.6647	-4.50354	C	3.803516	-2.92238	0.15981
C	1.599603	-2.46669	-2.56616	C	4.70185	-2.65013	-0.8827
H	2.392476	-3.10944	-2.93354	H	4.439485	-2.89217	-1.90773
C	-0.20328	-1.72962	0.719569	C	5.944128	-2.07978	-0.60685
C	-1.25217	-2.50522	1.18757	H	6.638348	-1.87267	-1.41648
C	-1.59983	-2.46636	2.566207	C	6.293736	-1.76822	0.708903
H	-2.39273	-3.10904	2.933649	H	7.254843	-1.30698	0.913468
C	-0.91336	-1.67179	3.449522	C	5.398093	-2.02382	1.747357
H	-1.17881	-1.66418	4.503503	H	5.660363	-1.76453	2.768912
C	0.168713	-0.87235	3.006994	C	4.157114	-2.60067	1.476518
C	0.93512	-0.07084	3.891423	H	3.446361	-2.80556	2.270454
H	0.675587	-0.06537	4.947093	C	2.376867	-5.13642	-1.13316
C	2.00558	0.662066	3.439113	C	3.599694	-5.81477	-1.2059
H	2.604345	1.229169	4.145064	H	4.471664	-5.41959	-0.69432
C	2.369125	0.659519	2.062541	C	3.699672	-6.99775	-1.9388
C	1.609779	-0.0968	1.186091	H	4.651381	-7.51868	-1.99729
H	1.84936	-0.08959	0.130539	C	2.578194	-7.50954	-2.59256
C	0.523031	-0.89036	1.623063	H	2.657165	-8.43081	-3.16359
C	-3.55541	1.40084	-1.58616	C	1.354235	-6.84072	-2.51106
C	-4.00825	2.571579	-2.21733	H	0.47949	-7.2416	-3.01531
H	-3.44671	2.985549	-3.04958	C	1.245172	-5.65652	-1.78483
C	-5.16625	3.219343	-1.80162	H	0.290409	-5.138	-1.71866
H	-5.50635	4.113522	-2.31326	C	-2.37719	-5.13619	1.133481
C	-5.90747	2.718768	-0.7211	C	-1.24553	-5.65624	1.785246
C	-5.44379	1.573158	-0.05973	H	-0.29076	-5.13774	1.719086
H	-6.00863	1.172788	0.774747	C	-1.35464	-6.84038	2.511575
C	-4.29777	0.924309	-0.49307	H	-0.47992	-7.24122	3.015906
H	-3.99587	0.011514	0.006354	C	-2.5786	-7.50918	2.59307
C	-8.21685	2.508754	0.038327	H	-2.65761	-8.43041	3.164167
C	-9.00128	2.798593	1.162267	C	-3.70005	-6.99744	1.939223

H	-8.76474	3.668881	1.765523	H	-4.65176	-7.51835	1.9977
C	-10.0696	1.973653	1.503906	C	-3.60003	-5.81451	1.206227
H	-10.6627	2.213712	2.383268	H	-4.47197	-5.41936	0.694579
C	-10.3831	0.832656	0.755343	C	-3.80375	-2.92223	-0.15972
C	-9.58778	0.550555	-0.36302	C	-4.15734	-2.60062	-1.47645
H	-9.81228	-0.32343	-0.9707	H	-3.44661	-2.80563	-2.27037
C	-8.52877	1.376188	-0.72764	C	-5.39829	-2.02372	-1.74733
H	-7.92827	1.146093	-1.60147	H	-5.66056	-1.76452	-2.7689
C	-7.23079	4.740399	-0.26427	C	-6.2939	-1.76798	-0.70888
C	-8.42413	5.376826	-0.63356	H	-7.25497	-1.30668	-0.91348
H	-9.26669	4.779399	-0.96531	C	-5.9443	-2.07945	0.606893
C	-8.53022	6.762967	-0.56707	H	-6.63849	-1.87222	1.416514
H	-9.46706	7.234931	-0.85406	C	-4.70205	-2.64984	0.882783
C	-7.45603	7.56154	-0.15673	H	-4.4397	-2.89182	1.907833
C	-6.26769	6.914014	0.203885	N	-7.11735	3.33071	-0.31505
H	-5.41879	7.504857	0.540258	N	7.117434	3.330315	0.314584
C	-6.15187	5.528253	0.162656	C	-11.5543	-0.04544	1.121429
H	-5.22694	5.047206	0.462698	H	-12.468	0.266211	0.597758
C	3.555359	1.400846	1.585902	H	-11.3696	-1.09155	0.854544
C	4.008292	2.571593	2.216972	H	-11.7655	-0.00271	2.195123
H	3.446802	2.985669	3.049201	C	-7.5645	9.066295	-0.12917
C	5.166356	3.219222	1.801211	H	-6.94544	9.497617	0.664959
H	5.506548	4.113396	2.3128	H	-7.23096	9.510234	-1.0769
C	5.90753	2.718502	0.720725	H	-8.59772	9.390128	0.034614
C	5.443729	1.572885	0.059437	C	7.565429	9.065874	0.130112
H	6.00853	1.172393	-0.775	H	6.951423	9.496985	-0.66807
C	4.297671	0.924172	0.49284	H	7.225784	9.51008	1.075547
H	3.995675	0.011368	-0.00652	H	8.599654	9.389648	-0.02721
C	7.23114	4.740008	0.264258	C	11.55462	-0.04533	-1.12226
C	6.152454	5.528127	-0.16286	H	12.47421	0.282901	-0.61932
H	5.227556	5.047255	-0.4633	H	11.38109	-1.08695	-0.83175
C	6.268481	6.913851	-0.20374	H	11.74925	-0.02279	-2.19977
H	5.41978	7.5049	-0.54027	P	2.152469	-3.66376	-0.09134
C	7.45683	7.561122	0.157425	P	-2.15273	-3.66364	0.091505
C	8.530745	6.762319	0.567935	O	-1.48906	-3.95027	-1.23009
H	9.467549	7.234087	0.85535	O	1.488764	-3.9502	1.230285

Table S15. Coordinates (Å) for the optimized structure (B3LYP-D3/6-31G(d)) in the ground state of **(*R*)-P3**							
Atoms	X	Y	Z	Atoms	X	Y	Z
C	1.23213	-2.99011	-1.15936	H	9.14576	4.411898	1.318081
C	0.201788	-2.16815	-0.72011	C	8.107492	2.289536	-0.01034
C	-0.52066	-1.35365	-1.64785	C	8.825491	2.676728	-1.14427
C	-1.58562	-0.52022	-1.2318	H	8.537315	3.580857	-1.67058
H	-1.8105	-0.46568	-0.17384	C	9.907128	1.92276	-1.60316
C	-2.34038	0.213391	-2.13171	H	10.44313	2.253929	-2.48467
C	-1.99417	0.14665	-3.51147	C	10.27038	0.747622	-0.93731
H	-2.5896	0.696378	-4.23385	C	9.551599	0.351113	0.199924
C	-0.94806	-0.63171	-3.94571	H	9.856053	-0.55418	0.715716
H	-0.70491	-0.67952	-5.00433	C	8.493367	1.118332	0.663341
C	-0.18733	-1.41096	-3.03683	H	7.946528	0.813262	1.549345
C	0.861985	-2.26708	-3.45599	C	3.761022	-3.27725	0.205159
H	1.105459	-2.32042	-4.51441	C	4.58841	-2.99972	-0.89514
C	1.546785	-3.03494	-2.54633	H	4.255542	-3.24617	-1.89756
H	2.312881	-3.72051	-2.8919	C	5.842482	-2.41799	-0.71288
C	-0.20173	-2.16821	0.720239	H	6.472929	-2.20893	-1.57302
C	-1.23203	-2.99022	1.159483	C	6.28784	-2.09801	0.571896
C	-1.54648	-3.0353	2.546492	H	7.25839	-1.62996	0.705037
H	-2.31252	-3.72093	2.892052	C	5.470214	-2.35498	1.671237
C	-0.86155	-2.2676	3.456189	H	5.800521	-2.08872	2.671141
H	-1.10487	-2.32113	4.514635	C	4.216152	-2.94065	1.488118
C	0.1877	-1.4114	3.037036	H	3.574598	-3.12929	2.344122
C	0.948562	-0.63231	3.945937	C	2.392005	-5.56114	-0.93591
H	0.705561	-0.68028	5.004588	C	3.642456	-6.18277	-1.04716
C	1.994615	0.146123	3.511687	H	4.516165	-5.72454	-0.59496
H	2.590154	0.695724	4.234073	C	3.776457	-7.38606	-1.74347
C	2.340637	0.213093	2.131885	H	4.754894	-7.85234	-1.82509
C	1.585752	-0.52037	1.231962	C	2.66501	-7.98506	-2.33493
H	1.810487	-0.46565	0.173982	H	2.771639	-8.92017	-2.87776
C	0.520842	-1.35385	1.64802	C	1.41191	-7.37706	-2.22135
C	-3.50521	0.999685	-1.67653	H	0.538608	-7.83756	-2.67532
C	-3.93718	2.154511	-2.34971	C	1.273797	-6.18011	-1.52372
H	-3.37297	2.523158	-3.20141	H	0.293845	-5.71532	-1.44159
C	-5.07611	2.84542	-1.95215	C	-2.39211	-5.56113	0.935769
H	-5.39768	3.725847	-2.49812	C	-1.27387	-6.18039	1.523225
C	-5.82311	2.405311	-0.84775	H	-0.29386	-5.71576	1.440913
C	-5.37896	1.274009	-0.14622	C	-1.41203	-7.37741	2.22073
H	-5.94461	0.917877	0.707392	H	-0.53871	-7.83813	2.674426
C	-4.25066	0.583882	-0.56087	C	-2.66522	-7.98519	2.334526
H	-3.96614	-0.3155	-0.02765	H	-2.77189	-8.92036	2.877256
C	-8.10752	2.289478	0.01009	C	-3.7767	-7.3859	1.74342
C	-8.82572	2.676505	1.143955	H	-4.7552	-7.85202	1.825215

H	-8.53762	3.580551	1.67045	C	-3.64265	-6.18254	1.047242
C	-9.90745	1.922486	1.602535	H	-4.51638	-5.72408	0.595328
H	-10.4436	2.253529	2.484003	C	-3.76104	-3.27701	-0.20486
C	-10.2706	0.747458	0.936442	C	-4.21653	-2.94069	-1.48776
C	-9.55163	0.351114	-0.20073	H	-3.57523	-3.12955	-2.3439
H	-9.85601	-0.55409	-0.71672	C	-5.47063	-2.35504	-1.67065
C	-8.4933	1.118384	-0.66384	H	-5.80123	-2.08901	-2.67052
H	-7.94631	0.813432	-1.54979	C	-6.28794	-2.09779	-0.57113
C	-7.13452	4.467881	-0.5644	H	-7.25851	-1.62974	-0.70411
C	-8.31764	5.050119	-1.02804	C	-5.84221	-2.41748	0.713585
H	-9.14566	4.411902	-1.31821	H	-6.47239	-2.20819	1.573873
C	-8.45195	6.436745	-1.11393	C	-4.5881	-2.9992	0.895622
H	-9.38547	6.853063	-1.47359	H	-4.25493	-3.24539	1.898004
C	-7.38296	7.264195	-0.75618	N	-7.01097	3.059851	-0.4575
C	-6.18994	6.686244	-0.29998	N	7.011024	3.059829	0.45757
H	-5.37154	7.340607	-0.01767	P	2.089257	-4.062	0.090753
C	-6.07156	5.308834	-0.19362	P	-2.08931	-4.06187	-0.0907
H	-5.14983	4.869905	0.173556	O	-7.40116	8.630129	-0.8114
C	3.505411	0.999458	1.676674	O	7.40103	8.630096	0.811803
C	3.937466	2.154176	2.349985	O	-11.2998	-0.07181	1.305558
H	3.373347	2.522696	3.201803	C	8.58398	9.254397	1.276748
C	5.076338	2.845153	1.9524	H	8.390992	10.32812	1.244563
H	5.397974	3.725497	2.498473	H	8.818241	8.958302	2.3082
C	5.823207	2.405222	0.847841	H	9.443596	9.020663	0.634025
C	5.378984	1.274025	0.146192	C	-8.58407	9.254415	-1.27646
H	5.944539	0.91803	-0.70754	H	-8.39113	10.32814	-1.24417
C	4.250731	0.583831	0.560864	H	-8.81819	8.958382	-2.30796
H	3.966157	-0.31547	0.02753	H	-9.44376	9.0206	-0.63387
C	7.134516	4.467858	0.564538	C	-12.0488	0.286709	2.453435
C	6.071481	5.308795	0.193964	H	-12.8081	-0.48812	2.571688
H	5.149715	4.869855	-0.17312	H	-11.4187	0.318343	3.352391
C	6.189823	6.686202	0.300407	H	-12.5402	1.260717	2.326444
H	5.371361	7.340557	0.018253	O	11.29954	-0.07161	-1.30674
C	7.382874	7.264165	0.756482	C	12.04825	0.28706	-2.45471
C	8.45195	6.436733	1.114038	H	12.80753	-0.48778	-2.57323
H	9.385499	6.853064	1.473603	H	11.41796	0.318855	-3.35353
C	8.31768	5.050109	1.028061	H	12.5397	1.261031	-2.32767

Table S16. Coordinates (Å) for the optimized structure (B3LYP-D3/6-31G(d)) in the ground state of **(*R*)-PO3**							
Atoms	X	Y	Z	Atoms	X	Y	Z
C	-1.27568	-2.74795	1.162727	C	-8.18683	2.279625	-0.01244
C	-0.21719	-1.97324	0.715438	C	-8.92657	2.605294	1.126783
C	0.491618	-1.13402	1.632836	H	-8.66685	3.49531	1.690626
C	1.58697	-0.34104	1.217103	C	-9.99358	1.807419	1.544032
H	1.846829	-0.33389	0.166398	H	-10.5474	2.091084	2.431083
C	2.329857	0.415353	2.107756	C	-10.3194	0.649698	0.830021
C	1.938663	0.418475	3.476855	C	-9.5791	0.315391	-0.31343
H	2.523527	0.985742	4.194286	H	-9.8553	-0.57667	-0.86682
C	0.858867	-0.31341	3.908244	C	-8.53638	1.126458	-0.73517
H	0.578348	-0.30698	4.958575	H	-7.97297	0.870649	-1.62636
C	0.10958	-1.11512	3.009382	C	-3.7995	-3.16528	-0.23739
C	-0.9819	-1.91338	3.430413	C	-4.72129	-2.89393	0.784717
H	-1.26858	-1.90476	4.478854	H	-4.48144	-3.13543	1.815408
C	-1.65125	-2.70797	2.534004	C	-5.95806	-2.32575	0.48095
H	-2.45218	-3.34959	2.885635	H	-6.67131	-2.11987	1.274148
C	0.217219	-1.97323	-0.71547	C	-6.27825	-2.01523	-0.84246
C	1.27571	-2.74793	-1.1628	H	-7.23647	-1.55841	-1.06918
C	1.651231	-2.70794	-2.53409	C	-5.35898	-2.26873	-1.86047
H	2.452142	-3.34956	-2.88575	H	-5.59863	-2.00993	-2.88766
C	0.981822	-1.91337	-3.43048	C	-4.12363	-2.84368	-1.56166
H	1.268456	-1.90476	-4.47893	H	-3.39494	-3.04764	-2.3394
C	-0.10965	-1.11512	-3.00941	C	-2.40059	-5.37823	1.087813
C	-0.85899	-0.31345	-3.90825	C	-3.62479	-6.05617	1.136574
H	-0.57852	-0.30702	-4.9586	H	-4.48622	-5.66108	0.607384
C	-1.93879	0.418414	-3.47683	C	-3.73982	-7.23866	1.868145
H	-2.5237	0.985657	-4.19424	H	-4.69272	-7.75922	1.907876
C	-2.32992	0.415314	-2.10771	C	-2.63183	-7.7504	2.544513
C	-1.58697	-0.34105	-1.21707	H	-2.72249	-8.67131	3.114439
H	-1.84679	-0.33388	-0.16636	C	-1.40626	-7.08202	2.486982
C	-0.49163	-1.13402	-1.63285	H	-0.54184	-7.48287	3.008791
C	3.524743	1.156056	1.65366	C	-1.28234	-5.89833	1.762293
C	3.968216	2.326204	2.292203	H	-0.32626	-5.38019	1.714664
H	3.393735	2.740101	3.115743	C	2.400842	-5.37816	-1.08791
C	5.131361	2.97618	1.895389	C	1.282622	-5.89848	-1.76225
H	5.460469	3.869667	2.415026	H	0.326431	-5.38056	-1.7145
C	5.892394	2.478438	0.825581	C	1.406693	-7.08217	-2.48694
C	5.438334	1.330806	0.157806	H	0.542284	-7.4832	-3.00863
H	6.013994	0.93018	-0.66889	C	2.632392	-7.7503	-2.54461
C	4.286309	0.681616	0.572826	H	2.723173	-8.6712	-3.11453
H	3.993795	-0.23101	0.067348	C	3.740361	-7.23832	-1.86838
C	8.186813	2.279772	0.012666	H	4.693363	-7.75868	-1.90822
C	8.926462	2.605415	-1.12663	C	3.625175	-6.05585	-1.13681

H	8.666668	3.495394	-1.69049	H	4.486587	-5.66056	-0.60773
C	9.993463	1.807557	-1.54391	C	3.799537	-3.16517	0.237362
H	10.54719	2.091199	-2.43102	C	4.1236	-2.84347	1.561618
C	10.31939	0.649882	-0.82987	H	3.394872	-3.04734	2.339331
C	9.579178	0.315603	0.313648	C	5.358956	-2.26852	1.860439
H	9.855447	-0.57642	0.867064	H	5.598555	-2.00963	2.887623
C	8.536461	1.126655	0.735428	C	6.278287	-2.01514	0.842457
H	7.973129	0.870877	1.626675	H	7.236508	-1.55833	1.069191
C	7.255947	4.499743	0.490189	C	5.958158	-2.32577	-0.48094
C	8.445236	5.073454	0.94871	H	6.671463	-2.11998	-1.27412
H	9.254051	4.428937	1.276711	C	4.721389	-2.89393	-0.78473
C	8.610059	6.459025	0.981844	H	4.481591	-3.13552	-1.81541
H	9.547538	6.868378	1.33918	N	7.102713	3.091619	0.437195
C	7.565608	7.295247	0.575257	N	-7.10274	3.091507	-0.43691
C	6.366484	6.726336	0.123802	O	7.614286	8.661517	0.576865
H	5.567478	7.387029	-0.19674	O	-7.61462	8.661361	-0.57722
C	6.218098	5.348758	0.070003	O	11.33062	-0.20899	-1.1562
H	5.291982	4.916403	-0.2939	C	-8.80477	9.277	-1.03537
C	-3.5248	1.156005	-1.65357	H	-8.63705	10.35264	-0.95778
C	-3.96835	2.326111	-2.29213	H	-9.01709	9.017077	-2.08121
H	-3.39394	2.739986	-3.11573	H	-9.66799	8.998574	-0.41571
C	-5.13149	2.976069	-1.89526	C	8.804402	9.27727	1.03494
H	-5.46066	3.869524	-2.41492	H	8.636631	10.35289	0.957234
C	-5.89242	2.478352	-0.82538	H	9.016742	9.017477	2.080813
C	-5.43829	1.330763	-0.15759	H	9.667643	8.998816	0.415318
H	-6.01388	0.93016	0.669166	C	12.10228	0.087538	-2.30675
C	-4.28627	0.681591	-0.57266	H	12.84278	-0.7101	-2.38649
H	-3.99368	-0.231	-0.06715	H	11.48406	0.101616	-3.21437
C	-7.25606	4.499615	-0.49008	H	12.61696	1.052862	-2.20934
C	-6.21826	5.348733	-0.06999	O	-11.3306	-0.2092	1.156315
H	-5.29212	4.916464	0.293961	C	-12.1024	0.087367	2.306796
C	-6.36671	6.726297	-0.12395	H	-12.8429	-0.71029	2.386516
H	-5.56774	7.387069	0.196518	H	-11.4842	0.101516	3.214461
C	-7.56587	7.295093	-0.57546	H	-12.6171	1.052668	2.209291
C	-8.61028	6.458772	-0.98195	P	-2.15422	-3.90636	0.04938
H	-9.54778	6.868036	-1.33933	P	2.154297	-3.90632	-0.04946
C	-8.44538	5.073212	-0.94866	O	1.463808	-4.19562	1.257767
H	-9.25417	4.428617	-1.27659	O	-1.46374	-4.19556	-1.25787

G: References

1 O. V. D. and L. J. B. and R. J. G. and J. A. K. H. and H. and Puschmann, *J. Appl. Cryst*, 2009, **42**, 339–341.
2 G. M. Sheldrick, *Acta Crystallogr. Sect. C Struct. Chem.*, 2015, **71**, 3–8.
3 B. Yang, S. Yan, S. Ban, Y. Zhang, H. Ma and W. Huang, *Chem. Mater.*, 2024, **36**, 7940−7952.
4 T. Lu and F. Chen, *J. Comput. Chem.*, 2012, **33**, 580–592.
5 A. D. and K. S. W. Humphrey, *J. Mol. Graph*, 1996, **14**, 33–38.
6 2016. J. Frisch, G. W. et al. Gaussian, Inc., Wallingford CT, *Gaussian 16, Revision A.03,* .
7 H. Kruse, L. Goerigk and S. Grimme, *J. Org. Chem.*, 2012, **77**, 10824–10834.
8 J. Tirado-Rives and W. L. Jorgensen, *J. Chem. Theory Comput.*, 2008, **4**, 297–306.
9 A. D. Becke, *J. Chem. Phys.*, 1993, **98**, 5648–5652.
10 F. Neese, *WIREs Comput. Mol. Sci.*, 2012, **2**, 73–78.
11 T. Lu, *J. Chem. Phys.*, 2024, **161**, 082503.